JULY 2017 Ph.D. in CIVIL ENGINEERING ABDULNASER A. KASHMOOLA

UNIVERSITY OF GAZİANTEP

GRADUATE SCHOOL OF

NATURAL & APPLIED SCIENCES

INVESTIGATION OF LOCAL SCOUR AND DISCHARGE CHARACTERISTICS OF SINGLE STEP BROAD CRESTED WEIRS

Ph.D. THESIS

IN

CIVIL ENGINEERING

BY

ABDULNASER A. KASHMOOLA

JULY 2017

Investigation of Local Scour and Discharge Characteristics of Single Step Broad Crested Weirs

Ph.D Thesis

in

Civil Engineering

University of Gaziantep

Supervisors

Prof. Dr. Mustafa GÜNAL

Assist. Prof. Dr. Hamid HUSSEIN

by

Abdulnaser A. KASHMOOLA

July 2017

REPUBLIC OF TURKEY
UNIVERSITY OF GAZİANTEP
GRADUATE SCHOOL OF NATURAL & APPLIED SCIENCES
CIVIL ENGINEERING DEPARTMENT

Name of the thesis: Investigation of Local Scour and Discharge Characteristics of Single Step Broad Crested Weirs.

Name of the student: ABDULNASER ABDULRAZZAQ AHMED KASHMOOLA

Exam date: 10.07.2017

Approval of the Graduate School of Natural and Applied Sciences

Prof. Dr. A. Necmeddin YAZICI
Director

I certify that this thesis satisfies all the requirements as a thesis for the degree of Doctor of Philosophy.

Prof. Dr. Abdulkadir ÇEVİK
Head of Department

This is to certify that we have read this thesis and that in our majority opinion; it is fully adequate, in scope and quality, as a thesis for the degree of Doctor of Philosophy.

Assist. Prof. Dr. Hamid H. Hussein
Co-Supervisor

Prof. Dr. Mustafa GÜNAL
Supervisor

Examining Committee Members:	Signature
Prof. Dr. Yalçın YÜKSEL	....
Prof. Dr. Esin ÇEVİK	....
Prof. Dr Mustafa GÜNAL	....
Prof. Dr. Aytaç GÜVEN	....
Assist. Prof. Dr. Ayşe Y. GÜNAL	....

I hereby declare that all information in this document has been obtained and presented in accordance with academic rules and ethical conduct. I also declare that, as required by these rules and conduct, I have fully cited and referenced all material and results that are not original to this work.

Abdulnaser A. KASHMOOLA

ABSTRACT

INVESTIGATION OF LOCAL SCOUR AND DISCHARGE CHARACTERISTICS OF SINGLE STEP BROAD CRESTED WEIRS

KASHMOOLA, A. Abdulnaser
Ph.D. in Civil Engineering
Supervisor: Prof. Dr. Mustafa GÜNAL
Co-Supervisor: Assist. Prof. Dr. Hamid HUSSEIN
July 2017
119 pages

Scour control process considered as the main objective to ensure safety and economical design of hydraulic structures to prevent any serious failure in the future. Many types of research showed that local scour downstream of single step broad crested weir decreased five times in comparison with a traditional weir. In this study single step broad crested weir with height (21) cm at downstream and ten models of them are investigated. The first group is four models of ramps with different angles at the downstream of weir and six models of hollow end sill with different heights and porosity. The measurements were tested under three discharges for a duration of 6 hours, and the velocity field was measured by using an Acoustic Doppler Velocimeter.

The present results showed that the ramp with an angle (10.8^0) is the best model to decrease local scour hole volume and a maximum depth of scour. It is also found that the end sill with height (24) cm and porosity (35%) give a low local scour hole volume and maximum depth of scour. The minimum distance of scour from weir is an important issue to prevent failure of weir in the future. In this research, the single broad crested weir was modified to produce minimum local scour at downstream and also reduces costs because there is no need to use countermeasures for reducing the scour depth by lining with rubbles and riprap to protect failure.

Keywords: Broad Crested Weir, Scour reduction, Local scour, Weir.

ÖZET

TEK BASAMAKLI GENİŞ YÜZEYLİ SAVAKLARDA YEREL OYULMA VE DEBİ KARAKTERİSTİKLERİNİN İNCELENMESİ

KASHMOOLA, A. Abdulnaser
Doktora Tezi, İnşaat Mühendisliği Bölümü
Tez Yöneticisi: Prof. Dr. Mustafa GÜNAL
Yardımcı Tez Yöneticisi: Y. Doç. Dr. Hamid HUSSEIN
Temmuz 2017
119 sayfa

Hidrolik yapıların emniyetli ve ekonomik tasarımını sağlamak için oyulma kontrol süreci ana hedef olarak düşünülmüştür. Birçok araştırma sonucuna göre tek basamaklı geniş yüzeyli savakların mansabında oluşan oyulma normal savaklara gore beş kat daha azdır. Bu çalışmada, basamak yüksekliği 21 cm olan geniş yüzeyli savak modelleri kullanılarak iki grup deney yapılmıştır. Birinci grup deneyler farklı açılarda basamak üzerine yerleştirilmiş rampa modelleri üzerinde, ikinci grup deneyler ise basamak sonuna yerleştirilmiş ve farklı boşluk oranına ve yüksekliğe sahip bloklar kullanılarak yapılmıştır. Ölçümler üç farklı akım debisinde 6 saat süre sonunda Akustik Dopler Hız ölçer ile yapılmıştır.

Bu çalışmada elde edilen ölçümler, 10.8^0 eğime sahip tek basamaklı, geniş yüzeyli savak modelinin oyulma derinliği ve oyulma çukuru hacmini azaltlığı için en iyi model olduğunu göstermiştir. Ayrıca 24 cm yüksekliğindeki basamak sonuna yerleştirilen %35 boşluk oranına sahip blok oyulma çukuru hacmin ve maksimum oyulma derinliğini azaltmıştır. Oluşan oyulmanın savaktan olan uzaklığı savakların hasar görmesinde önemli bir etkendir. Bu çalışmada, tek basamaklı geniş yüzeyli savak geliştirilmiş ve mansapta oluşacak yerel oyulma derinliği en aza indirilmiş olduğundan savak yapısından sonra yüzeyin taşlarla kaplanmasına veya riprap ihtiyacı ortadan kalktığından savak yapım maliyeti düşmüştür.

Anahtar Kelimeler: Geniş yüzeyli savak, Oyulmanın azaltılması, Yerel oyulma, Savak.

ACKNOWLEDGMENTS

The author wishes to express his deepest gratitude to his supervisor Professor Dr. Mustafa GUNAL for his valuable guidance and support throughout the conduction of experiments and preparation of this thesis.

Also, special thanks to my co-supervisor Associate Professor Dr. Hamid Hussein for his guidance and support during the study.

I am also grateful to my friends for their help during different phases of this study.

Finally, words cannot express my appreciation for my wife for her support and encouragement during the study.

TABLE OF CONTENTS

Page

LIST OF FIGURES

Page

LIST OF TABLES

Page

LIST OF SYMBOLS/ABREVIATIONS

e	Porosity (%)
$P1$	Height of weir in U/S (cm)
$P2$	Height of weir in D/S (cm)
dr	Diameter of the hole (cm)
ds	maximum depth of scour (cm)
Vs	volume of scour (cm^3)
Rd	Redaction depth of scour (%)
Rv	Redaction volume of scour (%)
ds/Yu	maximum depth of scour to U/S water depth
Yt/Yu	Tailwater depth to U/S water depth
Yd/Yu	D/S water depth to U/S water depth
θ^0	angle of the ramp
ρ	Density of fluid (kg/m^3)
Eu	energy at U/S (cm)
Et	energy at D/S (cm)
ΔE	The energy dissipation ratio between U/S and D/S (%)
Va	velocity of flow at downstream of the weir (m/s)
Vc	critical velocity (m/s)
g	Gravitational acceleration (m/s^2)
d_{50}	Median particle size (mm)
Fr	Froude number = $[v / (gh)^{0.5}]$
FD	Densimetric Froude number
R	Correlation coefficient
d_{16}	Grain size of which 16% by weight of the sediment is finer
d_{84}	Grain size of which 84% by weight of the sediment is finer
∂g	$= (d_{84}/d_{16})^{0.5}$ Geometric standard deviation of the grain size distribution

CHAPTER 1

INTRODUCTION

1.1 Information

The weir is an obstruction constructed across a river or stream for the purpose of rising water surface or water flow measurement. The primary objective of the traditional broad crested weir is to increase and control the upstream water level. Weirs with different shapes have been considered an important hydraulic structure which used in open channel flow. They are widely used in water flow measurements and control of water surface levels.

Local scour downstream of hydraulic structures may cause damage or complete failure of this structure. Scour in bed material at the downstream of weirs is considered the most unfavorable process which threats the overall stability of the weir. Structures built in rivers and canals are subject to scour near their foundations. If the depth of scour becomes big, the stability of the foundations jeopardizes, with a consequent danger to the structure of damage or failure. One of the important problems in weirs accumulated sediments and prevent their downstream current, resulting in erosion and scouring downstream of the weirs. It is established that the scope of scour depends on properties of flow, bed material texture, and shape of the structure. The erosion at downstream of the hydraulic structures is a big problem and was studied by many hydraulic designers to determine the variables governing this phenomenon and also to find the solutions for it. As a result of river damming by a weir and/or dam structure with a reservoir, the flow regime changes and the balance of sediment transport is distorted. As a consequence, an increased energy of water and the discontinuity of sediment transport cause local scour in loose soils below the weir structure. To reduce the risk of undermining the weir foundation, various of bed protection is used, which weaken the process of local scour and shift it to a safe distance from the foundation. One of them is single step broad crested weirs.

1.2 General

Broad-crested weirs and embankment weirs are standard engineered structures in irrigation systems, hydroelectric projects. The difference between these is generally the end-face slope, with the embankment weir has inclined end faces, and the normal broad-crested weir has vertical end faces. Some researchers have reviewed the achievement of a broad-crested weirs with various designs, all with the requirement that the weir crest is enough long to include parallel flow lines.

Broad-crested weirs can have a type of cross-sections in the control section, depending on the requirements. The simplest kind is the square-edged weir with a rectangular cross section. The edge refers to the inlet of the canal. Because weirs of such kind flow separation problems, the inlet cases have been improved by using of rounding with a radius proportional to the ultimate energy elevation to be arriving at the discharge value. Weirs with different forms have been considered hydraulic structures, which used in open channel flow. They are mostly used in water flow measurements and control of water surface profiles.

1.3 Broad Crested Weir

The streamline flows through a broad crested weir are parallel to the crest, critical depth happen along the crest, and the pressure distribution is hydrostatic (Chow, 1959).

The major aim of the traditional broad crested weir is to increase and control the inlet water head. Flow through a broad-crested weir depends on the weir's geometry. Simply discharge can be measured as follows:

$Q = CLH^n$ (1.1)

Where:

Q = Volumetric flow rate

C = Constant for the specific weir structure

L = Width of the weir

H = Height of water level inlet in relation to the weir's crest

n = structure different (usually 3/2 for a horizontal weir)

The formula above can also be used for sharp-crested weirs if the parameter constants are known

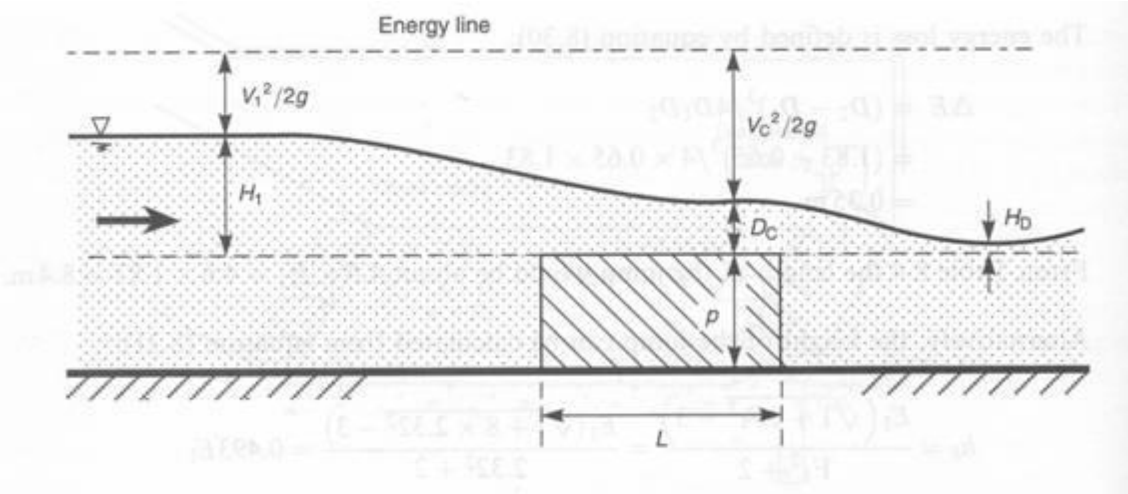

Figure 1.1 Schematic of the weir

To prevent erosion and scouring in downstream of weirs, the hydraulic energy should be dissipated. For this aim, several ways were used such as lining by rubbles and riprap, or by constructing steps at the downstream of weirs (Chanson, 2001).

1.4 Local Scour Downstream of Single Step Broad Crested Weirs with different ramps and hollow end sill

Scour control process considered as the main objective to ensure safety and economical design of hydraulic structures to prevent any serious failure in the future.

These new shapes gave the weir a new behavior by making it as an energy dissipator. The present study reduces costs in comparison with traditional weir and improves the hydraulic performance of the weir.

1.5 Thesis Objective

The main objectives of the thesis are as follows:

1. Experimental investigation of single broad crested weir shapes to mitigate and reduce the depth and volume of local scour at the downstream of the weir.
2. Reducing the depth and volume of local scour at the downstream of the weir, by using single step broad crested weir with different ramps.
3. minimize the depth and volume of local scour at the downstream of the weir, by using single step broad crested weir with different hollow end sill.
4. Choose the economic and safest model that produces minimum local scour as compared with a single step broad crested weir.

1.6 Thesis outline

To discuss the basics of the step broad crested weir problem the present thesis is composed of five chapters, Brief descriptions of each chapter are given as:

Chapter 1 Introduction:

Introducing a brief information of broad crested weir, also, explains the research objective and the layout of the thesis.

Chapter 2 Literature Review:

This chapter covered in previous work that deals with, the types of scour, Classification of broad crest weirs, weir coefficients of discharge, local scour around hydraulic structures, scouring downstream of weirs, methods to prevent scouring, development of maximum scour depth with time, flow regimes, numerical methods, numerical model simulations.

Chapter 3 Experimental Investigation:

This chapter gives a description of the laboratory models, and procedures.

Chapter 4 Results and Discussion:

This chapter gives results and discussions of results

Chapter 5 Conclusions and Recommendations:

Presents the major conclusions drawn from the results of this study and recommendations for future works.

CHAPTER 2

LITERATURE REVIEW

2.1 General

Weirs are among the most popular and simple hydraulic structures. Studies investigated symmetrical weirs, with inlet and outlet faces that were similar in slope. Hager and Schwalt (1994) presented behavior and design guidelines for a sharp cornered; vertical faced broad crested weir.

Schwalt (1994) were analyzed the flow lineaments experimentally through the broad-crested weir with vertical inlet wall and sharp-crested corner and suggested the discharge head correlation for submerged flow under a new approach.

Discharge computation is a necessary matter in hydraulic engineering. The weir is one of the flow scale apparatus for open canal. They are defined as structures where the flow lines parallel to each other through the weir and the crest of the weir is horizontal. Weirs are used as flow computation structures, for example, in hydropower structures, irrigation canals and experimental flumes (Haun et al., 2011). Contracted sharp crested weirs are also vertical barriers placed normal to the flow direction in which water shift through a contracted section over the weir plate (Aydın et al., 2011).

The broad crested weir is mostly flat horizontal blocks, but those have progressively raised inlet faces to pass better sediment and wreckages. The discharge efficiency has been the topic of much research.

Scour control process considered as the main objective to ensure safety and economical design of hydraulic structures to prevent any serious failure in the future.

2.2 Scour

2.2.1 Definition of Scour

The erosion of channel bed and bank due to water flow or bed erosion at the downstream of hydraulic structures is called scour (Ebrahim and Heydarnejad, 2014). Scouring in watercourses and drainage passage causes great damage to the environment and Hydraulic Structure therefore, scour must be taken into consideration while designing such structures. The convert of the flow caused by the existing structures and things submerged in moving frames of water. This change consists of local increases in velocity and of the starting of minor flows and turbulent wakes with eddies. The local scour eliminates material of the bottom around the frames and things and can put in danger their support, threatening their constancy and its security.

2.2.2 Classification of local scour

The critical velocity commonly used in determining to scour either clear-water or live-bed scour according to the ratio of average approach velocity to critical velocity (V_a/V_c).

Neill (1968) proposed that bedding material will convert in clear-water scour (Hamill, 1999) as the velocity of flow approach velocity (V_c):

$$\mathrm{V}c = 1.58[(S_s - 1)gD_{50}]^{1/2}(\frac{\mathrm{y}}{\mathrm{D}_{50}})^{1/6} \quad (2.1)$$

Where S_s is specific gravity or relative density of sediment (assumed to be 2650 kg/m^3 or $S_s = 2.65$), D_{50} is the Median particle size, and y is the depth of flow.

Assuming, as state above that Ss = 2.65, the threshold velocity becomes:

$$\mathrm{V}c = 6.3y^{1/6}\mathrm{D}_{50}{}^{1/3} \quad (2.2)$$

When flow intensity ($V_a/V_c < 1$) for uniform sediments clear-water scour cases are present, where V_a is the average approach velocity.

In the condition of live bed scour for uniform sediments, critical velocity is lower than the average approach velocity ($V_a/V_c>1$).

The initial eddies system in front of the weir is the major scour force, and it removes bed material from downstream of the weir. Since the average at which material is transferred far from the area is greater than the transportation average into it, a scour hole is created after the war. As the scour hole obtains deeper, the strength of the eddies at the downstream of the weir decreases and finally a case of equilibrium is arrived. For a clear-water situation that occurs when the shear stress from the eddies equals the critical stress for the sediment particles, and no more bed material is scoured. For a live-bed situation, equilibrium is arrived when the value of sediment inflow equals the value of outflow from the scour hole. In that situation, the scour depth vibrates, but the average depth remains constant.

2.3 Classification of Broad Crested Weirs

Based on the value of (h/L) the current over a broad crested weir with an upstream sharp corner is classified as follows (Subramanya, 1986):

1. (h/L) ≤ 0.1: In this range the critical flow control section plays at the downstream of the weir and the resistance of the weir surface as important role in determining the value of (Cd) (Fig 2.1a) this kind of weir , termed as long-crested weir, finds limited use as a reliable flow measuring device.

2. 0.1≤ (h/L) ≤ 0.35: The critical depth control occurs around the upstream end of the weir, and the discharge coefficient varies slowly with (h/L) in this range (Fig 2.1b) this kind can be called a true broad crested weir.

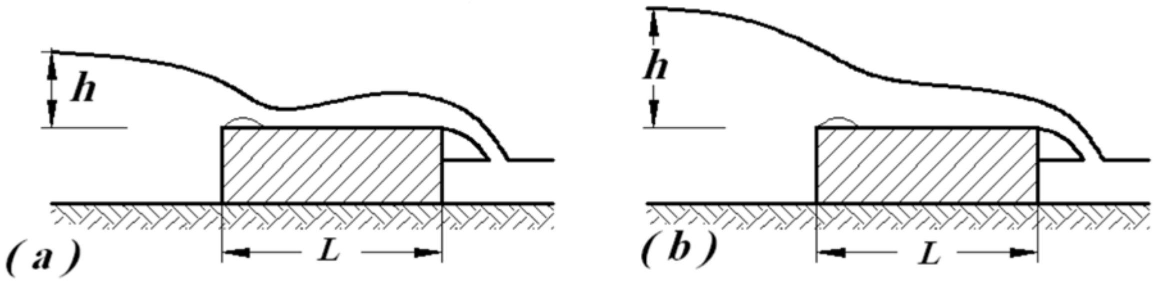

Figure 2.1 Flow types of broad crested weir (Subramanya, 1986)

3. 0.35 ≤ (h/L) ≤ about 1.5: The water surface profile will be curvilinear all over the weir. The control section will be at the upstream end (Fig 2.2c) the weirs of this kind can be termed as a narrow crested weir. The upper limit of this range depends upon the value of (h/P).

4. (h/L) > about 1.5: The flow separates at the upstream corner and jumps clear across the weir crest. The flow surface is highly curved (Fig 2.2d), and the weir can be classified as sharp crested.

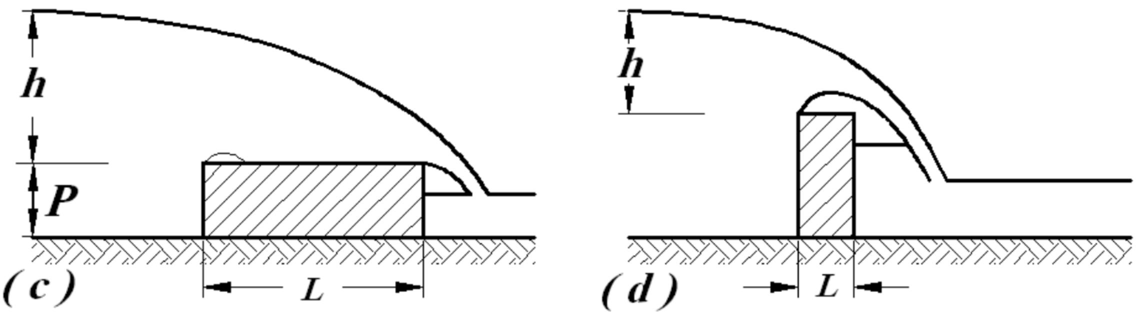

Figure 2.2 Flow types of broad crested weir (Subramanya, 1986)

2.4 Energy Dissipation

2.4.1 Energy Dissipation Ratio, ΔE%

A broad crested weir is a structure with a level crest above which the fluid pressure may be considered hydrostatic. If such a situation is to exist, then concerning (Fig 2.3) the following inequality must be satisfied. 0.08 <H/L< 0.5 (Bos, 1976).

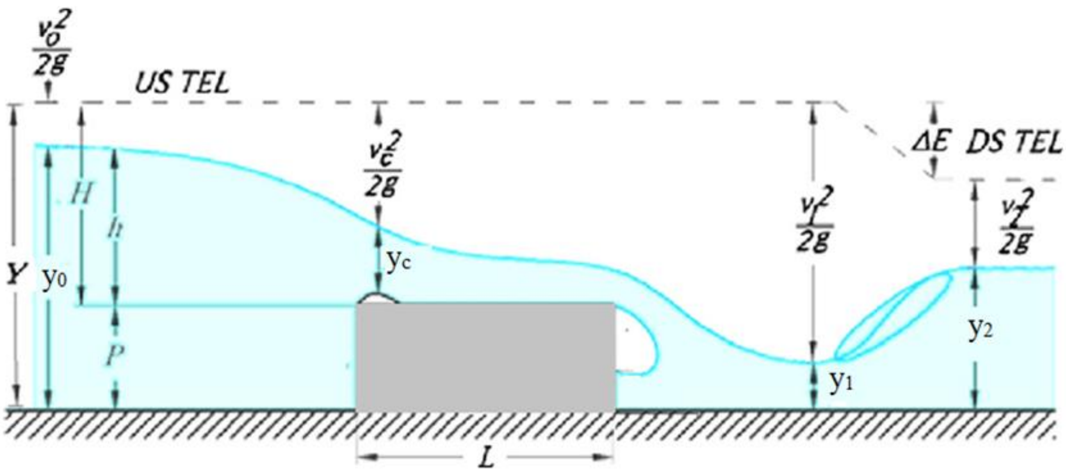

Figure 2.3 Broad crested weir (Bos, 1976)

If the upstream corner of the weir is sharp, then the flow will separate and then reattach enclosing a separation bubble. However, if the upstream corner is rounded this separation bubble will not exist.

Based on energy relations, the public relation for the flow energy dissipation can be verified.

Applying energy correlations between section (1) and section (2) in Figure above we obtained:

$$E_1 = P_1 + h_1 + \frac{V_1^{\ 2}}{2g} \tag{2.3}$$

$$E_2 = P_2 + h_2 + \frac{V_2^{\ 2}}{2g} \tag{2.4}$$

$$\Delta E = \frac{E_1 - E_2}{E_1} * 100 \tag{2.5}$$

Where:

P_1 : Height of weir in upstream (U/S) (cm).

P_2 : Height of weir in downstream (D/S) (cm).

h_1 : upstream (U/S) water head above the weir crest (cm).

h_2 : downstream (D/S) water head above the weir crest (cm).

V_1 : Velocity of flow in upstream (U/S) (cm).

V_2 : Velocity of flow in downstream (D/S) (cm).

E_1 : The energy of weir in upstream (U/S) (cm).

E_2 : The energy of weir in downstream (D/S) (cm).

ΔE : Energy Dissipation Ratio (%).

There are two main ways for the dissipation of energy in the flow, one is the viscous dissipation induced by the mean motion, and the other is the dissipation via the turbulent motion. By considering the energy equations of the flow, we can see that the turbulence dominates the loss of energy from the mean motion, and the work done by the Reynolds stresses is much bigger than the direct dissipation due to viscosity. Besides, for a flow at high Reynolds number, the turbulent shear stresses are much larger than the viscous shear stresses. That means the dissipation by work done against turbulent shear stresses also has a much bigger contribution to the energy loss in the flow.

The energy loss in the flow over a weir is due to incomplete conversion of kinetic energy into potential energy. Upstream of the weir, in the acceleration area, part of the potential energy of the flow is converted into its kinetic energy. While the water is flowing, it continuously loses energy against surface resistance, but this loss is negligibly small with regard to the loss in form resistance. The mechanism of form resistance here is: part of the kinetic energy of the flow is converted into energy of vortices of all scales, and turbulent fluctuations; then this supply of energy will eventually be dissipated as heat via the viscosity.

The following figure illustrates different zones in the flow over a weir according to (Hoffmans, 1992).

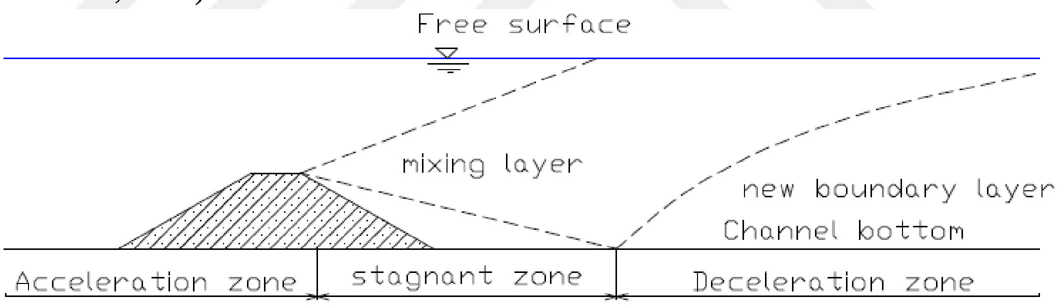

Figure 2.4 Definition of flow zones (Hoffmans, 1992)

As mentioned earlier, the energy loss of the flow over a weir, or form resistance, is much larger than the loss in surface resistance. In the existing theories, discharge relations are often used to express the energy loss. The discharge value can be used to calculate the water depth and speed of the flow. Knowing the water depth and velocity of the flow inlet and downstream of the weir, the decrease in energy height can be calculated. The discharge itself strongly depends on the downstream water level (depends on which flow regimes) and the weir geometry.

Chamani and Beirami (2002) introduced a style for estimating both subcritical and supercritical flow properties through drops and derived an empirical relationship to predict the relative energy loss.

Al-Talib (2007) investigated in an experimental study the stepped and non-stepped weirs to discover their activity in dissipating flow energy. She got that stepped weirs are more active than unstepped weirs and the ultimate energy dissipation ratio in stepped weirs was about 10% higher than unstepped weirs.

Ali Khani et al. (2010) studied the hydraulic jump in the stilling basin with vertical end sill. These stilling basins with continuous sills are much used as the energy dissipates end of hydraulic structures. All results of laboratory showed the important effect of the sill on the dissipation of energy. Also prove that an high in the maximum depth and a reduction in the sequent depth of the sill height is increased for a particular LB. Although smaller sill locations confirmed to have more effect on rising of y_3 and decreasing of y_2. However; sill positions larger than 167 cm from the beginning of the basin did not appear a big effect on y_2 and y_3. Where; h is the height of the sill, y_1 is upstream water depth, y_2 is the sequent depth of jump (or actually flow depth directly after sill for a forced jump), y_3 is an ultimate flow depth inlet of the sill. LB is the distance from the beginning of the stilling basin to the upstream face of the sill.

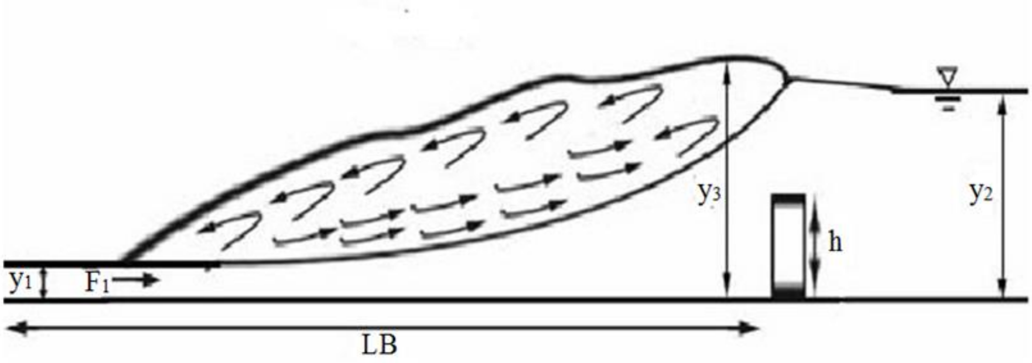

Figure 2.5 hydraulic jumps in the stilling basin with vertical end sill (Ali khani et al., 2010)

Hussein et al. (2010) they added a new performance to the traditional broad crested weir, by using it as an energy dissipater. To investigate the energy dissipation (ΔE%), the outlet height of the weir was minimized four times as 9.8, 8,6 and 3.8 cm. Thirty tests were carried out in a horizontal channel for a wide domain of discharge.

Laboratory results gave a high agreement between the calculated values of the suggested model. They obtained three empirical non-dimensional equations with high correlation coefficients. The laboratory results of the investigation proved that the energy dissipation ($\Delta E\%$) improved up to 46%. Further, discharge coefficient (C_d) was increased and obtained higher values in comparison with traditional weirs.

Hussein et al. (2011) improved the hydraulic efficiency of single step broad-crested weir. Through analyzing the factors that have an influence on the shape of the step and its effect on the flow properties, and energy dissipation ($\Delta E\%$) downstream (D/S) of the weir. The differential equation of progressively changing flow for the water surface profiles above the weir was solved analytically. Further, empirical relations for ($\Delta E\%$) and discharge coefficient (C_d) due to the affecting parameters were derived. The results proved that the ratio of the length of downstream step to the length of the weir equals to 0.5 gives a higher energy dissipation ($\Delta E\%$) in comparison with other weir models. The comparison between predicted values by the differential equation of progressively changing flow and experimental values gives a good agreement; the ultimate difference is about 7%. Two empirical relations were getting, the first to calculate discharge coefficient (C_d) regarding the ratio of inlet water head above the weir crest to upstream weir height and length of downstream step to the length of the weir. While the second equation to calculate energy dissipation ($\Delta E\%$) regarding the ratio of downstream water level to the upstream weir height, length of downstream steps to the length of the weir and the Froude number with a high correlation coefficient.

Elyass (2012) studied experimentally the influence of channel bed slope on energy dissipation of flow for single step broad crested weir under free flow cases. He tested five models of weirs. The laboratory results proved that water surface shapes were smooth and continuous and had a descending direction from the point of computation taking the shape of the weir with a decline drop near the outlet face of the weir. It was noted that for the same ratio of upstream weir height to downstream weir height the channel slope influence was inversely proportional on the energy dissipation. Also, the influence of effective upstream head above the crest of upstream weir height did not show when ratio of upstream weir height to downstream weir height, but in the other weirs appeared. He obtained four empirical non-dimensional equations to calculate the energy dissipation ratio regarding other parameters with a high correlation coefficient.

2.4.2 Energy Balance and Momentum Balance

The main mechanisms domination of the flow through a weir are gravity and inertia; other effects like viscosity and surface tension are of secondary importance. As mentioned earlier, for a steady flow, the Bernoulli equation, which is an energy equation, can always be applied taking into account certain portion of energy losses. Providing a proper allowance for all forces acting, the momentum equation always holds true as well.

Generally speaking, in the analysis of flow, the energy and momentum equations play a complementary role for each other. Usually, the information which is not supplied by one equation is provided by another. Together with the continuity equation, they provided the analytical means to assess the energy loss in the flow over a weir (Tuyen, 2006).

2.4.3 Turbulence and Energy Loss

Turbulent is one of the most prominent properties of the flow because most of the flows encountered in nature and technical installations are turbulent flows. It is the manner of flow in which different flow formulas show a random difference with time and space. The two most important types of turbulence are free turbulence and wall turbulence. Turbulence is capable of transfer energy of the flow from the mean motion to the turbulent fluctuations. Those fluctuations will then induce turbulent shear stresses, and energy will eventually be dissipated as heat via the viscosity (Uijttewaal, 2007).

2.5 Weir Coefficients of Discharge

In the last years, different researchers investigate the properties of flow through a broad- crested weirs. Rao and Rao (1973); Ackers (1978) verified an empirical equation for the discharge coefficient (C_d), with the gradient inlet face of the weir. Clemens (1984) produced a simplified design procedure taking a wide scope of parameters.

Ramamurthy et al. (1988) investigated the properties of a square and round edge (R) for broad crested weirs under free and submerged flow cases. They got a mathematical equation from momentum expressions for the coefficient of discharge (C_d). Further, they sight that the flow separation is basically discarded and the coefficient of discharge (C_d) has achieved the biggest value when the proportion of the radius of the inlet corner (R) to the height of the weir (P) is ($0.25 \leq R/P \leq 1$).

Fritzi and Hager (1998) calculated the discharge coefficient with respect to relative crest length for long broad-crested, broad-crested, short-crested, and thin-crested weirs with a side slope 1V:2H. They show that the sloping embankment has a bigger discharge capacity compared to a traditionally broad crested weir with vertical faces.

Farhoudi and Alami (2005) carried out tests to study the influence of the inlet gradient of rectangular broad crested weirs on discharge capacity. They indicated that the weir discharge capacity is arriving its maximum at an angle of 25°.

Gogus et al. (2006) studied experimentally the influences of the width of the down weir crest and a step height of broad-crested weirs of rectangular compound cross section on the amounts of the discharge coefficient, the average velocity factor, and the modular limit. They introduced wide data outlining the behavior of broad-crested weirs with compound cross section and various step heights.

Chinnarasri et al. (2008) estimated the Coefficients of Discharge (C_d) over a large broad-crested weir; two experimental equations were offered depending on the shape of the weir.

Noori and Juma (2009) improve the behavior of broad crested weirs. The behavior of broad crested weir was improved by using an inlet face gradient, rounding the upstream corner and capping the upstream corner with a semi-cylinder to minimize the influence of flow separation. All experiments increased the discharge capacity and improved the behavior of the weir. They show that the value of the upstream face slope of 0.5H: 1V are quite enough to give high amounts of discharge coefficient. Two experimental relations were got to predict the amount of the discharge coefficient with respect to active elevation to crest length ratio, inlet corner radius to crest length ratio and radius of the cap to crest length ratio with high correlation coefficients.

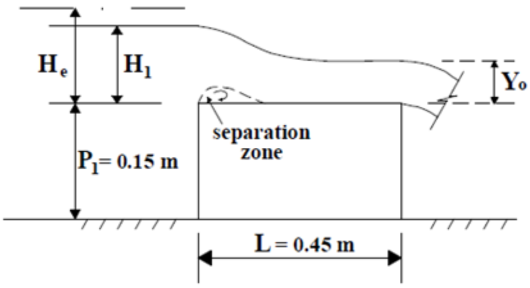

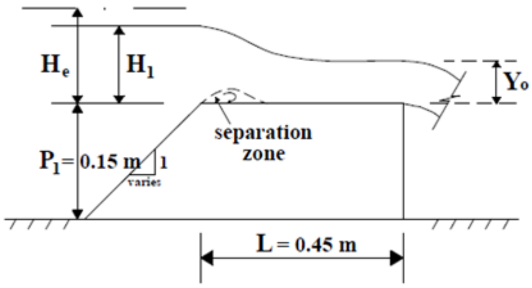

a) Flow through square edge weir with vertical upstream face

b) Flow over inclined upstream face weir

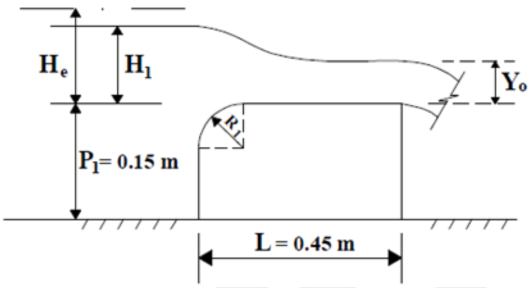

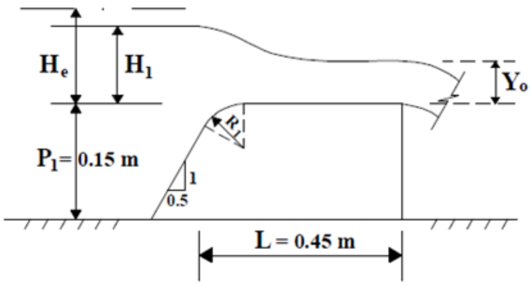

c) Flow through round edge weir with vertical upstream face

d) Flow over the rounded edge inclined upstream face weir

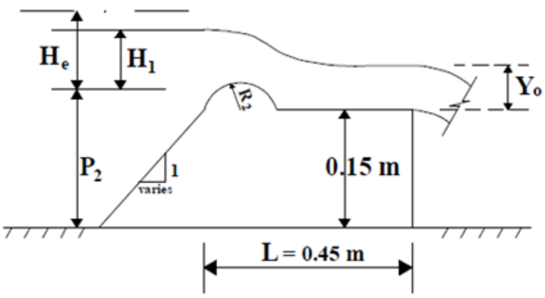

e) Flow over capped edge weir with inclined upstream face

Figure 2.7 Definition sketches showing different cases tested (Noori and Juma, 2009)

Azimi and Rajaratnam (2009) analyzed discharge properties for vertical face weirs with a square edge, or rounded inlet is wide.

The investigate of Sargison and Percy (2009) related to the flow through a trapezoidal broad-crested weir with changing inlet and outlet gradients were analyzed. Data are offered comparing the influence of gradients of 2H: 1V, 1H: 1V and vertical in different combinations of the inlet and outlet faces of the weir.

Increasing the inlet gradient to the vertical decreased the length of the surface profile and, hence, the static pressure of the crest. It also reduced the discharge coefficient.

Goodarzi et al. (2012) studied the hydraulic properties of flow through sloped-face broad-crested weirs. A new relation factor to predict the discharge coefficient for sloped-face broad-crested weirs were given.

The investigate of Parilkova et al. (2012) related to the effect of surface roughness on the difference of the discharge coefficient for broad-crested weirs. Because of this investigate, a style for finding of the head-discharge relationship for broad-crested weirs with a rough crest surface is suggested.

Salmasi et al. (2012) offered data that will be of use in the design of hydraulic frames for flow control and computation. A measurements were carried out to research the influences of the length of the minimal weir crest and a step length of broad-crested weirs with a rectangular complex cross section on the amount of the discharge coefficient (C_d) and the average velocity factor. Results show that a cut out happen to head-discharge ratings.

Azimi et al. (2013) They studied the influence of inlet and outlet ramps by providing the inlet and the outlet length scales, respectively. They found that for tall-crested weirs, a rising gradient increases the discharge coefficient compared to the state of the level crest, while for the broad-crested weir, the gradient does not influence the discharge coefficient (C_d). A falling gradient of the crest causes an increase in the discharge coefficient (C_d) for both broad-crested and narrow-crested weirs. The discharge coefficient (C_d) of embankment weirs is greater than the discharge coefficient (C_d) amounts of weirs without the inlet and outlet ramps as illustrated in Figure 2.6.

Where:

(a) Flow through broad-crested weir with positive or negative crest gradient.
(b) Flow through broad-crested weir with inlet and/or outlet ramps.
(c) Flow through triangular (hump) weir with inlet and/or outlet ramps.

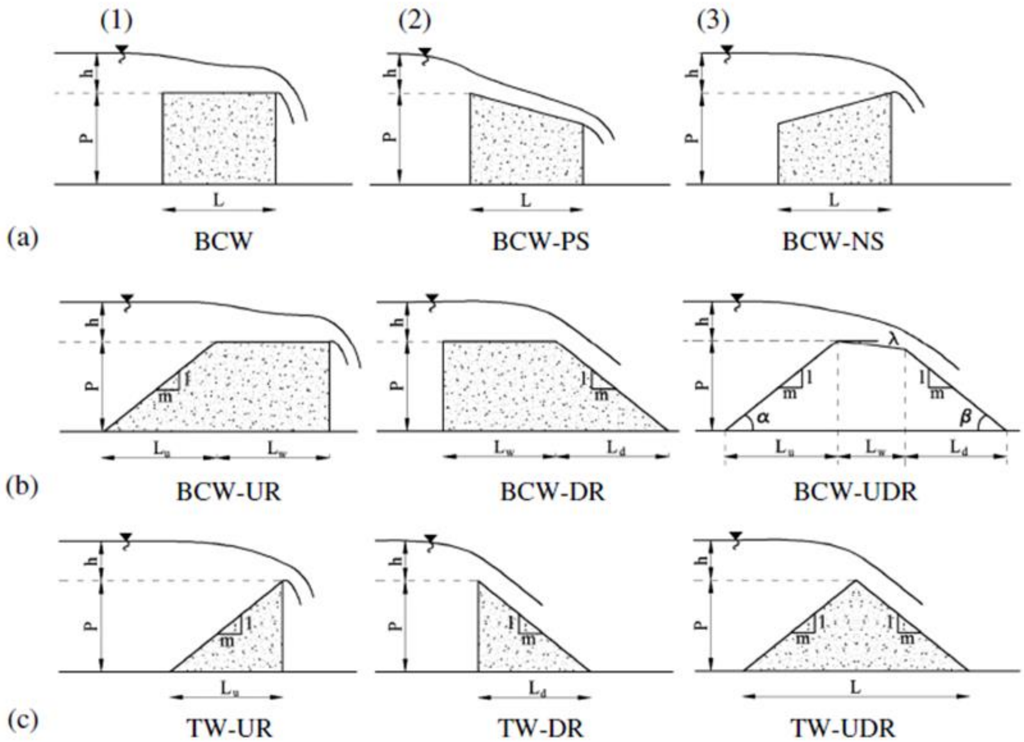

Figure 2.6 Definition sketch of flow over rectangular, trapezoidal (embankment), and triangular (hump) weirs with several configurations of U/S and/or D/S ramps (Azimi et al., 2013)

Jalil et al. (2014) studied the influence of the surface roughness on the discharge coefficient for broad-crested weirs. Lobrotary results of this study show that the behavior of the broad-crested weirs improves with decreasing the relative roughness height and with increasing the relative total head.

In the study of Madadi et al. (2014) the influence of the inlet face gradient of a trapezoidal broad-crested weir on discharge coefficient and water surface profile was studied using the experimental models.

The results proved that decreasing the inlet face gradient prevents the progression of separation zone. Reducing the inlet face gradient to 21^0, increased the discharge coefficient up to 10% and decreased the separation relative length and height up to 80% and 95% respectively.

In Zachoval et al. (2014) investigate, computation of the discharge coefficient for rectangular sharp-edged broad-crested weir was empirically analyzed. The influence of friction and surface tension on the difference of discharge coefficient was taken into account.

Badr and Mowla (2015) carried out an empirical study of the influence of the inclined inlet side of broad-crested weirs on the discharge coefficient and flow properties. They showed that reducing the gradient of the inlet side cause increasing the discharge activity and the discharge efficiency of the weir.

Aksoy and Dogan (2016) studied experimentally the influence of the approach angle on the discharge capacity of the broad crested weir. Four variant approach angles were examined under steady case cases by using three variant discharge amounts.

2.6 Local scour around hydraulic structures

The problem of the scour end of the hydraulic control structure is of great importance because it can affect the stability of the structure.

Grade control structures are considered to be one of the most important ways to prevent failure in channels. Many laboratory investigations on the scour depths under different flow cases and structure configurations are available. Mason and Arumugam (1985) observed that there are many formulae which have been developed for predicting scour under a dropping. A list of these formulae is reported by Whittaker and Schleiss (1983) and Mason and Arumugam (1985). Experimental results obtained all these formulae. The scour end of a grade-control structure was studied by Bormann and Julien (1991). The authors define an equilibrium scour formula founded on the concept of the jet diffusion and particle stability in the scour hole of grade-control structure and tested it comparing the results of large-scale experiments.

Scour is a natural happening caused by the erosion effect of the flowing current on alluvial beds. Scour happens normally, as a part of the morphological changes of rivers and as a result of human-made structures (Hoffmans and Pilarczyk, 1995).

Mossa (1998) found that the higher the tailwater depth, the lower the amount of the ultimate scour depth. The experimental results show that scour outlet of the grade-control structure depends on the face angle of the structure, that is the impingement angle of the jet. The study deal with the scour downstream of the grade-control structure providing different case studies of such phenomena for several configurations of wall jets. To investigate the scouring process features, several experimental tests were carried out with two different configurations of the grade-control structure. The experimental data were compared with those calculated using some literature formulae, which generally are not dimensionally homogeneous. A dimensional analysis of the scour phenomena was proposed, and the experimental results of the study were compared with the proposed formula.

Noori and Al- Hafith (2007) conducted a laboratory study to investigate the scour downstream gabions protecting rock fill weirs. The study contains the values of the ultimate scour depth and length of a scour hole end the weir. The shape of scour hole was also investigated. Two empirical relations were obtained; one for the predicting of relative scour depth and the other for the predicting of the relative length of scour hole.

Emiroglu and Tuna (2011), carried out a laboratory study of the influence of tail water depth of local scour end of stepped chutes. The results show that ultimate depth and area of scour are strongly dependent on tailwater depth. Also, the ultimate scour depth increases with increases in the discharge and the tailwater depth.

2.7 Scouring downstream of weirs

Flow and sediment characteristics determine the scour process. The sediment transport is mainly dependent on the bed shear-stress and the turbulent case near the bed on the one hand and the density of the bed material, the sediment size distribution and the porosity of the (non-cohesive) material on the other hand.

The scour outlet of a grade-control structure was studied by Bormann and Julien (1991). The authors defined an equilibrium scour formula founded on the concept of the jet diffusion and particle stability in the scour hole of grade-control structure and tested it comparing the results of large-scale experiments.

Dehghani and Bashiri (2009) studied the scouring downstream of combined flow through the weir and under the gate. The results show that the conceptual model of flow field downstream of combined flow through the weir and under the gate indicates that there are interactions between the flows over the weir and under the gate and the scour hole cuts and fills alternatively. The comparison of the results shows that the main part of scour in combined flow is due to flow over the weirs.

Hussein et al. (2009) were performed an experimental comparison study between two weir models. First of the models was a traditional broad-crested weir while the other was a single step broad-crested weir. Experimental results indicated that local scour downstream (D/S) of single step broad-crested weir decreased five times in comparison with a traditional weir. Scour depth decreased from 9.2 cm to 2.6 cm with the increase of sand size from 0.48 mm to 1.3 mm. The relative depth of scour increases with respect to the relative time to scour. On the other hand, an empirical relation was obtained to estimate the ratio of scour depth to upstream (U/S) water head with respect to the ratio of downstream (D/S) water height to upstream (U/S) water head, densimetric particle Froude number, the ratio of median size of sand to upstream (U/S) water head and geometric standard deviation of sand sizes with high correlation coefficients.

Sobeih et al. (2012) investigated the effect of using openings in weirs at scour hole depth end of this structure. The investigation was dependent on a laboratory program included 171 experiments. Three states of opening arrangements were contained, no opening, one opening and three openings. Finally, an empirical equation was developed for predicting scour hole depth with respect to end flow conditions.

Fahmy (2013) studied experimentally to estimate the scour geometry outlet of the weir and to reduce the scour using a row of semi-circular baffle blocks. All experiments were tested considering different heights and locations of baffle blocks with various flow cases. The results show that the time required for settling the operation of scour was 6 hours.

The installation of baffle blocks was a significant influence on the scour hole, which is smaller than the case with no baffles, for the baffled floor tests, the slope angles increase, but the downstream slopes are steeper than the upstream slopes.

2.8 Methods to prevent scouring

Scour control process considered as the main objective to ensure the safety of hydraulic structures to prevent any serious failure in the future.

In the early nineties a morphological model for the development of scour holes back hydraulic structures was modified (Hoffmans, 1992), founded on the 2-D Navier-Stokes and convection-diffusion relations.

The length of the bed protection depends on the permissible value of scour (ultimate scour depth and the inlet scour gradient) and Geotechnical structure of the soil involved (Van Rijn, 1985).

Hoffmans and Pilarczyk (1995) showed that due to shear failures or flow slides or small-scale shear failures at the end of the bed protection, the scour process could gradually deterioration the bed protection, leading finally to the failure of the hydraulic structure.

The flow type end of hydraulic structures and in the scour hole is shown in Figure 2.9 in which the separated shear layer shows to be much same to plane mixing layer. The axis of the mixing layer are formed at the very start of the flow as a little curved due to the effect on the bed.

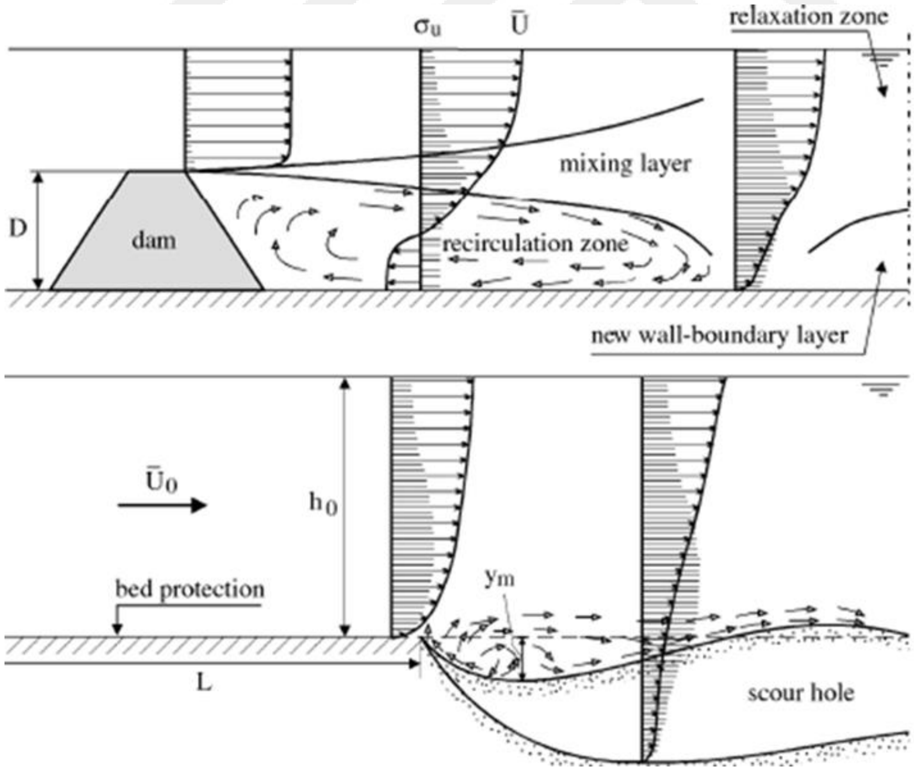

Figure 2.9 Schematized flow pattern below a dam (Hoffmans and Pilarczyk, 1995)

The scour process can be divided into various time levels. At the first, the development of scour is very quick, and finally, an equilibrium situation will be achieved. During closing operations of dams in rivers (Figure 2.8), which take place within a limited time, equilibrium will not be achieved.

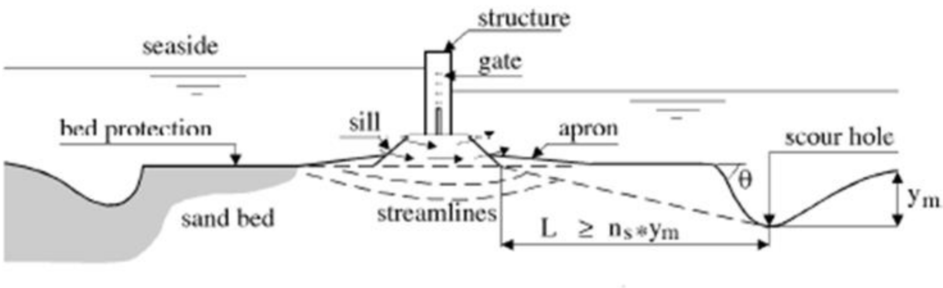

Figure 2.8 Schematization of a storm surge barrier (Hoffmans and Pilarczyk, 1995)

Eddies with a vertical axis happen when the flow pattern is affected by the support and/or vertical end walls. Then the bed material is picked up by the rotating ascending stream in the eddy and is shooting out aslant (Hoffmans and Pilarczyk, 1995).

2.9 Development of scour depth with time

To give some prudence into the scour process back hydraulic structures, the flow type and the sediment convey along the upstream slope of the scour hole are described in several phases in the scour process. Founded on tests with scale model with small Froude numbers (Breusers, 1966 and Dietz, 1969), Zanke (1978) described four phases in the development of a scour hole (Figure 2.10).

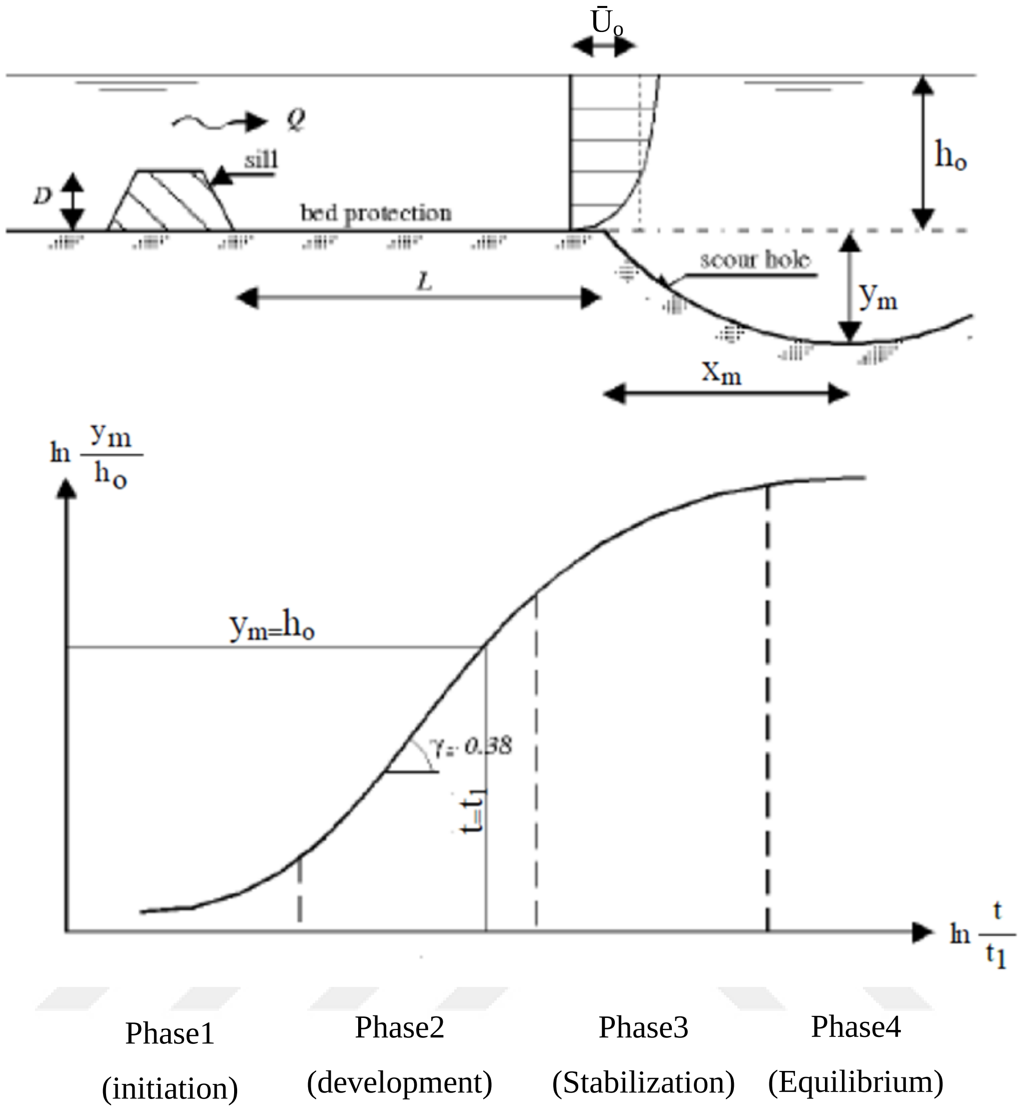

Figure 2.10 Development of the scour process(Breusers, 1966 ; Dietz, 1969; Zanke, 1978)

2.9.1 Initial phase

The flow in the scour hole is almost uniformly in the longitudinal direction. This phase of the scour process can be described as the phase in which the scour capacity is most sharp. tests with fine sediments by (Breusers, 1966) indicated that at the starting of the scour hole evolution a certain value of bed material near the inlet scour gradient goes into suspension.

2.9.2 Development phase

During the development phase, the scour depth increases frequently, but the shape of the scour hole still similar.

Computations by Hoffmans (1990) indicate that the upper part of the inlet scour gradient is in equilibrium, whereas the bottom is remains developing.

2.9.3 Stabilization phase

The rate of development of the ultimate scour depth reduces. The scour capacity in the deepest part of the scour hole is tiny compared to the scour capacity outlet of the point of reattachment.

2.9.4 Equilibrium phase

The dimensions of the scour hole do no longer change much. Generally, in this phase of the scour process the bed particles at the upstream scour gradient are only rolling and sliding beneath a saltation height.

Rouse (1950) emphasized that the scour has been proportional to the geometrical progression of time such as final equilibrium depth could not be expected. However, as shown by Mason and Arumugarn (1985) that the concept of a maximum scour depth can be accepted for all practical purposes and thus, expressions can be developed for it ignoring time as a parameter.

Mossa (1998) traced the scour hole profiles at different time intervals starting at the beginning of each experiment on the right wall to study their timely development and the geometrical change under the effect of the applied jet. Experiences show an increase of the scour depth value with time until it reaches the maximum value of the equilibrium condition. He also shows an increase in the length of the deposit with a slight change in the location of the maximum scour with time advance. All cases the experiments showed that the scour rate is higher at the beginning of the runs and it slows down until reaching the equilibrium scour depth and increase in the maximum scour depth with a shift in the location of maximum scour when the discharge increases and the tailwater decreases. He also shows that generally, the equilibrium time increases for higher discharge values.

2.10 Flow regimes

The classification of flow regimes is really necessary and helpful in the experimental process. An early classification by Escande (1939) divides the flow into four types.

Although his classification refers to the circular crested weir, it can be equally applied to all other overflow structures. Recently a study by Fritz and Hager (1998) has strengthened this classification by extending it with a trapezoidal weir with the downstream slope of 1V:2H.

Depending on the downstream water depth, the flow regimes can be divided into four main types (Escande, 1939) as shown in Figure 2.11 In the order of raising downstream water depth, they are:

A. Hydraulic jump: with a clear bore (roller) located at or downstream of the weir structure. In this case, the flow is not influenced by the downstream water depth.
B. Plunging flow: with the mainstream following the downstream slope of the weir and with a clear surface roller. The flow is almost independent of the downstream water depth.
C. Surface wave flows: with the mainstream following the free and wavy surface and a recirculation zone near the bottom.
D. The surface jet flows: the flow depth is larger; the surface is nearly horizontal and smooth. The flow strongly depends on the downstream water depth.

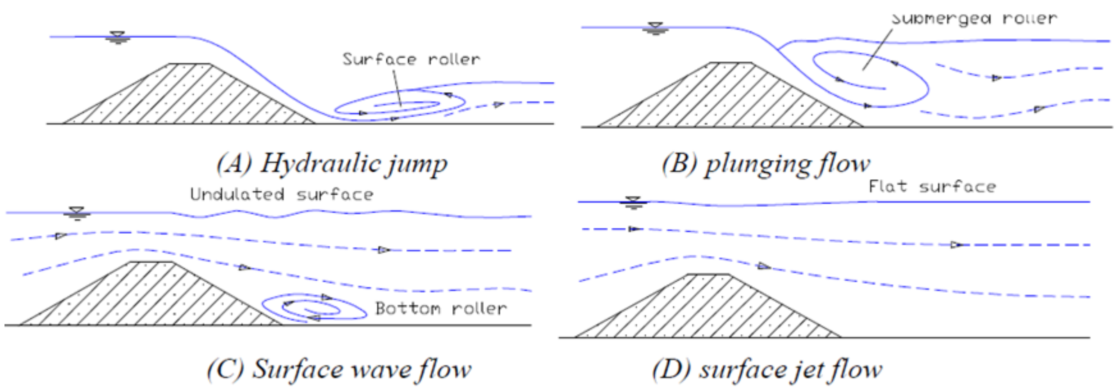

Figure 2.11 Four main types of flow (Escande, 1939)

For the sake of simplicity, the flow is divided into three regimes. According to Kolkman (1989), they are:

1. Free flow: the flow is entirely independent of the downstream water depth. A roller can be observed. (A combination of types A and B).
2. Submerged flow: the downstream water depth influences the flow. The flow surface is nearly horizontal. (Type D).

3. Transition regime: analogous to type C. It is also called the Undulated flow. The transition flow regime also has the clearest backward movement behind the weir, the so-called recirculation, in comparison with the two other flow regimes. In other words, the size of the recirculation zone in the case of transition state flow has the biggest size.

2.11 Numerical Methods

Several numerical studies were achieved to find the flow properties behind weirs by Computational Fluid Dynamics (CFD).

Hirt and Nichols (1981) used Volume of Fluid (VOF) method to describe the water surface profile in each cell, which is used in many hydraulic problems because it represents the sharp interface between the air and water phases.

The Re-Normalized Group Theory (RNG), k-ε turbulence model of (Yakhot and Orsag, 1986), was used with standard wall functions. This is one of a range of turbulence models classed as Reynolds-Averaged Navier-Stokes (RANS) models as defined by (Ferziger and Peric, 1997).

Fluctuating velocity describes turbulent flows. These fluctuations are also computationally expensive to simulate directly in practical engineering calculations. (Lien and Leschziner, 1994).

The governing equations of FLUENT software for unsteady incompressible 2D flows through weirs are continuity. Navier-Stokes relations are based on basics of physics mass conservation and Newton’s Second Law (Liu et al., 2002).

Empirical data for the contracted weir got from the studies of Şisman (2009) and Aydın et al. (2011) were used in the verification of numerical simulations.

Earlier work involving flow modeling through a rectangular broad crested weir has been conducted by (Sarker and Rhodes, 2004) who studied a weir empirically as well as numerically.

The results of (Sarkar and Rhodes, 2004) indicated that the comparison of the position of the free surface profiles through a experimenter rectangular broad crested weir with the numerical CFD model.

Hargreaves et al. (2007) used the volume of a liquid method to calculate the discharge also through a vertical faced broad crested weir.

Gonzalez and Chanson (2007) studied the pressure and velocity computation numerically on the broad crested weir, where the fast redistributions of both velocity and pressure fields at the upstream behind of the weir crest were estimated.

Hargreaves et al. (2007) described the effectiveness of CFD for free surface flows through a broad crested weir by using a published laboratory data set of (Hager and Schwalt, 1994) and discussed the accuracy of CFD to estimate the free surface profile.

The study of (Yazdi et al., 2010) simulated a spur dike with three-dimensional, and Reynolds-averaged Navier-Stokes equations with the volume of fluid and standard $k - \varepsilon$ method has been utilized to predict the free surface of the flow through the wires.

Afshar and Hoseini (2013) described the free surface profile of water on a broad crested weir by using (VOF). The results indicated that the good agreement with laboratory results.

Hoseini and Afshar (2014) used experimental study with CFD model that was achieved on broad crested weir located on a rectangular channel to estimate the Cd amount, and it gave good agreements between the two values got.

Al-Hashimi et al. (2015) studied the influence of inclination from 90˚ to 23˚ weir in the inlet face of rectangular broad crested weirs and flow properties by using CFD and experimental model that were applied to develop the behavior of broad crested weirs to minimize the influence of flow separation. Also, the discharge efficiency was increased 22% higher than the standard weir (90˚) with a slope of 23.

2.12 Numerical Model Simulations

Al-Hashimi et al. (2016) were used FLUENT software as a numerical model which represent a type of Computational Fluid Dynamics model to simulate flow through the weirs. A new behavior was added to this weir, by using a step at the end of the weir. The maximum value 28.78 of E% was got in single step broad crested weir in the laboratory result and 27.35 in the numerical result at S = 0.004.

Fatah, A. K. (2017) Was used Flow-3D to simulate the numerical model which is based on an experimental data in the present thesis. The bed-load transport model in Flow-3D can simulate the scour hole development. Four models of an inclined single Step Broad Crested Weirs [A, B, C, D] with different downstream reverse angles (0^0, 4.5^0, 8.7^0,13^0) respectively was tested under the same flow intensity (25 l/s) and the same duration of 6 hours. There was a good agreement between experimental and Flow-3D results. The values of flow depth simulated for the central axis of the channel in the longitudinal direction has been shown. Notably, the exact values of flow depth can be extracted from an Analyze section of Flow3D model. Based on the results extracted from the diagram of water surface profile on weirs' crest, it can be predicted that there is a clear influence of the change in downstream gradient of the water surface profile which results in the change of the hydraulic parameters of the system in addition, leads to changes in the rate of the scouring.

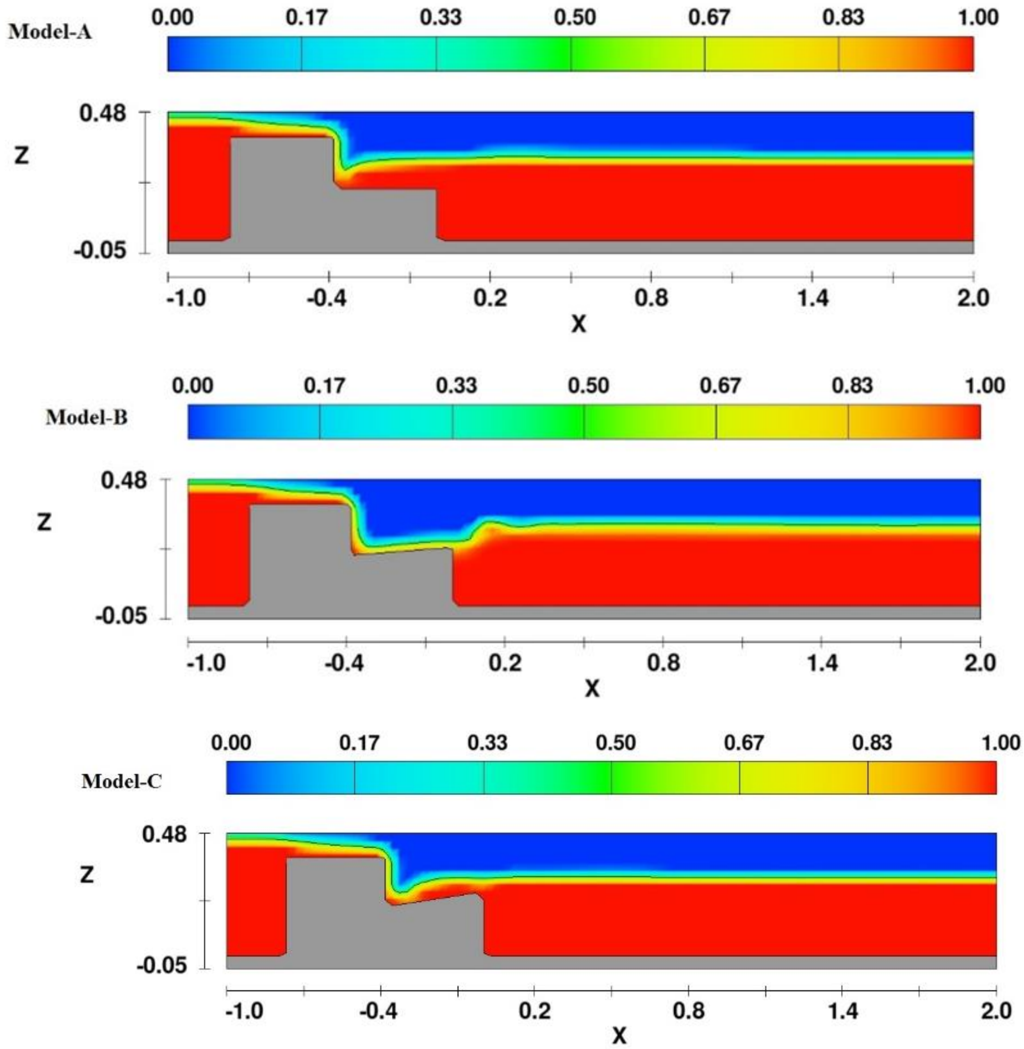

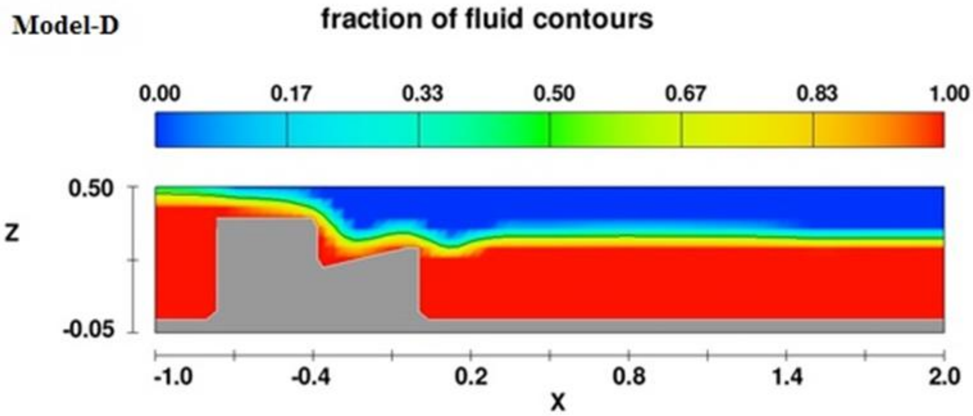

Figure 2.12 Comparison of longitudinal water surface and distances from the weir for each model and discharge (25 l/s) (Fatah, 2017)

Figure 2.12 shows there is a good agreement between the Flow-3D and experimental results in the present thesis.

Figure 2.13 presents the calculated scour profiles for all models. Good agreement is observed between the measured values from present thesis and the calculated values from Flow-3D. The maximum scour hole depth is only slightly underestimated.

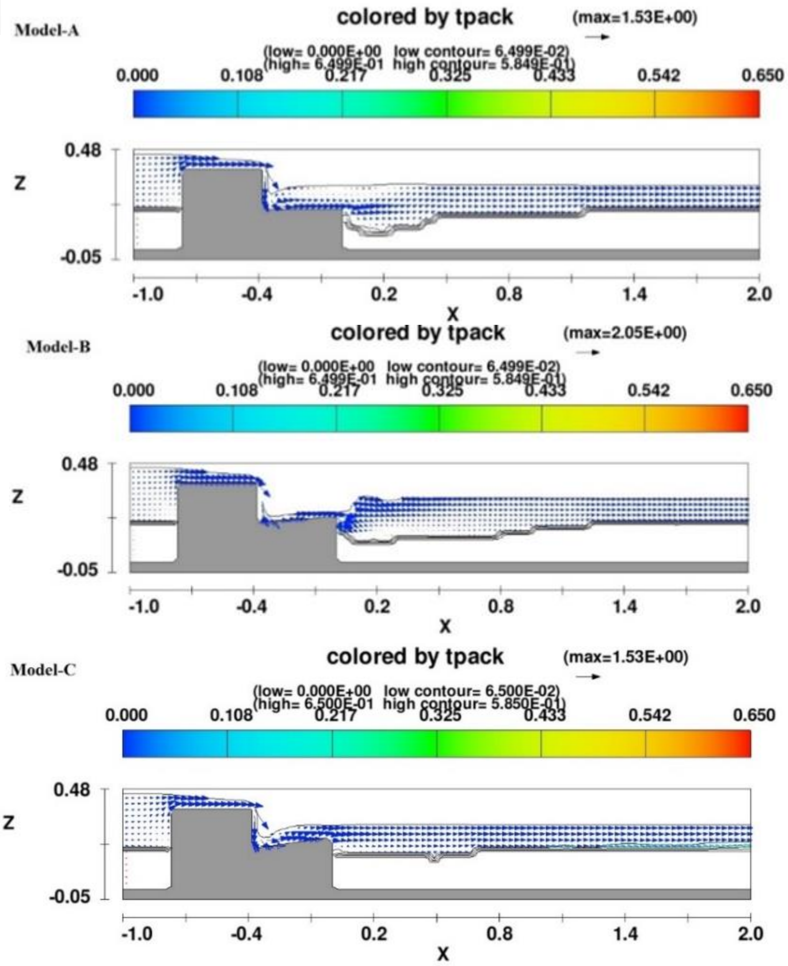

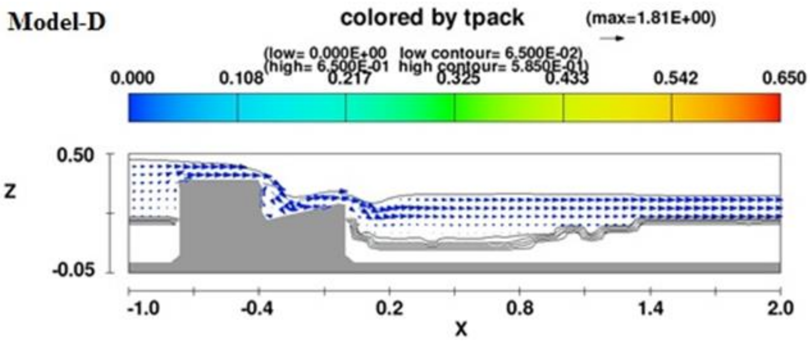

Figure 2.13 Calculated Results of longitudinal scour holes and distances from the weir for each model (Q=25 l/s) (Fatah, 2017)

As shown in Figure 2.13 the maximum scour depth was initiated after the weir model D for the reason that the drop of water adjacent from the toe of the weir. This case increases the danger of failure of the weir, while model C reduces the scour depth and producing least scour in the front the weir and pushes the drop of water away from the weir.

It is Obvious from Figure 2.14 that the maximum velocity was found on the sloped bed and then decreased immediately after the weir structure due to the energy dissipation on the sloped bed, as model C D/S slopes caused energy dissipation more than other models which resulted in the high scour reduction.

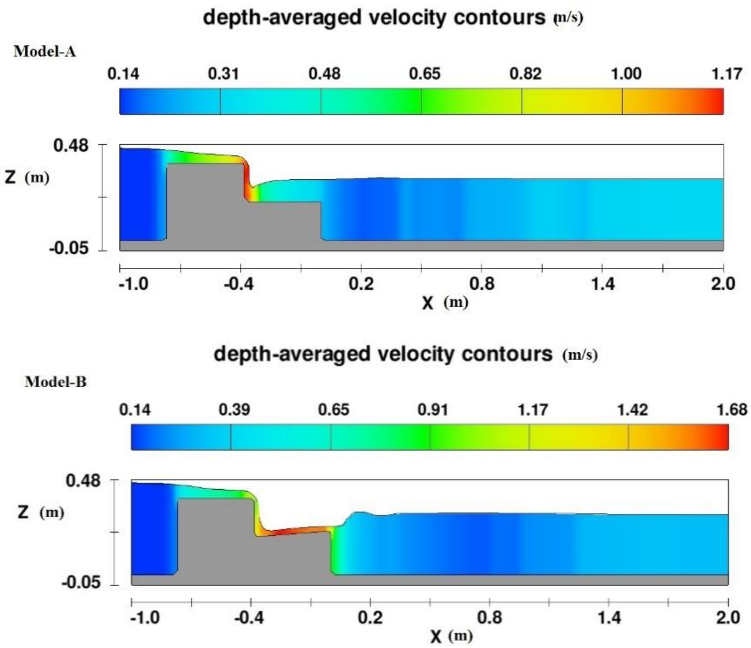

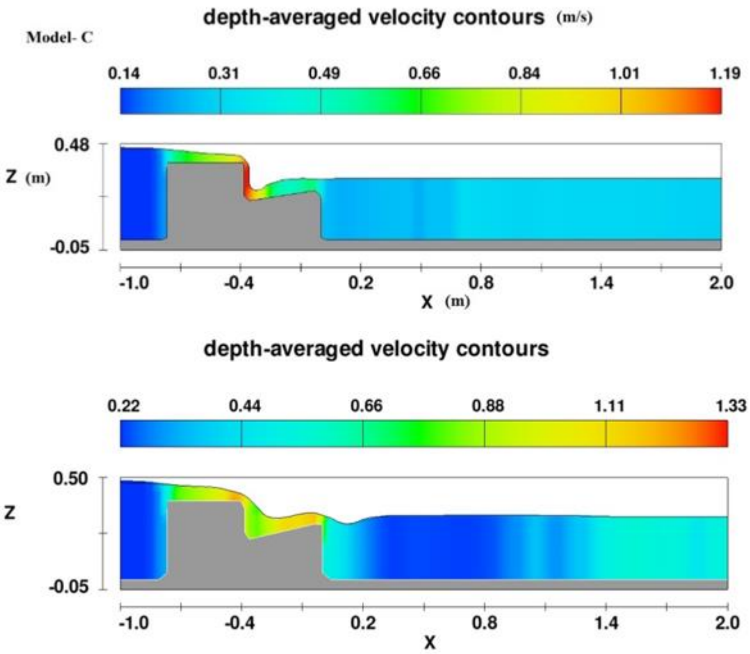

Figure 2.14 Depth Average velocities at the central axis (Q=25 l/s) (Fatah, 2017)

Figure 2.15 shows the contour related to the scour process for different models. The area of scour for model A, B and D has more erosion rate of sediment and covers a larger area than that of model C shown in Figure 2.15, which is reasonable qualitatively which indicates that model C is the best among the others in the reduction of scour process.

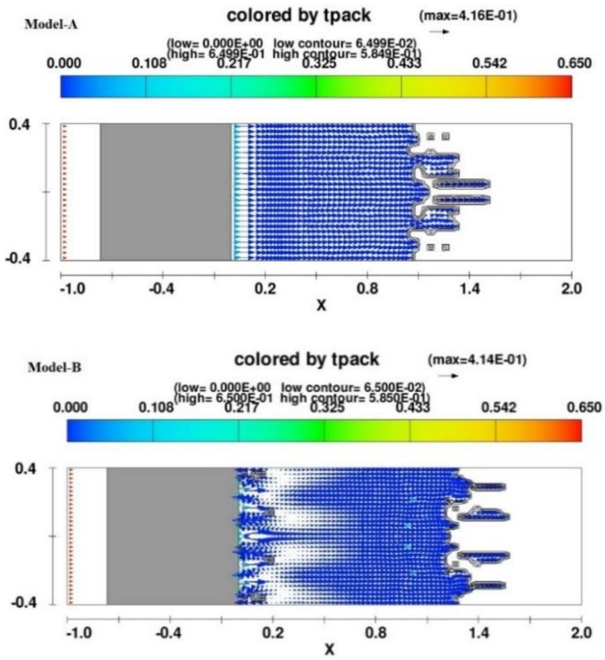

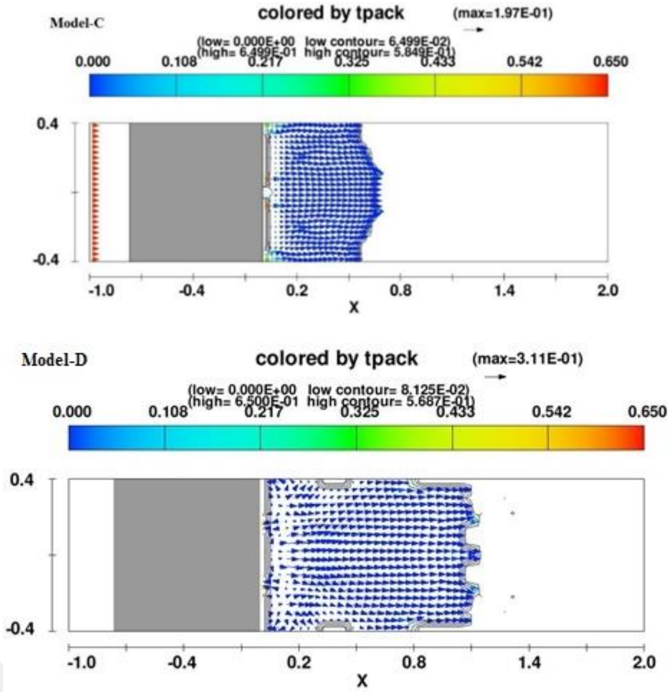

Figure 2.15 the scour pattern in front of models (A) (B) (C) and (D) (Q=25 l/s) (Fatah, 2017)

Figure 2.16 illustrates the distribution of turbulent energy in the pressure flow condition. The high energy of turbulence is located in the region of maximum scour downstream of weirs crest, which explains that the increased turbulent energy downstream of the weirs crest results from the pressure flow. Correspondingly, the maximum turbulent energy at the same times is distributed in the maximum hole region immediately after downstream of the weirs crest of model D, While the minimum turbulent energy at the same times is distributed in the maximum hole region immediately after downstream of the weirs crest of model C. Hence, it shows that model C can be taken into consideration in the design stage of such structures for the purpose of scour reduction to avoiding the damage to the structure, such as weirs.

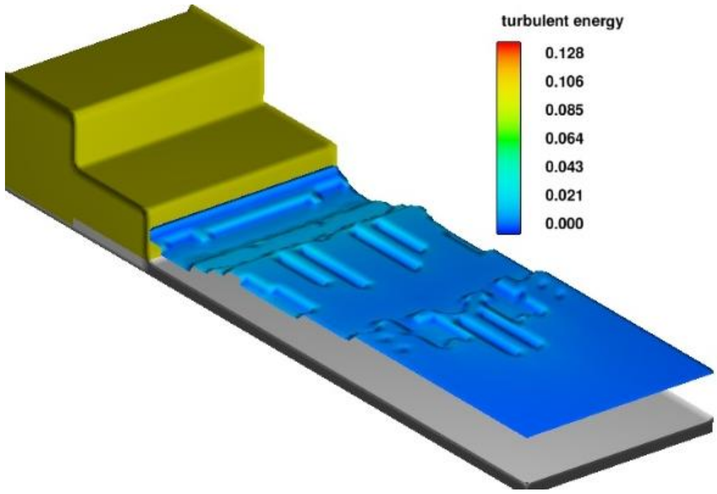
turbulent energy
0.128
0.106
0.085
0.064
0.043
0.021
0.000

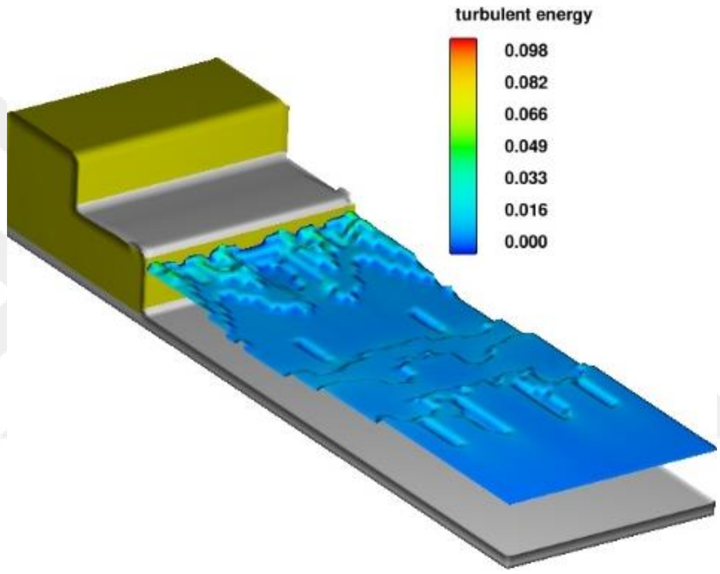
turbulent energy
0.098
0.082
0.066
0.049
0.033
0.016
0.000

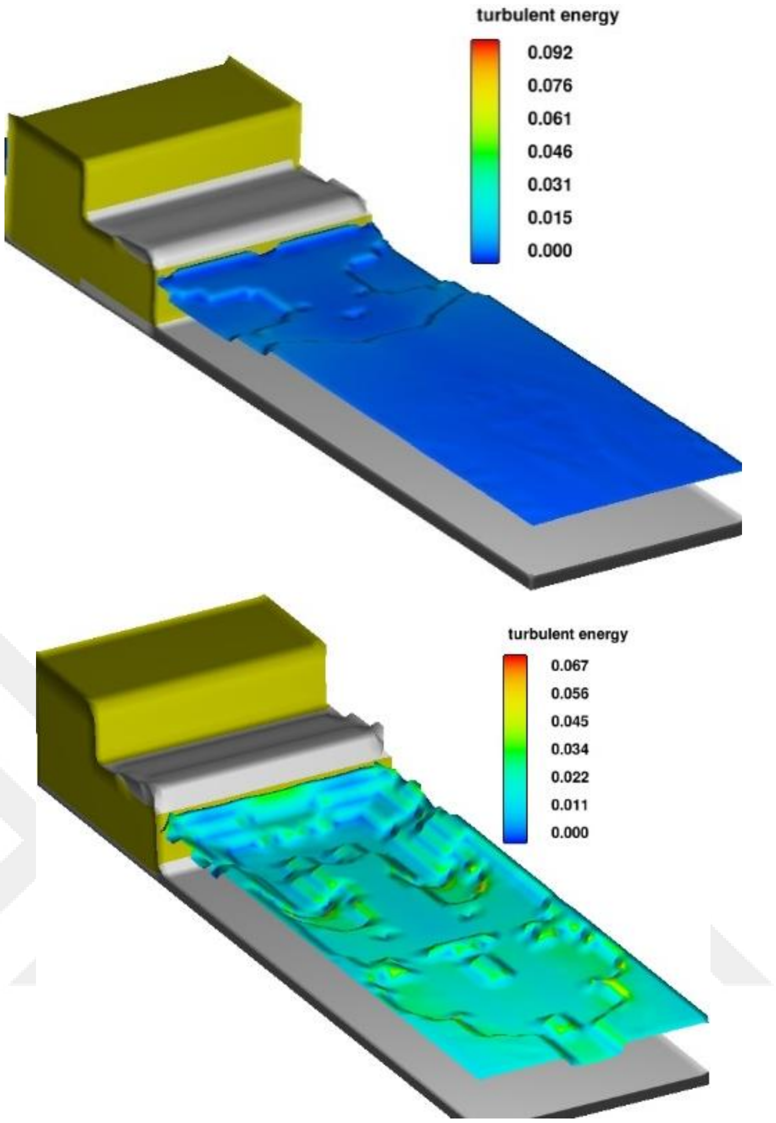

Figure 2.16 illustrates the distribution of turbulent energy (Q=25 l/s) (Fatah, 2017)

CHAPTER 3

EXPERIMENTAL INVESTIGATION

3.1 Introduction

The following sections include the developed experimental installation, measuring techniques, and experimental procedures. All the tests were carried out in Hydraulic Laboratory at the University of Gaziantep.

3.2 Flume

The tests were performed in the hydraulic Laboratory of Civil Engineering Department of Gaziantep University. The flume is 12 m long, 0.8m width and 0.9 m depth. The test section of the flume bed is 2 m long, 0.8 m wide was prepared at a distance 3 m downstream of the inlet flume as shown in Figure (3.1).

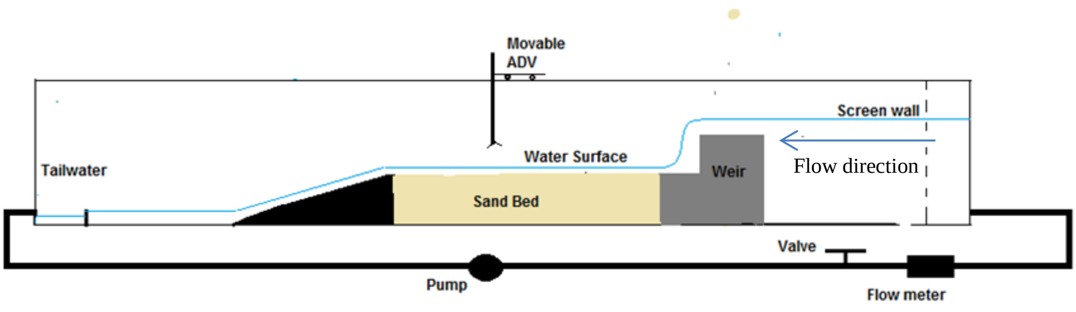

Figure 3.1 Experimental setup

The depth of the sand section is 21 cm at single step broad crested weir with the hollow end sill and the same depth of downstream inclined single step broad crested weir.

The surface water elevation was obtained by using digital point gage that installed on the top of the flume wall in the figure below:

Figure 3.2 digital point gage

Magnetic flow meter to measure discharge were installed in the pipe system before the inlet of the channel as illustrated in Figure (3.3).

Figure 3.3 Magnetic flow meter installed in the pipe system

The water provider by using a pump with a capacity 100-150 l/s as figure below:

Figure 3.4 pump system

The scour hole and the elevation of the bed were measured by laser meter as shown in Figure (3.5).

Figure 3.5 Laser meter installed in the channel

3.3 Sand bed

A series of experiments were carried out to characterize the sand bed material present in the flume used for the study. The soil tests performed included a mechanical sieve analysis and a specific gravity test. The results of the tests showed that the bed material consists of cohesionless sand with a median particle size d_{50} of 1.8 mm and a specific gravity of 2.65. The geometric standard deviation of the sand size σ_g is 3.87, which implies that the sand is of non-uniform size distribution. The σ_g is defined as, σ_g = $(d_{84}/d_{16})^{0..5}$. The plot of the grain size distribution (sieve analysis) test is depicted in Figure 3.6.

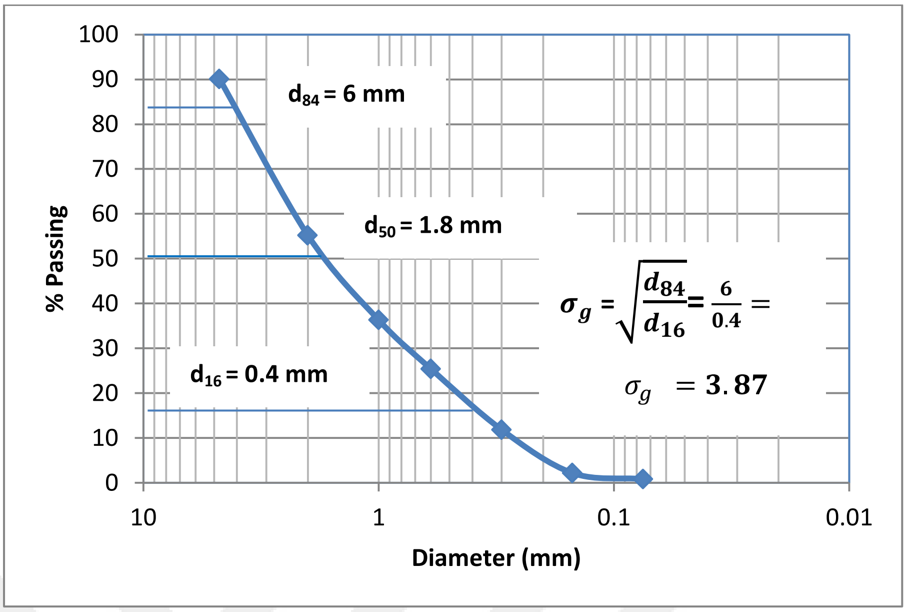

Figure 3.6 Grain size distribution

3.4 Velocity Measurement

An Acoustic Doppler Velocimeter ADV, developed by SonTek (5cm down-looking and a sampling rate up to 50 Hz) was mounted together with a vertical positioning on the carriage to measure the three-dimensional velocity components as well as the turbulence intensities. This instrument carriage was mounted on rails on the top of the flume sides allowing the movement of ADV in both longitudinal and transverse direction of the flume. Scales were fitted in the flume wherever necessary to provide a reference datum. The ADV probe and its operating mechanism are shown in Figure 3.7.

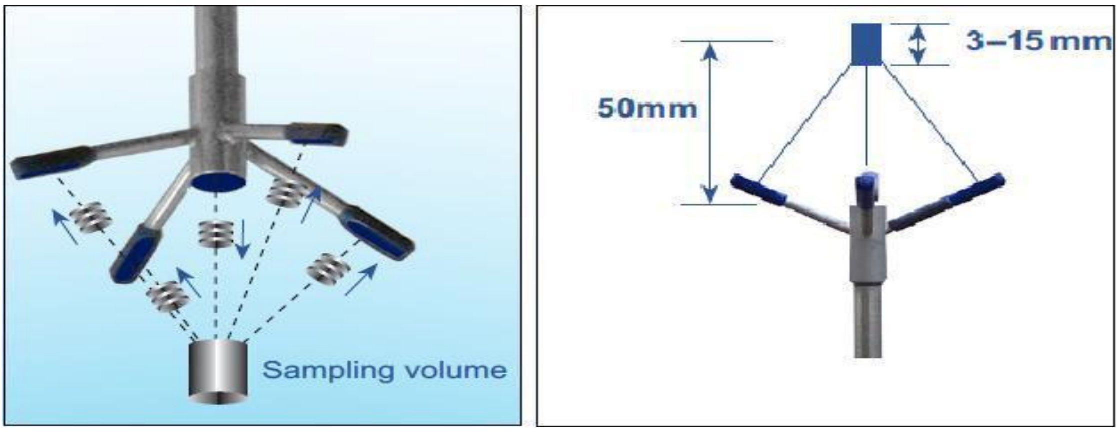

Figure 3.7 Nortek ADV probe with the transducer, receiver, and sampling volume (Tuyen, 2006)

The Cartesian coordinates system (x, y, z) was utilized to represent the flow velocity field as shown in Figure 3.8. Here, the time-averaged velocity components in (x, y, z) were represented by (*u*, *v*, *w)* and their fluctuations were (*u*', *v*,' *w'*), respectively. The lowest possible point of ADV reading was 1 cm above the bed Velocity components and turbulence intensities were plotted in *xz* planes using EXCEL and SURFER 11 programs.

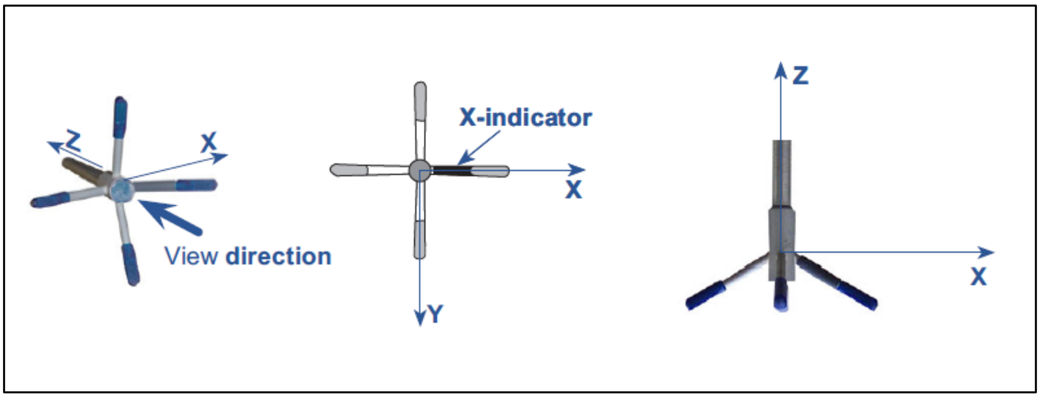

Figure 3.8 Defining the XYZ coordinates (Tuyen, 2006)

3.4.1 Acoustic Doppler Velocimeter Measurements

During each experiment, the velocity is periodically monitored using ADV. Stream velocity is measured in front of models using the ADV in the center of the flume.

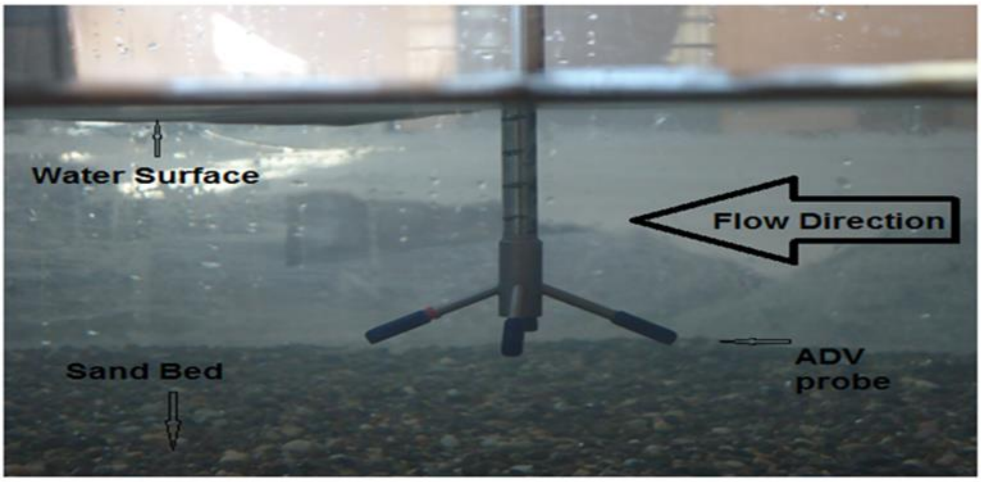

Figure 3.9 Typical ADV Setup

The typical ADV setup is shown in Figure 3.9. The ADV probe was then positioned above the scour hole and velocities were recorded for a period of 60 seconds. The sample period of 60 seconds was chosen to ensure that sufficient flow differences were captured.

The stream velocity components (u, v, w) were recorded with three directions. The velocity component (u) is the velocity in the direction of flow. While the velocity component (v) is the velocity perpendicular to the flow direction. However, the velocity component (w) is the velocity in the direction of the hole depth. The velocity components in (u, v, w) were recorded in the center of the flume with the direction of flow and different depths of hole.

The Isometric view for weir and axis measurement are shown in Figure (3.10).

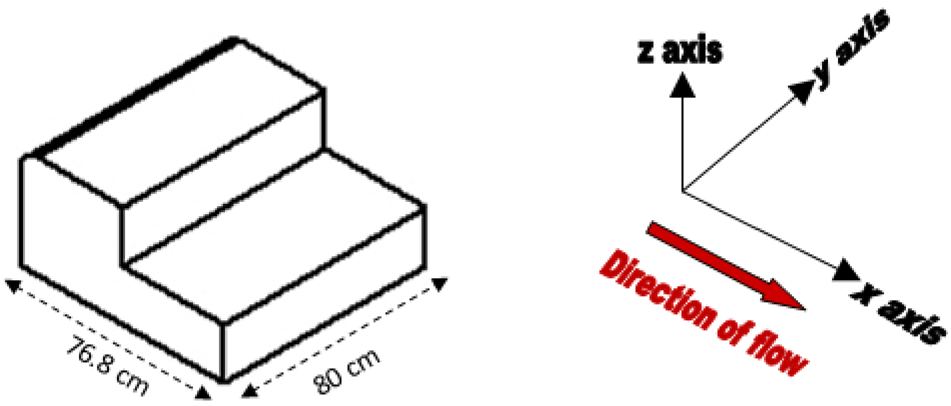

Figure 3.10 Axis measurement uses in Acoustic Doppler Velocimeter

3.5 Weir model

In this study, ten different types of single broad crested weir models are used. The first four models are inclined single step broad crested weir with different angles as shown in Figures (3.12,3.13,3.14,3.15). The second six models have end sill with different heights, porosity and the diameter of the holes. The hole diameter is (1.0, 1.5, 1.7, 1.0, 1.1, 1.0) cm respectively as shown in Figures (3.16, 3.17, 3.18, 3.19, 3.20, 3.21). One row of holes is used for the weir model of having 24 cm step height, two rows of holes are used for the weir model of having 27 cm step height and three rows of holes are used for the weir holes of having 30 cm. Each model, which are used in the experiment has 39 cm step height. The experiments were carried out using 15,20 and 25 l/s for duration of 6 hours.

Table 3.1 Summary of test conditions for inclined single step broad crested weir

Model	θ^0	Q (l/s)	P1(cm)
A1	0	15	39
B1	4.5	15	39
C1	8.7	15	39
D1	13	15	39
E1	10.8	15	39
A2	0	20	39
B2	4.5	20	39
C2	8.7	20	39
D2	13	20	39
E2	10.8	20	39
A3	0	25	39
B3	4.5	25	39
C3	8.7	25	39
D3	13	25	39
E3	10.8	25	39

Table 3.2 Summary of test conditions for single step broad crested weir with hollow end sill

Model	Q (l/s)	P2 (cm)	P1 (cm)	dr (cm)	e (%)
A1	15	21	39	0	100
F1	15	24	39	1	20
G1	15	24	39	1.5	30
H1	15	24	39	1.7	35
K1	15	27	39	1	25
M1	15	27	39	1.1	30
N1	15	30	39	1	30
A2	20	21	39	0	100
F2	20	24	39	1	20
G2	20	24	39	1.5	30
H2	20	24	39	1.7	35
K2	20	27	39	1	25
M2	20	27	39	1.1	30
N2	20	30	39	1	30
A3	25	21	39	0	100
F3	25	24	39	1	20
G3	25	24	39	1.5	30
H3	25	24	39	1.7	35
K3	25	27	39	1	25
M3	25	27	39	1.1	30
N3	25	30	39	1	30

3.6 Test Program

The test program was developed to deal with the evaluation of the efficiency of using different models to reduce local scour in front of the weir. The idea of this method is dependent on these models on the downstream of the weir so that the local scour was reduced.

The test program was divided into six series of tests, with each test series representing a complete set of tests. The six series of tests are referred to as series 1, series 2, series 3, series 4, series 5, and series 6. The tests were performed under live-bed conditions at three different flow discharges (15 l/s, 20 l/s, and 25l/s) for a duration of 6 hours.

A summary of the basic test and flow conditions are shown in Table 3.1. The series of tests (Series 1, 2 and 3) were designed to investigate the effect of ramp shapes on local scour. The shapes used to be single step broad crested weir with height (21) cm, inclined single step broad crested weir with ramp angle (4.5^0), inclined single step broad crested weir with ramp angle (8.7^0), inclined single step broad crested weir with ramp angle (10.8^0), inclined single step broad crested weir with ramp angle (13^0) at different discharges under live-bed scour conditions. The series of tests (Series 4, 5 and 6) were conducted to study the effect of the hollow end sill as a mitigation technique against weir scour.

Results from Series 1, 2 and 3 tests were analyzed together with the first group of the thesis and Series 4, 5, and 6 tests were analyzed together with the second group of the thesis. An empirical relationship was developed from experimental results. The scour contours were also plotted using software called Surfer version 11, and the results were discussed. Surfer version 11 is a full-function 3-D surface modeling/mapping program and contouring package. The Surfer is capable of quickly and easily converting XYZ data into contour, surface, wireframe, vector, image and shaded relief plots. The Surfer tool was employed to convert the scour hole topographical data into a contour map as well as into a three-dimensional profile of the scour hole region. The surfer is also capable of calculating the volume of the contoured hole using inbuilt Trapezoidal and Simpson rules. It can also calculate the surface area of the scour hole.

Table 3.3 Summary of test conditions for Series 1, 2, 3, 4, 5and 6 tests

Test	Run No.	Q (l/s)	Yu(cm)	Yd(cm)	Yt(cm)	Va(m/s)	Fr	FD
Series 1	**A1**	15	5.5	1.2	10	1.563	4.554	53.628
	B1	15	5.5	1.4	4.5	1.339	3.614	45.967
	C1	15	5.5	1.7	3.75	1.103	2.701	37.855
	D1	15	5.5	2.6	2.7	0.721	1.428	24.752
	E1	15	5.5	3	6	0.625	1.152	21.451
Series 2	**A2**	20	6.3	1.5	13	1.667	4.345	57.204
	B2	20	6.3	1.7	6.5	1.471	3.601	50.474
	C2	20	6.3	1.9	4.95	1.316	3.048	45.161
	D2	20	6.3	2.9	4.17	0.862	1.616	29.588
	E2	20	6.3	3.7	6.3	0.676	1.122	23.191
Series 3	**A3**	25	7.3	1.8	14	1.736	4.131	59.587
	B3	25	7.3	2	7.5	1.563	3.528	53.628
	C3	25	7.3	2.4	6	1.302	2.683	44.690
	D3	25	7.3	3.5	8.45	0.893	1.524	30.645
	E3	25	7.3	4.2	7	0.744	1.159	25.537
Series 4	**F1**	15	5.5	3	4.5	0.625	1.152	21.451
	G1	15	5.5	2.8	4.6	0.647	1.212	22.191
	H1	15	5.5	2.6	4.5	0.721	1.428	24.752
	K1	15	5.5	2.9	4	0.647	1.212	22.191
	M1	15	5.5	2.9	4	0.647	1.212	22.191
	N1	15	5.5	2.9	3.6	0.647	1.212	22.191
Series 5	**F2**	20	6.3	3.7	5	0.676	1.122	23.191
	G2	20	6.3	3.9	5	0.641	1.036	22.001
	H2	20	6.3	3.2	5.5	0.781	1.394	26.814
	K2	20	6.3	3.6	5.2	0.694	1.169	23.835
	M2	20	6.3	3.7	4.8	0.676	1.122	23.191
	N2	20	6.3	3.4	4.5	0.735	1.273	25.237
Series 6	**F3**	25	7.3	4	5	0.781	1.247	26.814
	G3	25	7.3	4.2	5.8	0.744	1.159	25.537
	H3	25	7.3	3.7	5.5	0.845	1.402	28.988
	K3	25	7.3	3.2	5.5	0.977	1.743	33.518
	M3	25	7.3	4	5.5	0.781	1.247	26.814
	N3	25	7.3	3.5	5	0.893	1.524	30.645

In which;

Yu = water head upstream of the model.

Yd =downstream water head above step.

Yt =tail water head.

Va = downstream velocity above step.

Fr = Froude number and it is expressed as:

$$Fr = \frac{Va}{\sqrt{gYd}} \tag{3.1}$$

In which:

g = acceleration due to gravity.

FD = densimetric particle Froude number and it is expressed as:

$$FD = \frac{Va}{\sqrt{((\sigma g - 1)D_{50}\, g)}} \tag{3.2}$$

σg = geometric standard deviation of the sand.

D_{50}= median size of sand.

a) Picture of model A

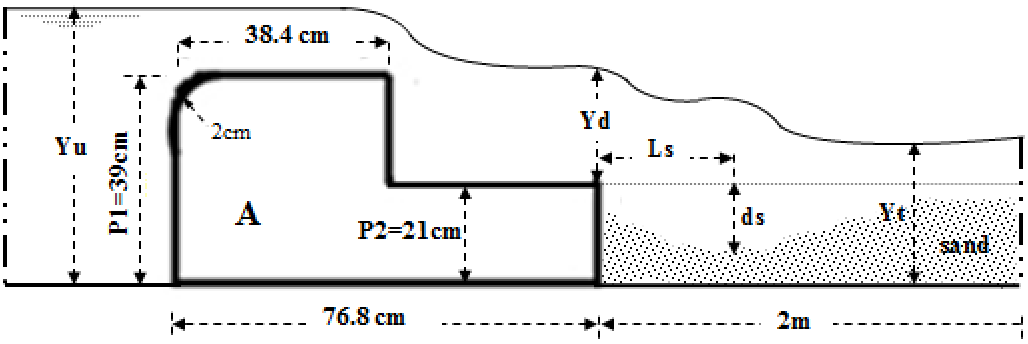

b) Sketch and dimensions of model A

Figure 3.11 Picture and sketch of testing model A

The model A is a single step broad crested weir

Ls = the distance of maximum scour depth from downstream of the weir.

ds = maximum scour depth.

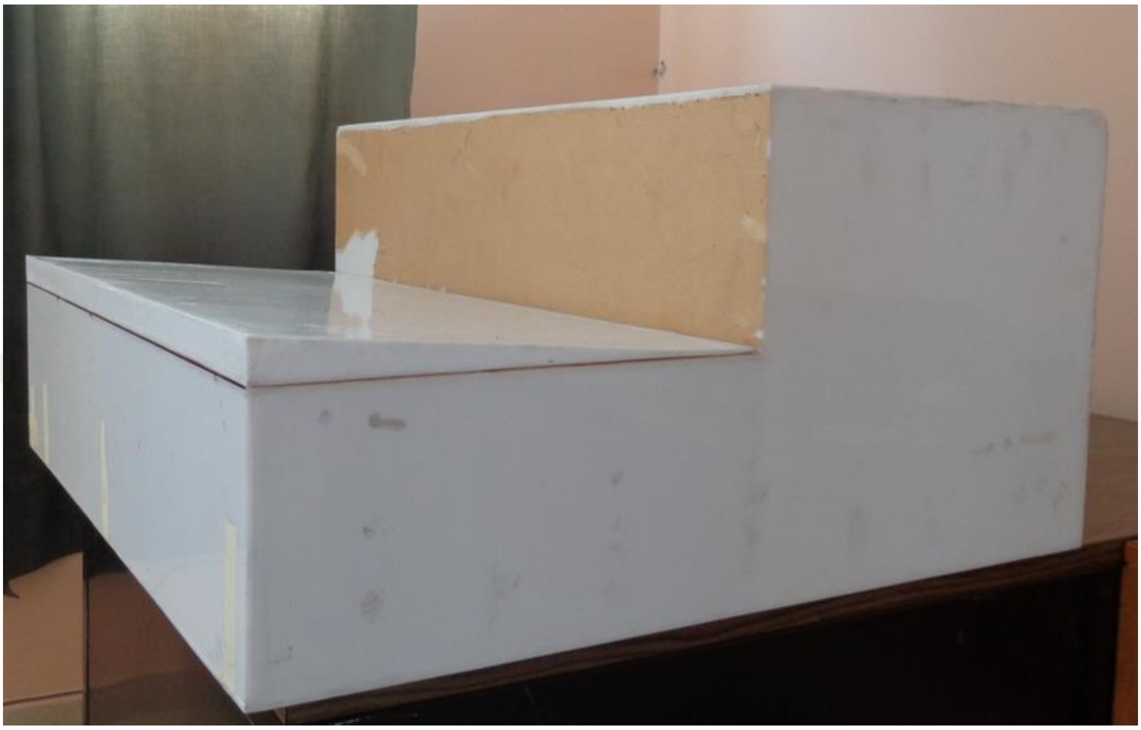

a) Picture of model B

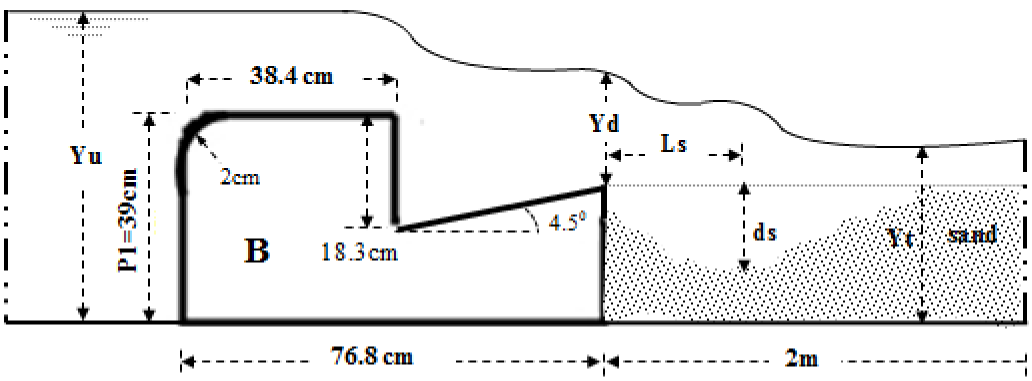

b) Sketch and dimensions of model B

Figure 3.12 Picture and sketch of testing model B

The model B is an inclined single step broad crested weir with a ramp angle (4.5^0).

a) Picture of model C

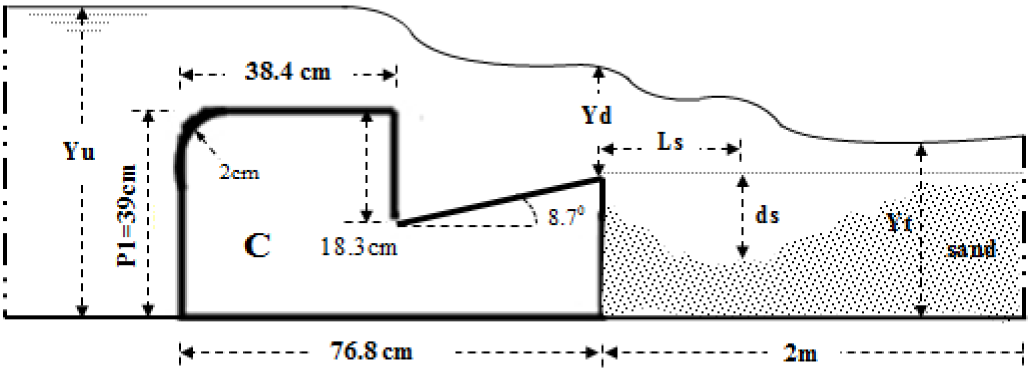

b) Sketch and dimensions of model C

Figure 3.13 Picture and sketch of testing model C

The model C is an inclined single step broad crested weir with a ramp angle (8.7^0).

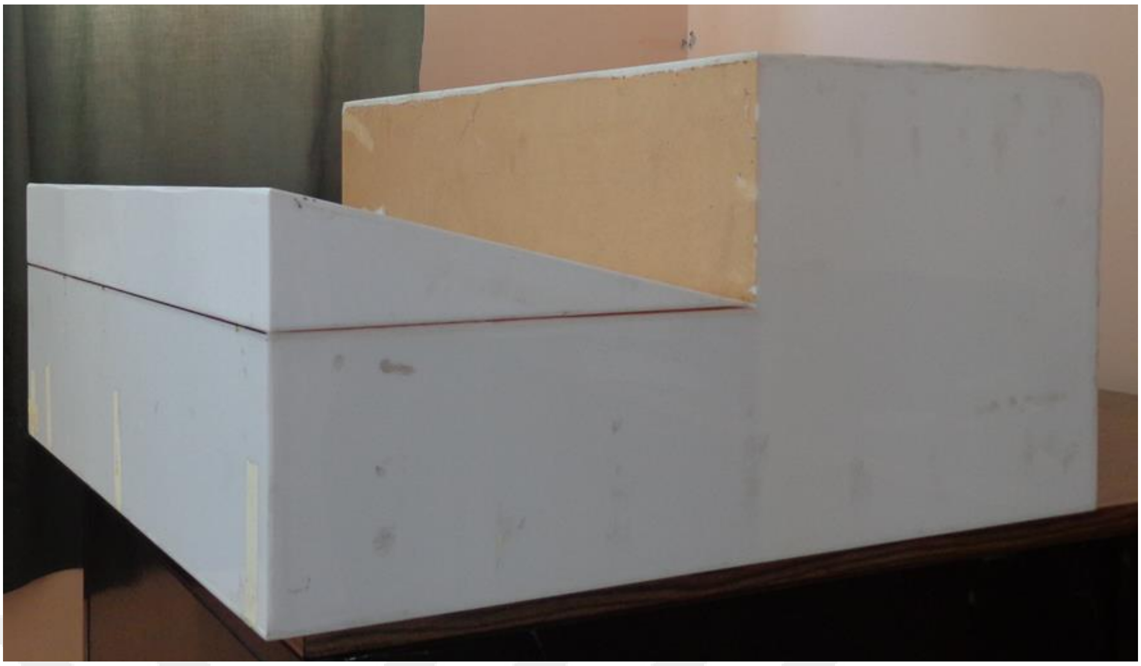

a) Picture of model D

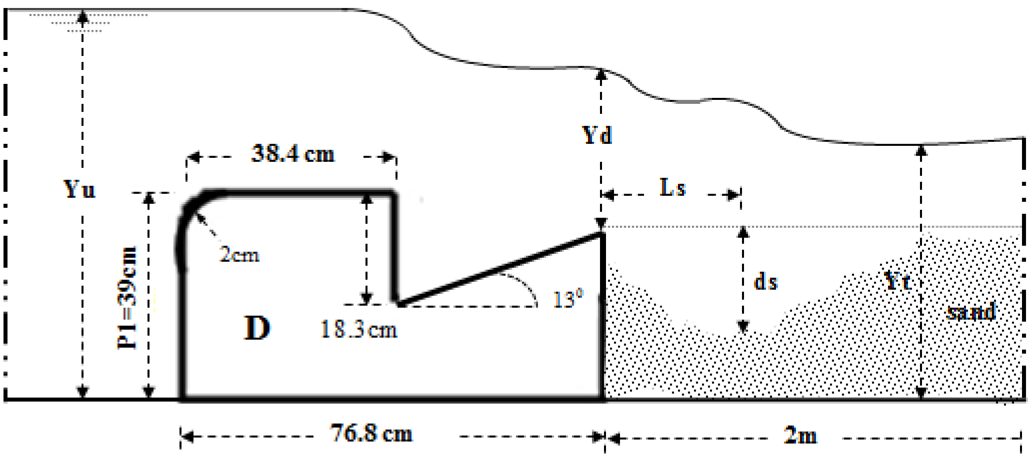

b) Sketch and dimensions of model D

Figure 3.14 Picture and sketch of testing model D

The model D is an inclined single step broad crested weir with a ramp angle (13^0).

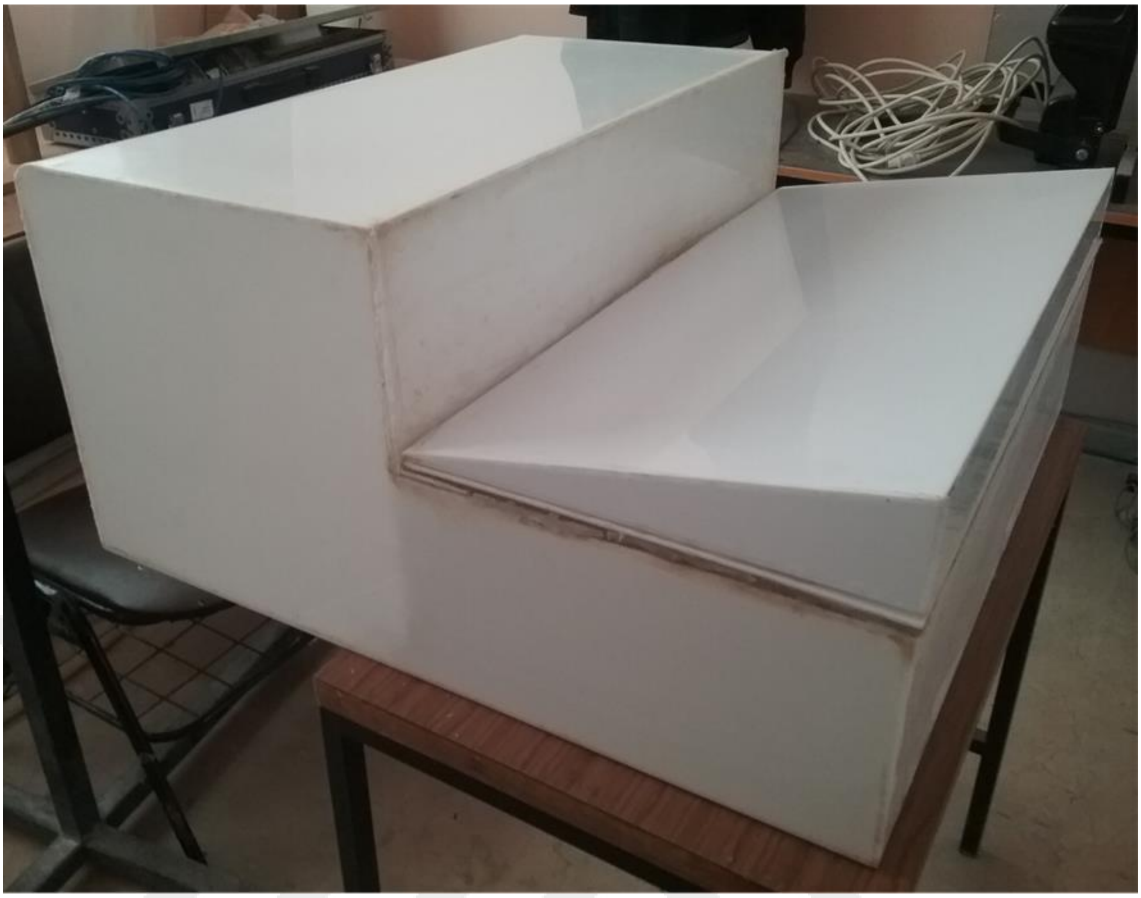

a) Picture of model E

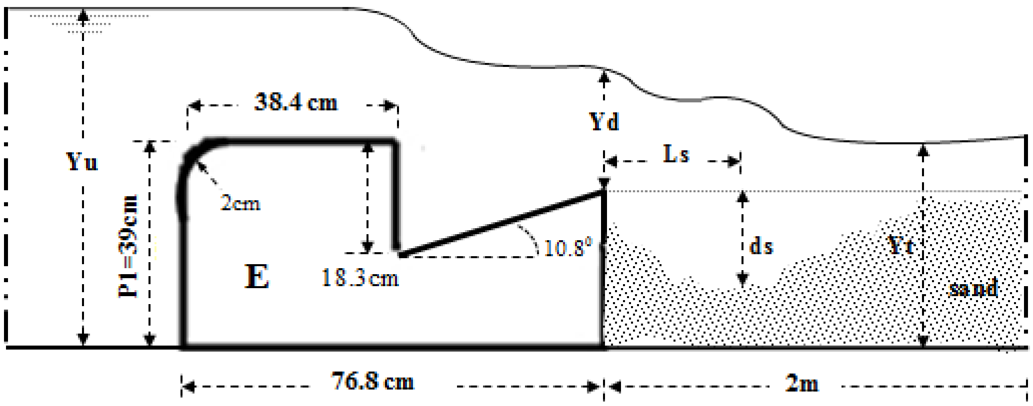

b) Sketch and dimensions of model E

Figure 3.15 Picture and sketch of testing model E

The model E is an inclined single step broad crested weir with a ramp angle (10.8^0).

a) Picture of model F

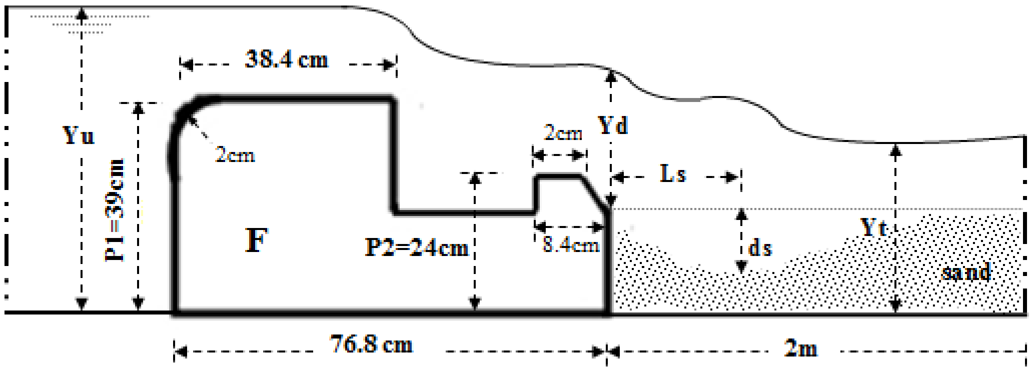

b) Sketch and dimensions of model F

Figure 3.16 Picture and sketch of testing model F

The model F is a single broad crested weir with hollow end sill [height (24) cm and porosity (20%)].

a) Picture of model G

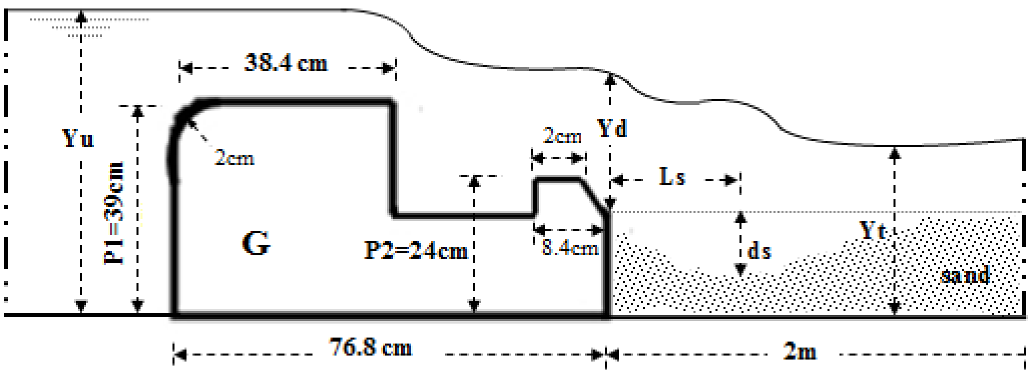

b) Sketch and dimensions of model G

Figure 3.17 Picture and sketch of testing model G

The model G is a single broad crested weir with hollow end sill [height (24) cm and porosity (30%)].

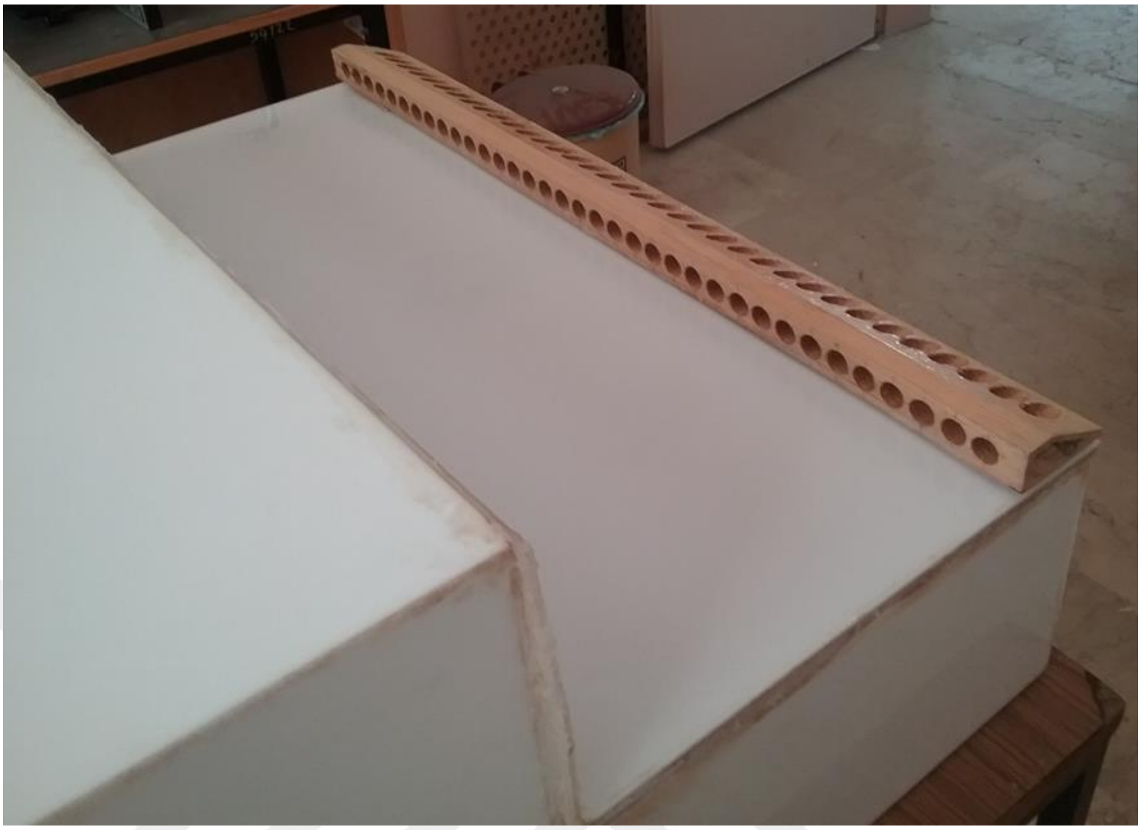

a) Picture of model H

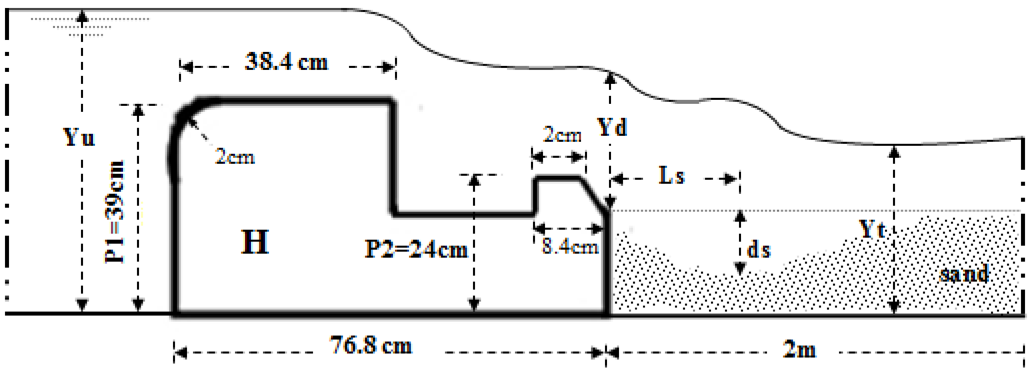

b) Sketch and dimensions of model H

Figure 3.18 Picture and sketch of testing model H

The model H is a single broad crested weir with hollow end sill [height (24) cm and porosity (35%)].

a) Picture of model K

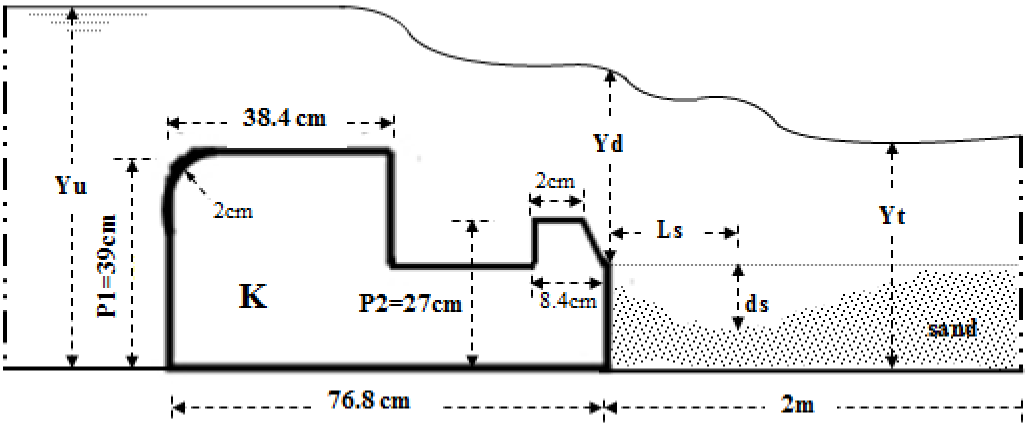

b) Sketch and dimensions of model K

Figure 3.19 Picture and sketch of testing model K

The model K is a single broad crested weir with hollow end sill [height (27) cm and porosity (25%)].

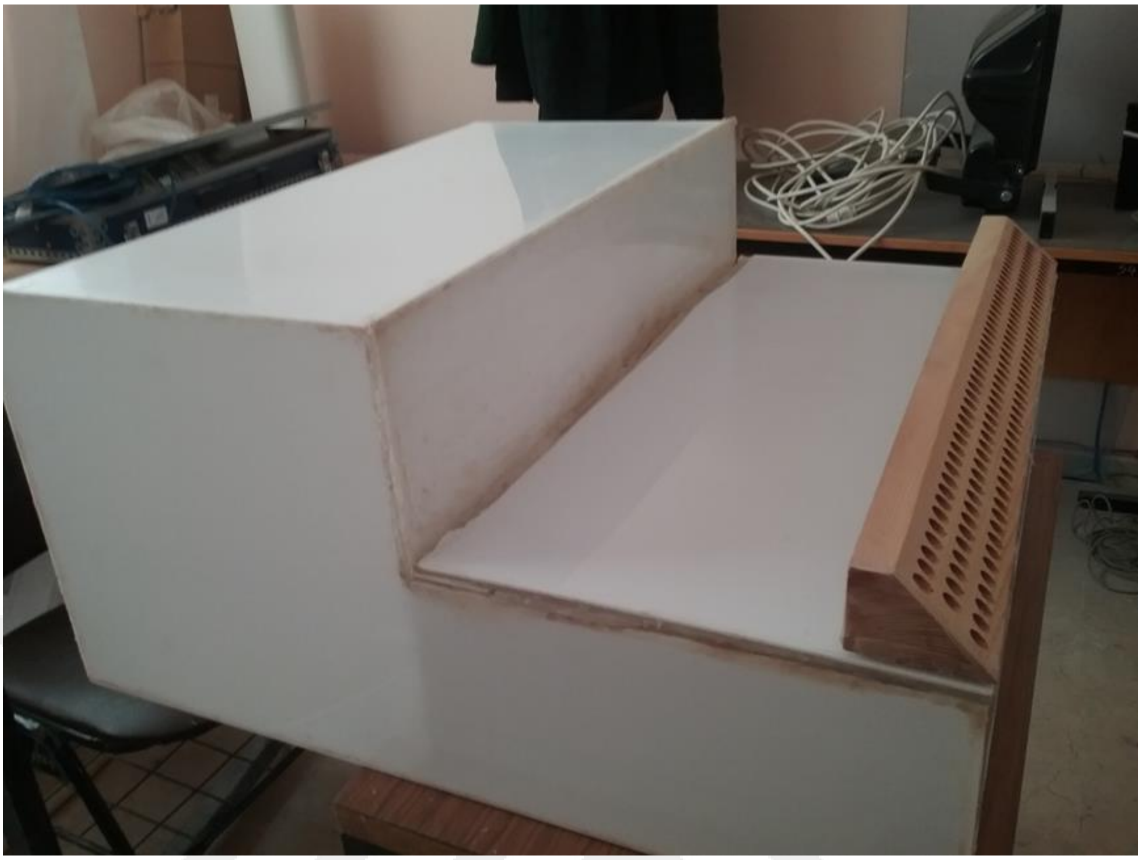

a) Picture of model M

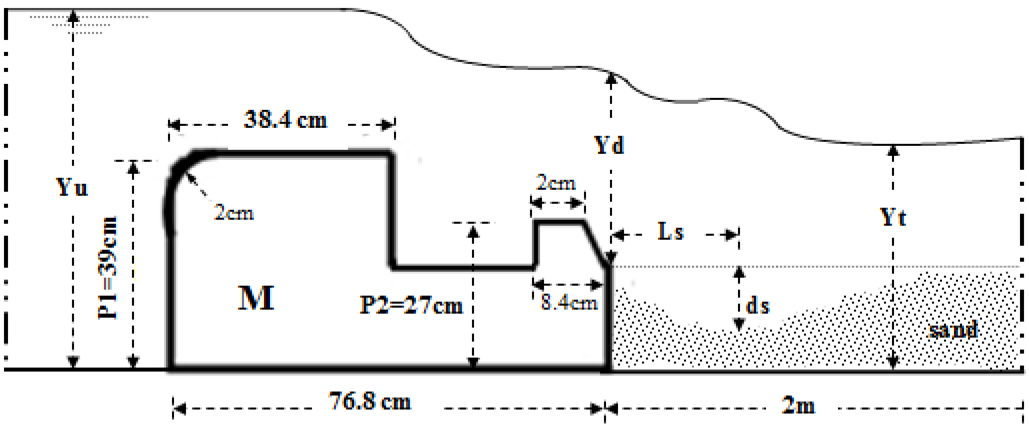

b) Sketch and dimensions of model M

Figure 3.20 Picture and sketch of testing model M

The model M is a single broad crested weir with hollow end sill [height (27) cm and porosity (30%)].

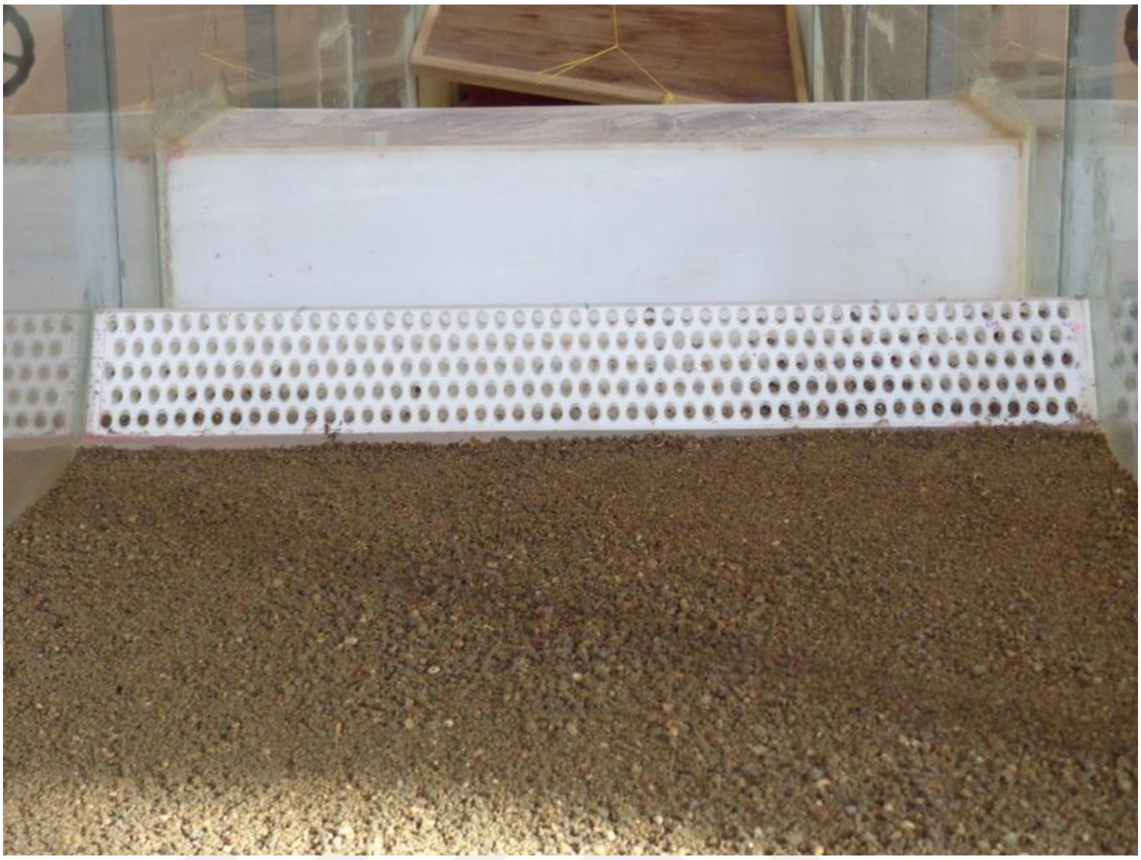

a) Picture of model N

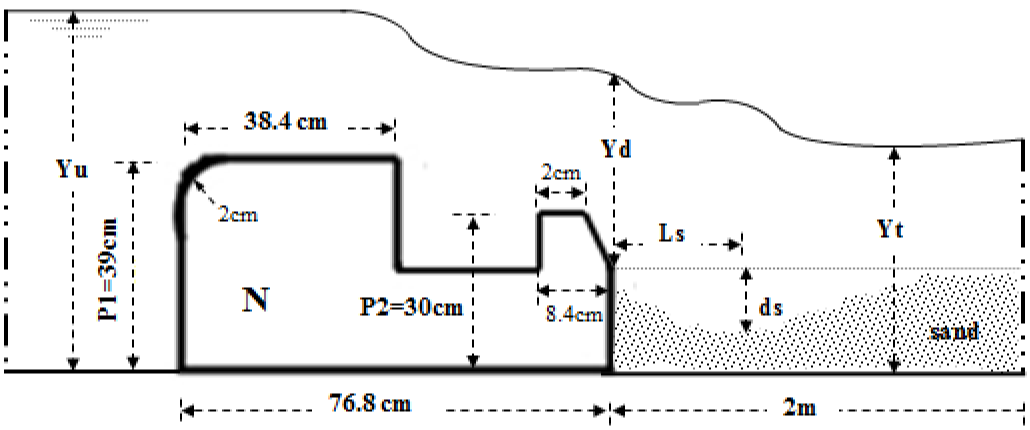

b) Sketch and dimensions of model N

Figure 3.21 Picture and sketch of testing model N

The model N is a single broad crested weir with hollow end sill [height (30) cm and porosity (30%)].

3.7 Implication of Scale effect

The difficulty of obtaining a sufficiently complete set of field data for the scale effect of weir scour experiments has implications for further research on weir scour. Because of the typical dimensions of laboratory flumes as well as the lower limit of cohesion-less sediment size, it is difficult to satisfy the similitude requirements relating scour in the flume to scour in the river. This difficulty limits the use of laboratory flumes in developing accurate predictors of scour depths at full-scale weirs. It is also affects laboratory experiments on local scour at other structures, such as abutments. Many researchers are investigating median particle size in the Tigris river as shown in Table (3.4) (Nedico 1976, Najib 1980, Khaleel 1986, Al-Taiee&Othman 1993 and Othman 2009). The discharge of the Tigris river was $150m^3/sec$ (Mohammad 2005).

Table 3.4 Values of d_{16}, d_{50} and d_{84} for the bed surface layer of the Tigris River

	Nedico 1976	Najib 1980	Khaleel 1986	AL-Taiee&Othman 1993	Othman 2009
$d_{84(mm)}$	71	49	58	56	43
$d_{50(mm)}$	40	22	38	37	32
$d_{16(mm)}$	25	10	27	27	15

3.8 Froude Scaling

Froude numbers are used to determine dynamic similarity between flows. Where a geometric scale is applied to scale the flow depth and height, the Froud number is used to scale flows due to the importance of gravity on free-surface flow. It is used to compare the resistance of weir within the fluid between the realistic and scale model experiments.

Froude scaling uses the ratio of inertia forces to gravity forces to scale between models used in this research.

$$\frac{\text{Innertia force}}{\text{Gravety force}} = \frac{F_i}{F_g} \alpha \frac{\rho V^2 L^2}{\rho g L^3} = \frac{V^2}{gL} \tag{3.3}$$

Where Fi is the force of inertia, Fg is gravity force, L is length, V is general velocity, g is gravity. Using Equation (3.3) scale from prototype to scale model,

$$(\mathbf{Fr})_m = (\mathbf{Fr})_p \tag{3.4}$$

$$\left(\frac{Va}{\sqrt{gL}}\right)_m = \left(\frac{Va}{\sqrt{gL}}\right)_p \tag{3.5}$$

$$\frac{V_m}{V_P} = \sqrt{\frac{L_m}{L_p}} \tag{3.6}$$

$$\frac{Q_m}{Q_P} = \frac{A_m V_m}{A_p V_P} = \frac{L_{m^2}}{L_{P^2}} \sqrt{\frac{L_m}{L_p}} = \frac{L_{m^{2.5}}}{L_{P^{2.5}}} \tag{3.7}$$

$Q_{m=}\ Q_P\ L_R^{2.5}$

The experimental setup in the laboratory is capable of having 58 l/s of discharge.

Q_p River=150 m^3/sec

Q_m pump= 0.058 m^3/sec

$0.058_{=}\ 150\ L_R^{2.5}$

L_R=0.0406

d_{50m}= d_{50p} L_R

d_{50m} = median particle size in the model=1.8mm

1.8= d_{50p} *0.0406

d_{50p}=41.7 mm

d_{50p} = median particle size in the Tigris river bed = 42 mm (Othman et al. 2012)

41.7 mm $\cong$ 42.0 mm

therefore, there is no scale effect.

3.9 Experimental Procedure

1. The weir was installed in the flume at the desired location.

2. Before each run, the bed was carefully leveled throughout its length using a trowel with screed. This trowel with screed is of the same width as the flume and can be dragged along the flume rails. Some measurements to check the leveling of the bed were taken randomly using the laser meter.

3. To start the test, the flume was very slowly filled with water to the required water depth, taking care for escaping of the air bubbles from the bed and no sediment movement is allowed.

4. The pump was then turned on until the desired flow rate has been achieved.

5. The temporal variation of scour was monitored. The progress of scour depth was observed 6 hours.

6. At the end of each test, the pump was shut down, and the water was slowly drained without disturbing the scour topography. The test section was then allowed to dry.

7. Photos of the scour topography were taken, and the final maximum scour depth was recorded using the laser meter. The contour profile of the scour hole was taken with the laser meter supported by the movable carriage of the flume.

8. After the test section was dried, the bed was frozen by pouring glue material (varnish).

9. Measurement of the flow velocity field in front of models was made by using ADV.

10. The above procedures were repeated for each test run.

CHAPTER 4

RESULTS AND DISCUSSION

4.1 Ramp angle inclined step

Analysis of results included four main aspects; local scour dimension, energy dissipation, water surface profiles, velocity distribution for inclined single step broad crested weir with different angles.

4.1.1 Local Scour Dimensions

The depth of local scour for weir with inclined step was measured and experimental results of the models will be compared with model A, and discussed in this section. The total scour volume (Vs), maximum local scour depth (ds) and the distance of maximum local scour from the weir (Ls) were compared for each of the four models as shown in Table (4.1).

Table 4.1 Total scour volume, maximum depth of scour and local scour distance from the weir for inclined single step broad crested weir

Model	θ^0	Q (l/s)	Vs (cm^3)	ds (cm)	Ls (cm)
A1	0	15	27993	11	40
B1	4.5	15	19597	9.5	32
C1	8.7	15	7974	3.8	12
D1	13	15	64326	14.3	8
A2	0	20	42537	12.8	52
B2	4.5	20	32405	12.8	40
C2	8.7	20	31338	11.6	36
D2	13	20	70556	17.2	24
A3	0	25	48583	12.4	68
B3	4.5	25	52680	12.4	48
C3	8.7	25	43784	12.2	76
D3	13	25	79316	16.1	48

It is clear that the model C minimizes the scour depth and the volume of local scour more than the other models at each discharge.

The energy loss in the flow over a weir is due to incomplete conversion of kinetic energy into potential energy (Al Naib, 1997). Upstream of the weir, in the acceleration area, part of the potential energy of the flow is converted into its kinetic energy. While the water is flowing, it continually loses energy against surface resistance, but this loss is negligibly small with regard to the loss in form resistance. The mechanism of form resistance here is: part of the kinetic energy of the flow is converted into energy of vortices of all scales, and turbulent fluctuations; then this cause the scour at the downstream of the weir. The low height of shape for model C help to dissipate vortices led to decrease depth of scour. The minimum distance of maximum scour depth from weir downstream for each discharge has occurred at model D because the height of shape enough to make it as traditional weir led to drop water at a low distance from the weir.

The reduction of depth and the total volume of local scour for each run of experiments were measured and shown in Table (4.2).

Table 4.2 Reduction of total volume and depth of scour for weir with inclined step comparing with model A

Model	**θ^0**	**Q (l/s)**	**Rv (%)**	**Rd (%)**
B1	4.5	15	29.99	13.64
C1	8.7	15	71.51	65.45
D1	13	15	0	0
B2	4.5	20	23.82	0
C2	8.7	20	26.33	9.38
D2	13	20	0	0
B3	4.5	25	0	0
C3	8.7	25	9.88	1.61
D3	13	25	0	0

Scour depth was reduced 65.5%, 9.38% and 1.61% for model C comparison with the model A at each discharge. Also, the model C reduces the total volume of local scour about 71.51%, 26.33%, and 9.88 % compared with model A at each discharge. It is clear that the model C minimizes the depth and volume of local scour more than other models because the effect of the vortex was reduced due to the slope of downstream (D/S) of the weir.

The values of average and critical velocities for each model are shown in Table (4.3).

Table 4.3 Experimental measurements of average and critical velocities for weir with inclined step

Model	θ	Va (m/s)	Vc (m/s)	Va / Vc
A1	0	1.563	0.319	4.892
B1	4.5	1.339	0.328	4.087
C1	8.7	1.103	0.338	3.259
D1	13	0.721	0.363	1.985
A2	0	1.667	0.331	5.028
B2	4.5	1.471	0.338	4.345
C2	8.7	1.316	0.345	3.816
D2	13	0.862	0.370	2.330
A3	0	1.736	0.342	5.081
B3	4.5	1.563	0.348	4.493
C3	8.7	1.302	0.358	3.632
D3	13	0.893	0.382	2.339

The values of average velocity are more than critical velocity lead to occurrence live bed because the effect of the slope of downstream (D/S) of the weir on the velocity of water.

The water surface profiles for each run were measured and shown in Figures (4.1, 4.2, and 4.3).

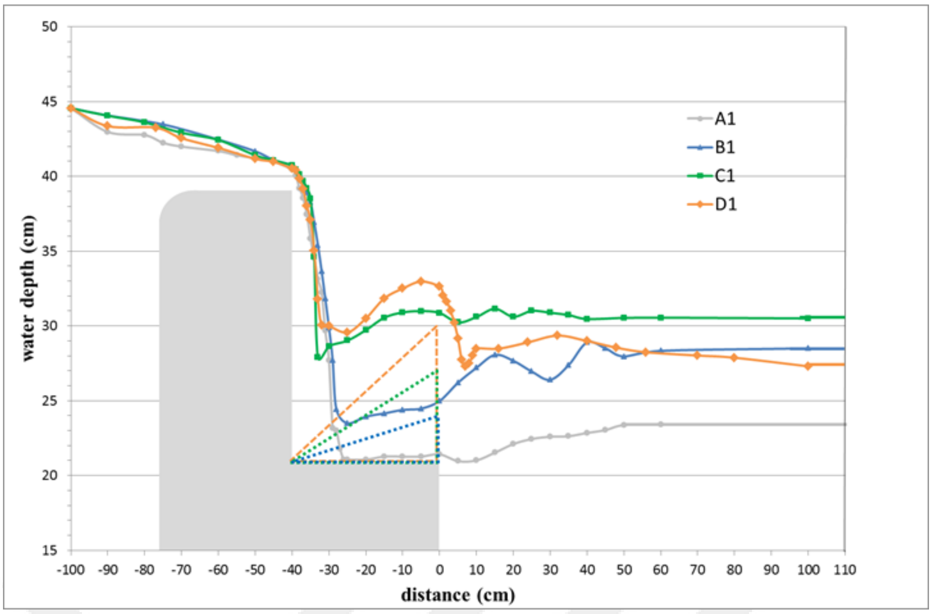

Figure 4.1 Longitudinal water surface profiles at the discharge of 15l/s for weir with inclined step

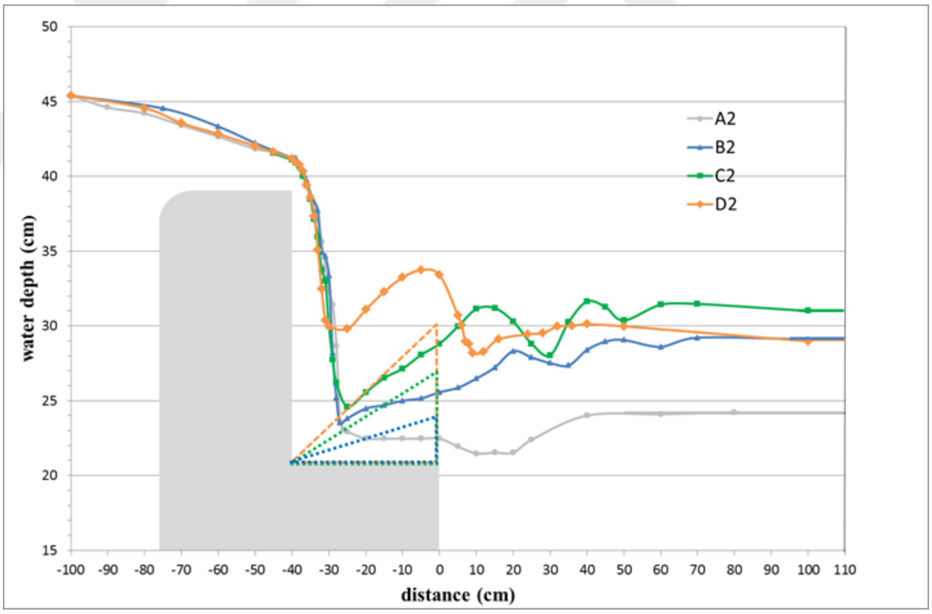

Figure 4.2 Longitudinal water surface profiles at the discharge of 20l/s for weir with inclined step

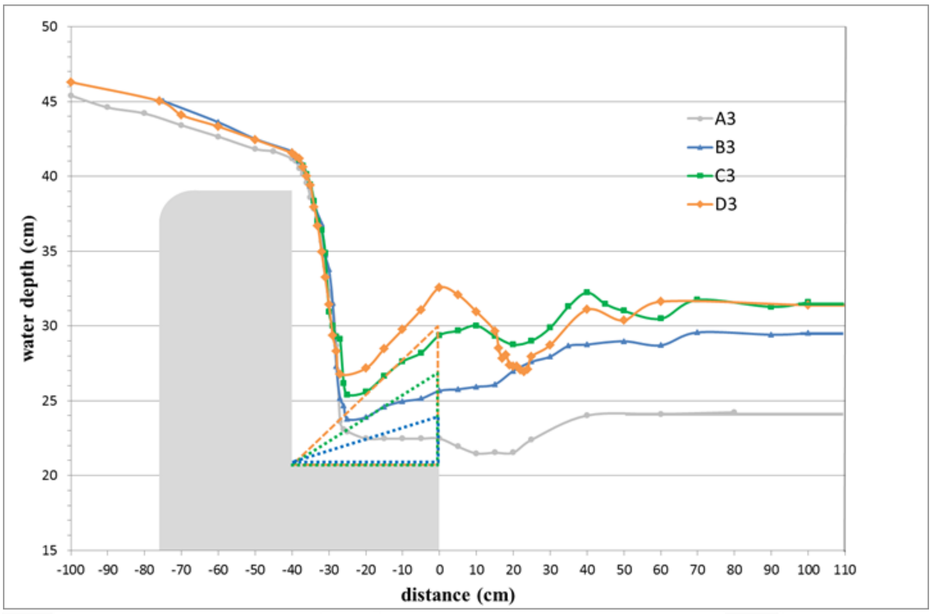

Figure 4.3 Longitudinal water surface profiles at the discharge of 25l/s for weir with inclined step

It is seen that, the trends of these water surface profiles for all discharges were mostly similar, follow the shape of the model, and the water surface at model A and C are smooth and effect on long distance on the downstream (D/S) of the weir, but the water surface at model B and D are more turbulent. The flow regime over the model A and C were surface jet flow because the surface is nearly horizontal and smooth, but the flow regime over models B, D was surface wave flow because of the mainstream following the free and wavy surface and a recirculation zone near the bottom (Tuyen, 2006).

The inlet energy of the flow is dissipated by inclined single step broad crested weir with different angles.

The total energies in the inlet Eu and at the end of weir Et are calculated and shown in Table (4.4).

Table 4.4 Energy dissipation for weir with inclined step

Model	θ	Eu (cm)	Et (cm)	ΔE%
A1	0	45.092	30.179	33.072
B1	4.5	45.092	29.385	34.834
C1	8.7	45.092	28.274	37.297
D1	13	45.092	31.458	30.237
A2	0	46.103	30.688	33.434
B2	4.5	46.103	30.254	34.377
C2	8.7	46.103	28.750	37.639
D2	13	46.103	30.802	33.189
A3	0	47.234	31.254	33.832
B3	4.5	47.234	30.885	34.613
C3	8.7	47.234	29.383	37.794
D3	13	47.234	31.647	32.999

It is clear that the high energy dissipation occurs at model C because it has an optimum height where energy dissipation occurs in the step is greater than the potential energy of the flow on the step, on the contrary, in model D, the energy dissipation occurs in the step nearly the same but the potential energy of the flow is greater comparing to model C.

Therefore the rate of scour at each run reduces considerably by increasing the step slope as shown in Figures (4.4, 4.5, and 4.6).

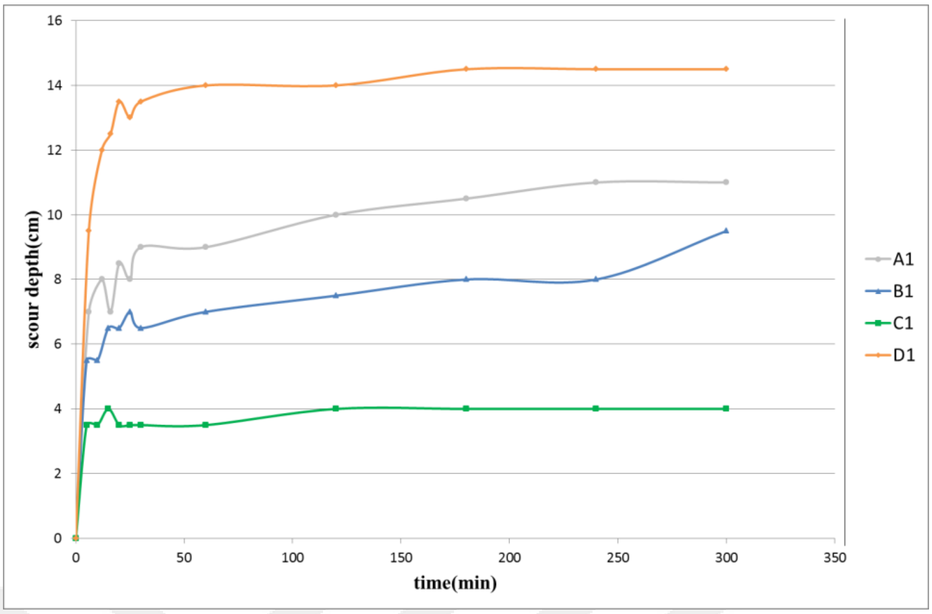

Figure 4.4 Downstream scour development with respect to time at the discharge of 15 l/s for weir with inclined step

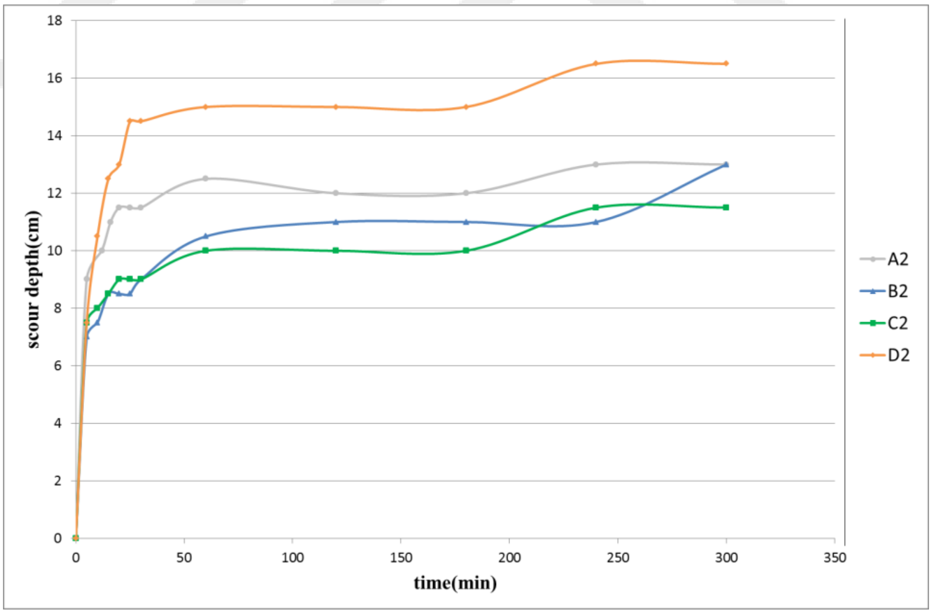

Figure 4.5 Downstream scour development with respect to time at the discharge of 20 l/s for weir with inclined step

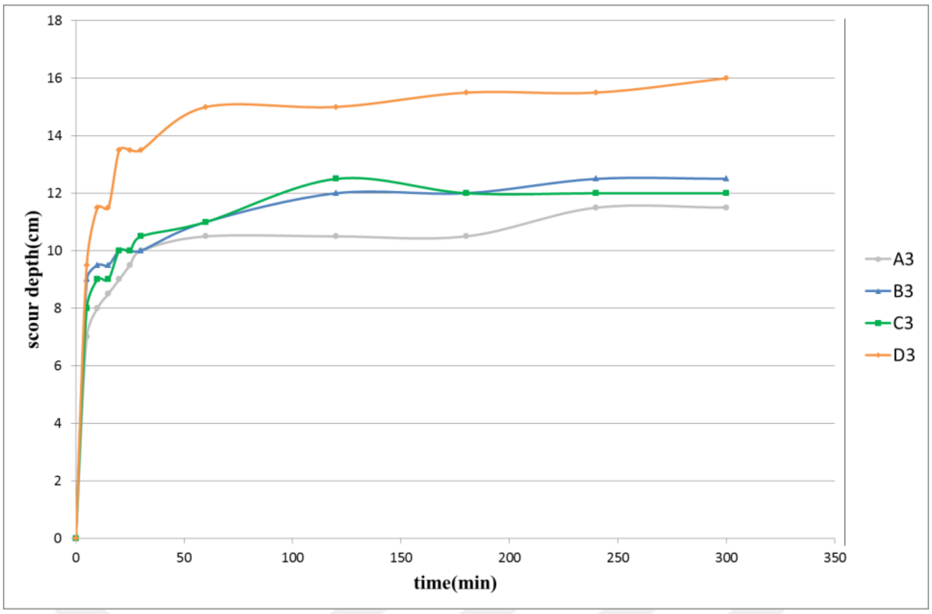

Figure 4.6 Downstream scour development with respect to time at the discharge of 25 l/s for weir with inclined step

It is seen that all models reach equilibrium case after 250 minutes. The model C is more stable and very slow in scour hole development when compares with other models because the height of shape makes stable the surface profile, on the contrary, the other models are more turbulence.

The bed profile for each run is given in Figures (4.7, 4.8 and 4.9).

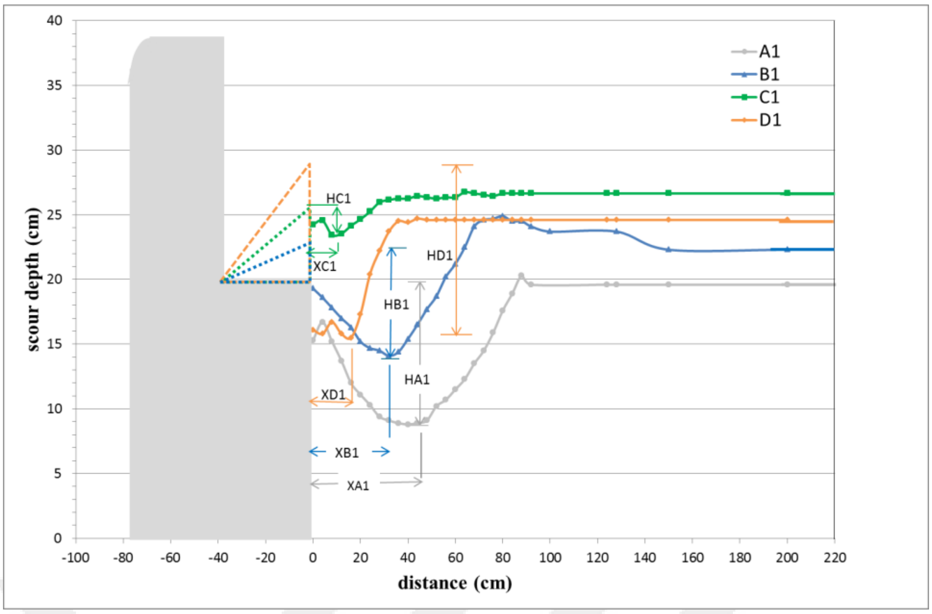

Figure 4.7 Bed profile at the discharge of 15l/s for weir with inclined step

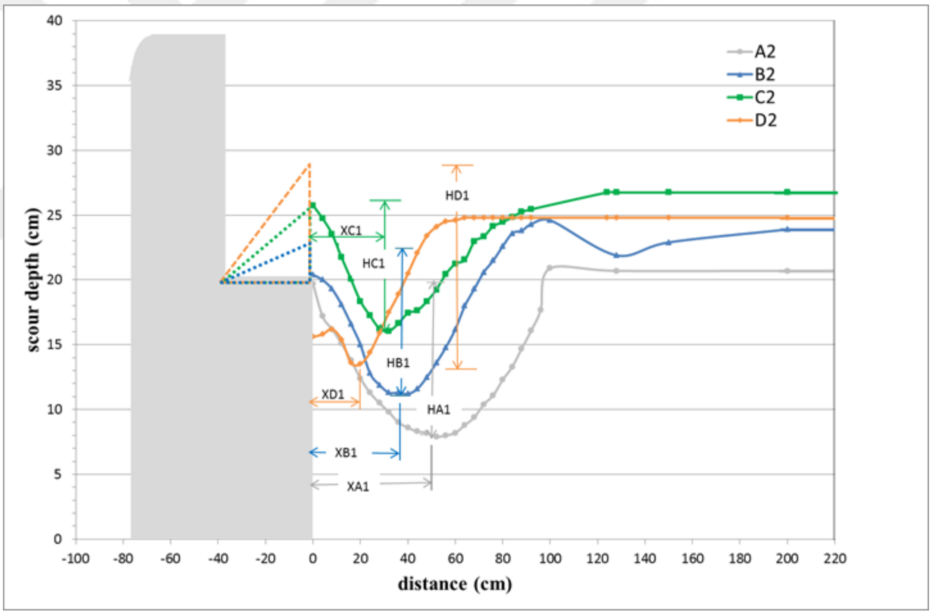

Figure 4.8 Bed profile at the discharge of 20l/s for weir with inclined step

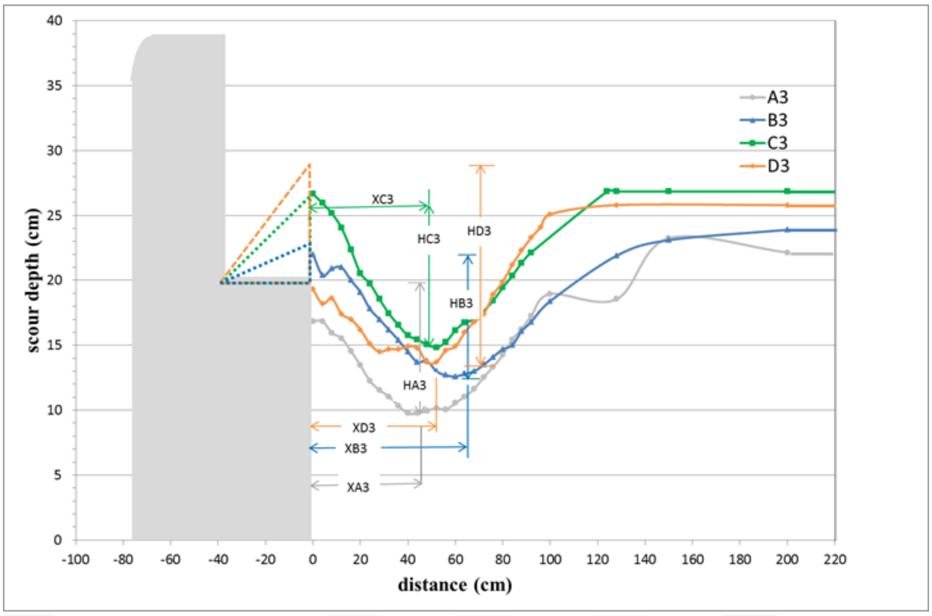

Figure 4.9 Bed profile at the discharge of 25l/s for weir with inclined step

Turbulence is capable of transfer energy of the flow from the mean motion to the turbulent fluctuations. Those fluctuations will then induce turbulent shear stresses, and energy will eventually be dissipated as heat via the viscosity (Uijttewaal, 2007).

There are two main ways for the dissipation of energy in the flow, one is the viscous dissipation induced by the mean motion, and the other is the dissipation via the turbulent motion. By considering the energy equations of the flow, we can see that the turbulence is dominant to the loss of energy from the mean motion.

That means the dissipation by work done against turbulent shear stresses also has a much larger contribution to the energy loss in the flow (Uijttewaal, 2007).

As shown in Figures 4.7, 4.8 and 4.9 that, the total volume of scour at model A is higher than other models because the effect of turbulent shear stresses at downstream (D/S) of the weir on long distance, but the maximum scour depth, and minimum distance of scour from weir were found after the weir model D because turbulent shear stresses is higher than other models lead to exposure to failure in the future.

The minimum depth and volume of scour for each discharge have occurred in model C because the height of the shape is optimum to dissipate the energy of flow at downstream (D/S) of the weir.

Figures 4.10, 4.11 and 4.12 show the scour pattern at each model after each run. The model C minimizes the scour depth and longer distance of scour from the end of the weir.

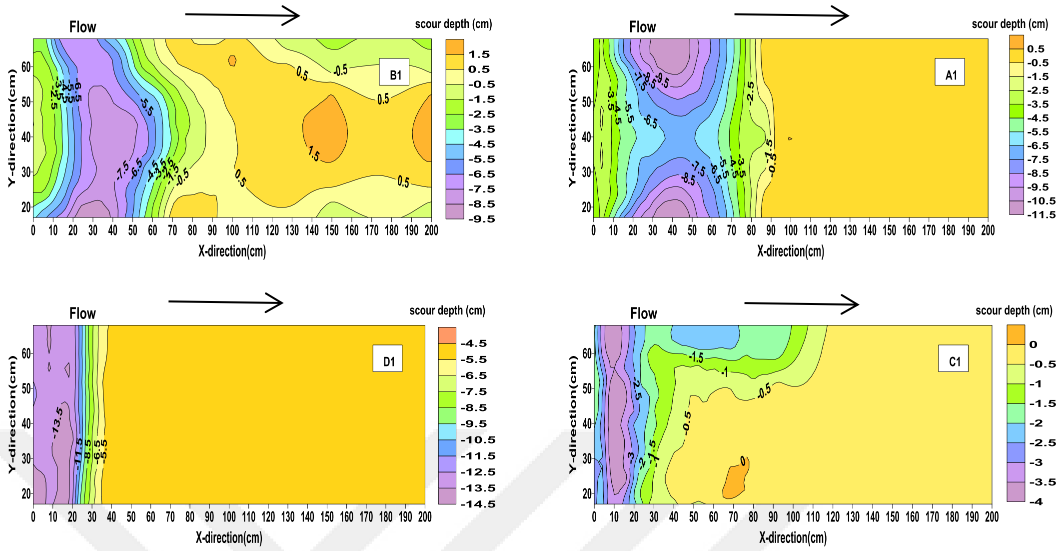

Figure 4.10 The scour pattern in front of models A1, B1, C1 and D1

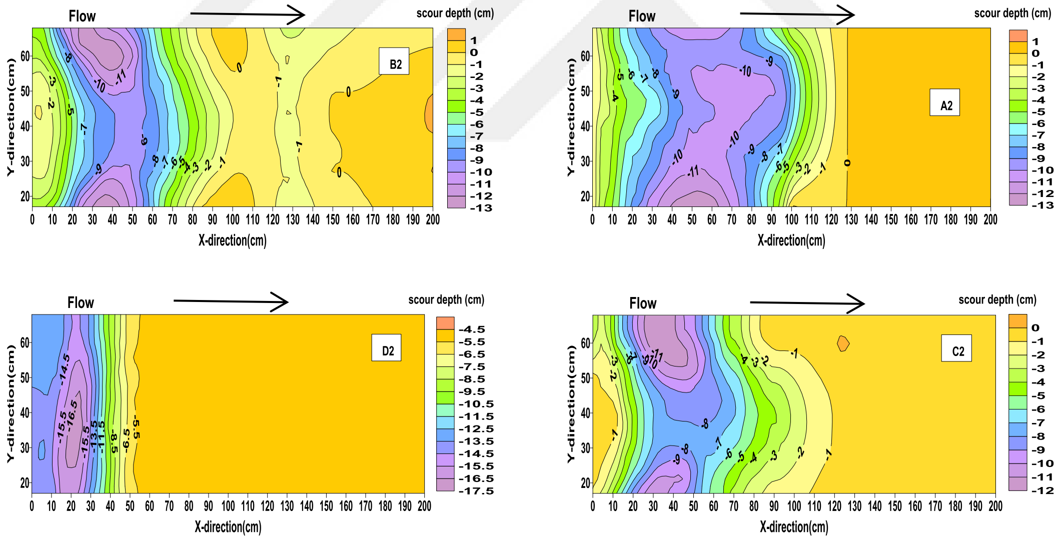

Figure 4.11 The scour pattern in front of models A2, B2, C2 and D2

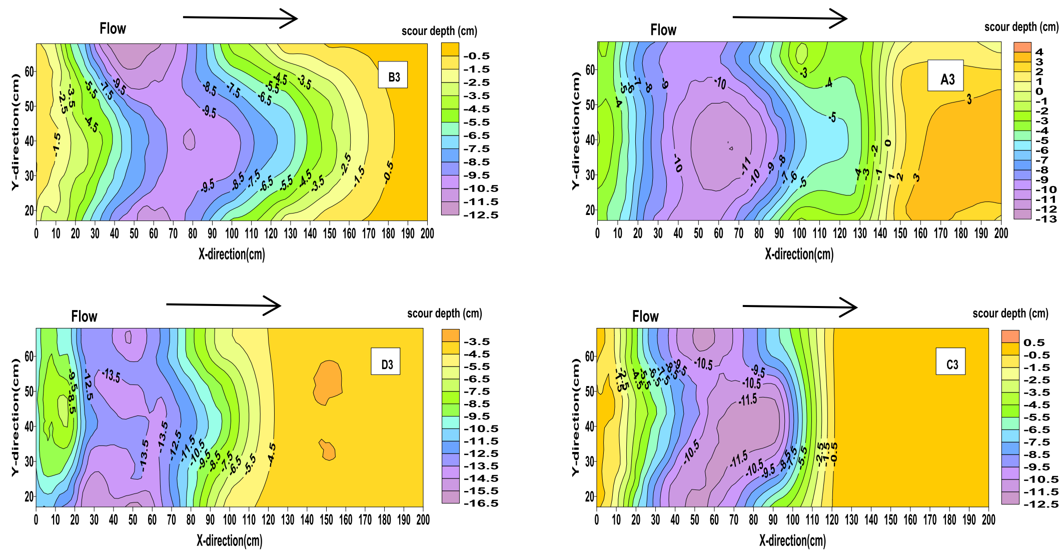

Figure 4.12 The scour pattern in front of models A3, B3, C3 and D3

It is seen from Figures (4.13,4.14 and 4.15) that, the effect of the vortex is very strong for model D, but the effect of the vortex is reduced for model C due to large energy dissipation.

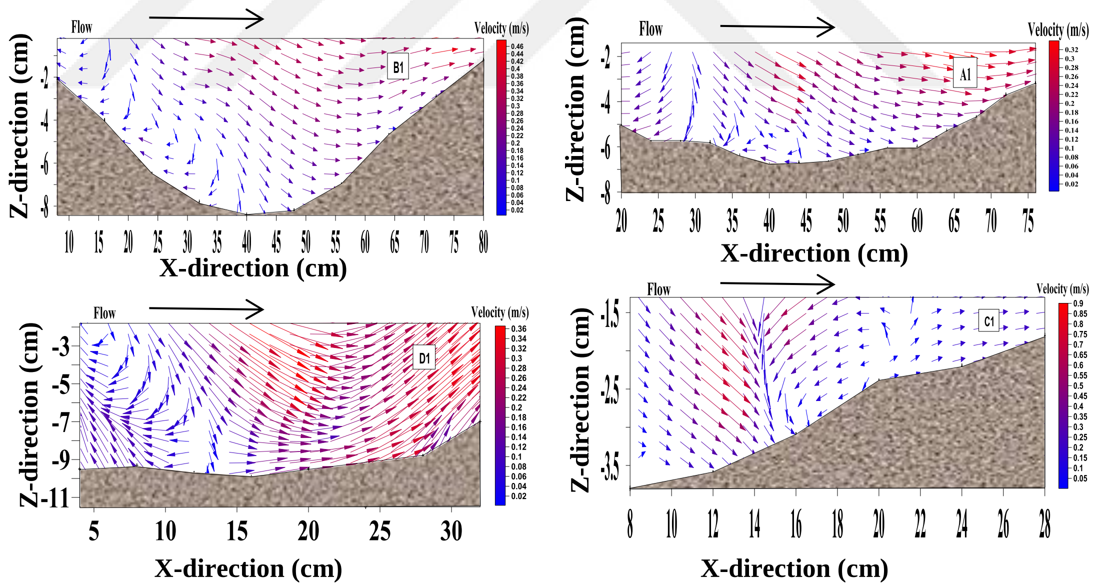

Figure 4.13 Velocity vectors in vertical plane along the center line of the channel for models A1, B1, C1 and D1

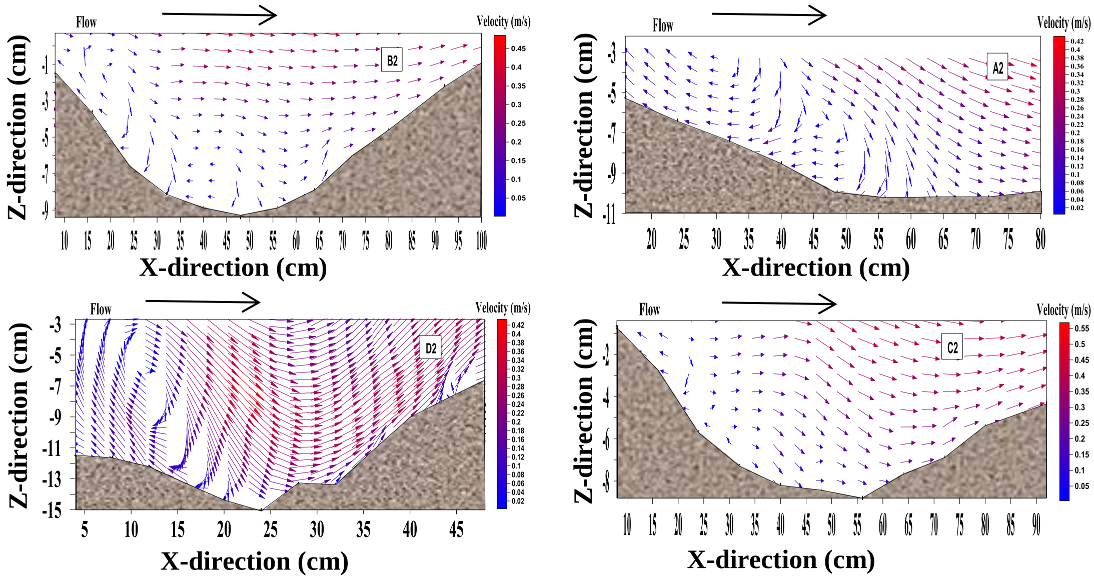

Figure 4.14 Velocity vectors in vertical plane along the center line of the channel for models A2, B2, C2 and D2

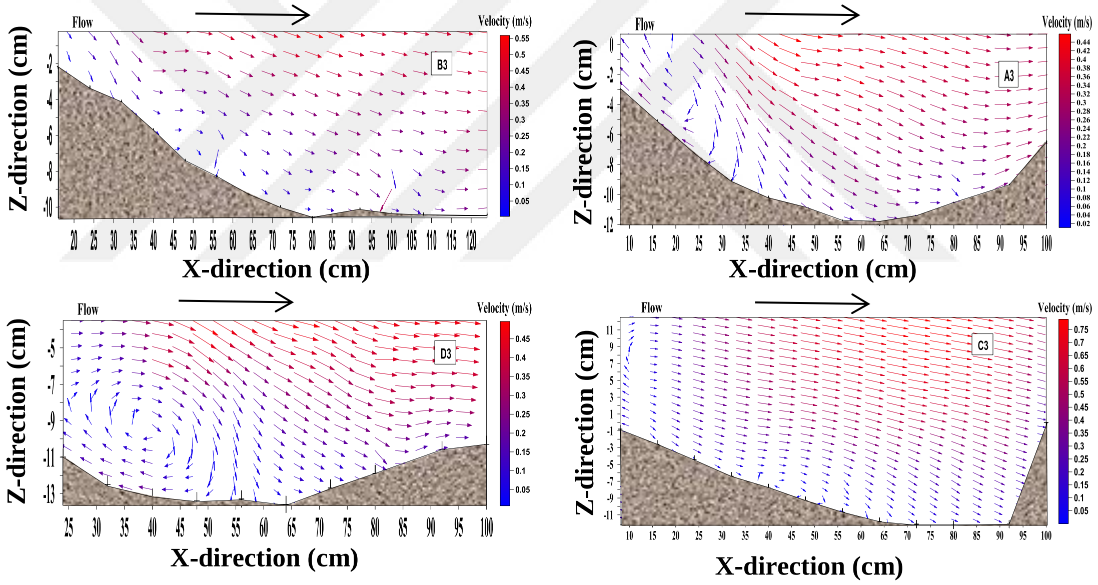

Figure 4.15 Velocity vectors in vertical plane along the center line of the channel for models A3, B3, C3 and D3

The biggest part of the kinetic energy of the flow is converted into energy of vortices, therefore, turbulent fluctuations are very strong at models A, B, and D, but the effect of the vortex is reduced for model C because the biggest part of the kinetic energy of the flow was dissipated (Uijttewaal, 2007).

The vortices at the models B and D are bottom roller because the flow regime is transition flow also called recirculation, but The vortices at the models A and C are surface roller because the flow regime is free flow (Tuyen, 2006).

4.1.2 Analyses by using Minitab program

In order to select an optimal model from experimental results, minitab program was used in the present thesis.

1) Copy data from a spreadsheet to Minitab:
we can copy data from Excel or other spreadsheet packages and paste into Minitab. This method works best for small amounts of data.

Table 4.5 All data used by the Minitab program for weir with inclined step

Model	**ΔE%**	**ds/Yu**	**$Vs^{1/3}$/Yu**	**Fr**	**FD**	**Yd/Yu**	**Yt/Yu**	**θ**
A1	33.072	2.000	5.521	4.554	53.628	0.218	1.818	0
B1	34.834	1.727	4.902	3.614	45.967	0.255	0.818	4.5
C1	37.297	0.691	3.632	2.701	37.855	0.309	0.682	8.7
D1	30.237	2.600	7.285	1.428	24.752	0.473	0.491	13
A2	33.434	2.032	5.541	4.345	57.204	0.238	2.063	0
B2	34.377	2.032	5.061	3.601	50.474	0.270	1.032	4.5
C2	37.639	1.841	5.004	3.048	45.161	0.302	0.786	8.7
D2	33.189	2.730	6.559	1.616	29.588	0.460	0.662	13
A3	33.832	1.699	4.998	4.131	59.587	0.247	1.918	0
B3	34.613	1.699	5.135	3.528	53.628	0.274	1.027	4.5
C3	37.794	1.671	4.828	2.683	44.690	0.329	0.822	8.7
D3	32.999	2.205	5.886	1.524	30.645	0.479	1.158	13

2) Define Custom Response Surface Design:
Define Custom Response Surface Design allow us to specify which columns contain

us factors and other design characteristics. After we define our design, we can use Modify Design, Display Design, and Analyze Response Surface Design.

The functional relationship for ΔE%, ds/Yu and $Vs^{1/3}$ /Yu with the main flow parameters may be expressed in dimensionless form as follows:

$$\Delta E\% = f_1\left(\frac{Yt}{Yu}, \frac{Yd}{Yu}, Fr\ , FD, \theta\right) \tag{4.1}$$

$$ds/Yu = f_3\left(\frac{Yt}{Yu}, \frac{Yd}{Yu}, Fr\ , FD, \theta\right) \tag{4.2}$$

$$Vs^{1/3}/Yu = f_3\left(\frac{Yt}{Yu}, \frac{Yd}{Yu}, Fr\ , FD, \theta\right) \tag{4.3}$$

We get equations as below.

ΔE%=-37.256+36.573Fr--0.949FD+176.709Yd/Yu+0.347Yt/Yu-0.235θ+2.74Fr*Fr +0.0466FD*FD-214.848Yd/Yu*Yd/Yu+1.216Yt/Yu*Yt/Yu+0.0629778θ*θ-1.10172 Fr*FD (4.4)

ds/Yu=-271.965+125.6Fr-6.0313FD+782.451Yd/Yu-2.066Yt/Yu+0.661θ+ 8.434Fr*Fr+0.164FD*FD-571.637Yd/Yu*Yd/Yu+2.535Yt/Yu*Yt/Yu-0.0717 θ*θ-3.146 Fr*FD (4.5)

$Vs^{1/3}$ / Yu=-256.546+124.8 Fr-6.332 FD+741.854 Yd/Yu-6.0531 Yt/Yu+1.244 θ+ 9.773 Fr*Fr+0.174 FD*FD-511.78 Yd/Yu*Yd/Yu+4.0304 Yt/Yu*Yt/Yu-0.103 θ*θ-3.312 Fr*FD (4.6)

The correlation coefficient (R^2) for each equation is 99%.
A comparison between predicted values by each equation and observed values experimentally is shown in Figures (4.16,4.17 and 4.18).

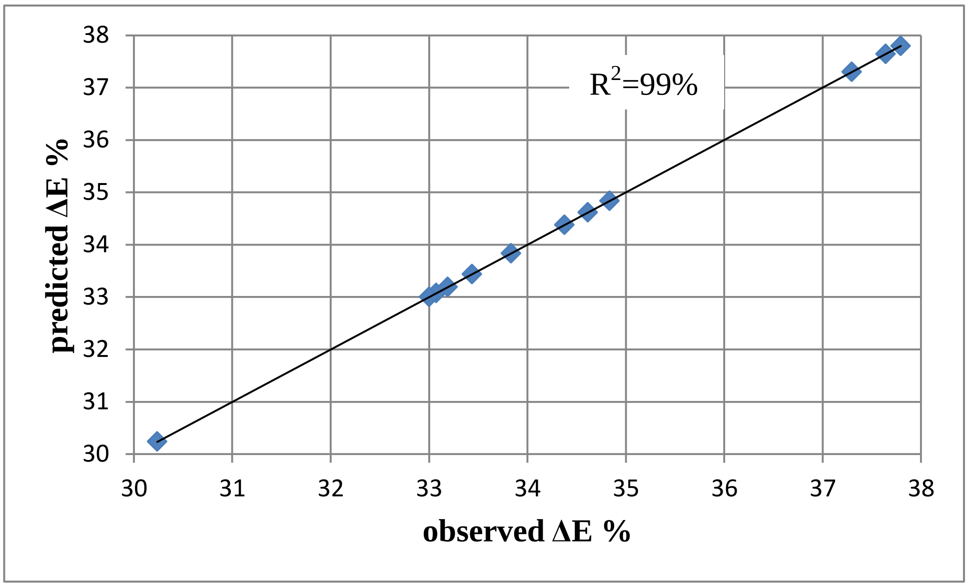

Figure 4.16 Variation of predicted values of ΔE % with observed ΔE % for weir with inclined step

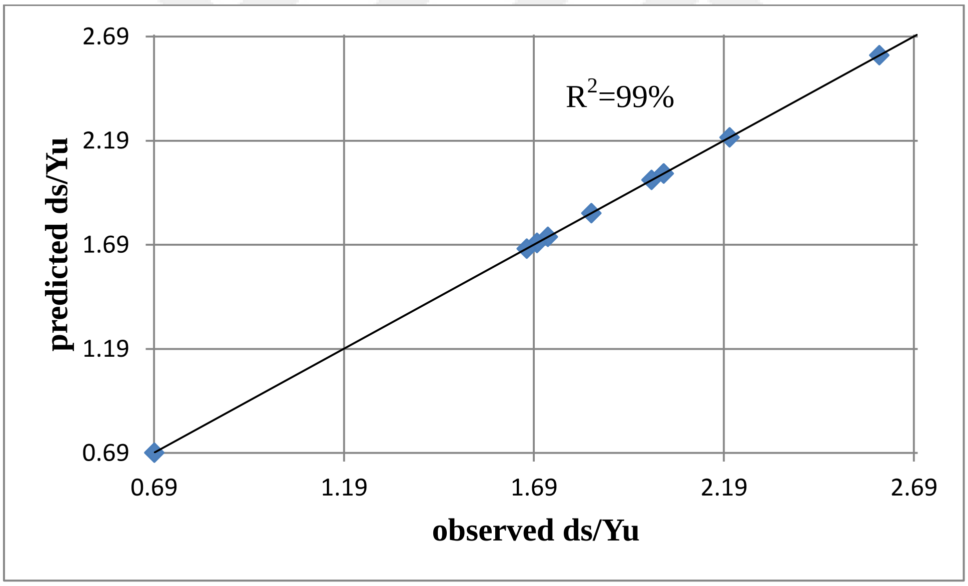

Figure 4.17 Variation of predicted values of ds/Yu with observed ds/Yu for weir with inclined step

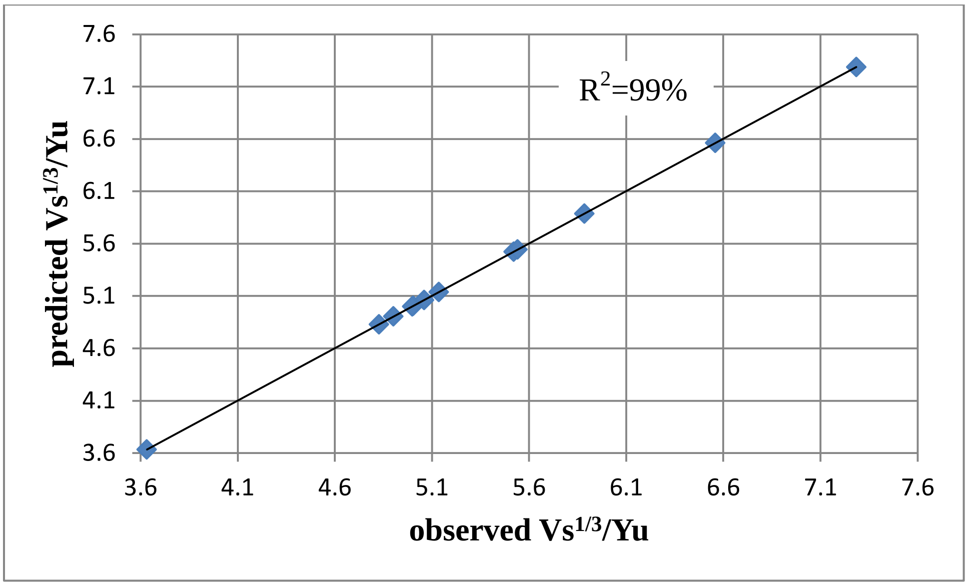

Figure 4.18 Variation of predicted values of $Vs^{1/3}/Yu$ with observed $Vs^{1/3}/Yu$ for weir with inclined step

Each figure indicates that all equations represented the measured data very well and hence could be used safely to predict the relative maximum depth of scour and energy dissipation.

3) Specifying Bounds:

To calculate the optimal numerical solution, we need to specify a response target and lower and/or upper bounds.

In Figure 4.19 the specify a response target, lower and/or upper bounds are shown .

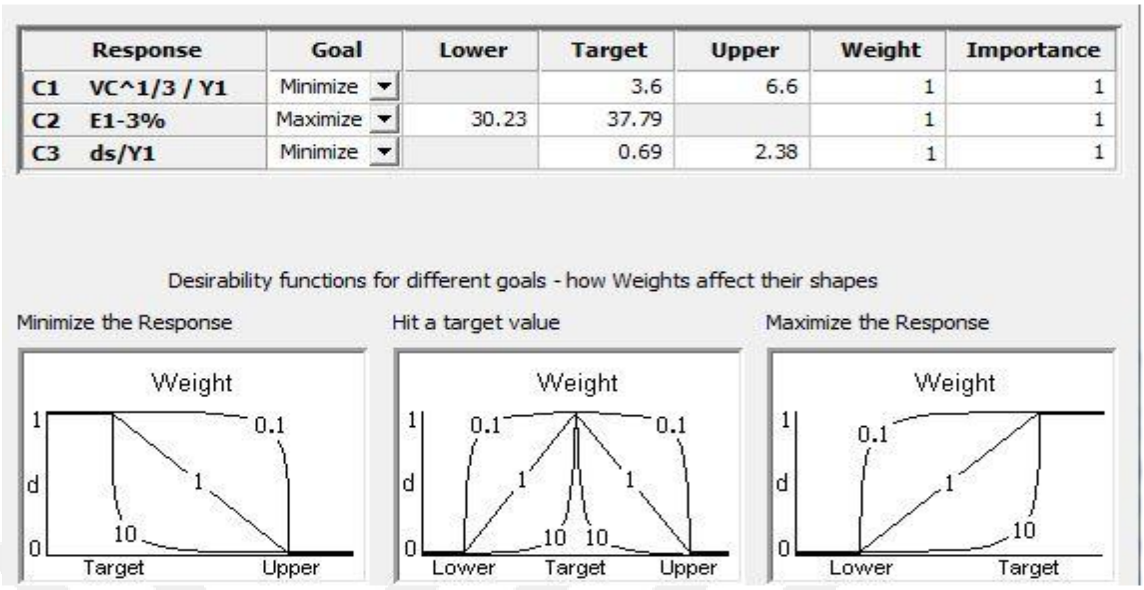

	Response	Goal	Lower	Target	Upper	Weight	Importance
C1	VC^1/3 / Y1	Minimize		3.6	6.6	1	1
C2	E1-3%	Maximize	30.23	37.79		1	1
C3	ds/Y1	Minimize		0.69	2.38	1	1

Figure 4.19 Specify a response target

After using Minitab analysis, we get the results as shown below.

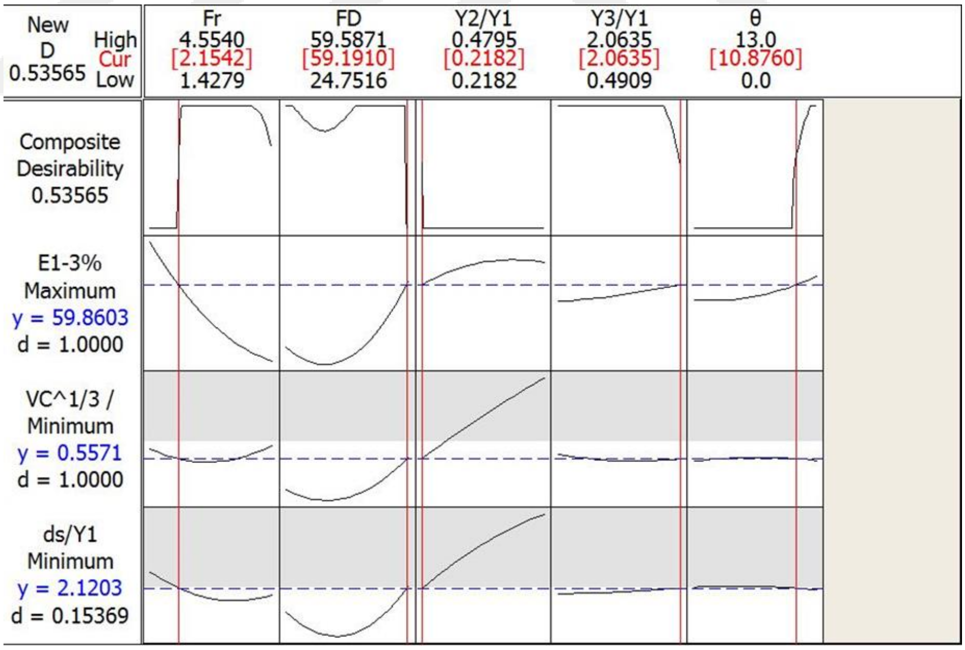

Figure 4.20 Results Minitab analysis

To prove these results from Minitab program; new model was tested under different flow intensity 15,20 and 25 l/s for the duration of 6 hours and was compared with the best model which we got from all experiments, and it was a model (C) with an angle (8.7^0).

Table 4.6 Total scour volume, maximum depth of scour, maximum local scour depth distance from the weir and Redaction volume and depth of scour comparing with model A

Model	**Q (l/s)**	**θ^0**	**Vs (cm^3)**	**ds (cm)**	**Rv %**	**Rd %**	**Ls (cm)**
C1	15	8.7	7974	3.8	71.51	65.45	12
E1	15	10.8	7846	3.5	71.97	68.18	12
C2	20	8.7	31338	11.6	26.33	9.38	36
E2	20	10.8	8247	4	80.61	68.75	15
C3	25	8.7	43784	12.2	9.88	1.61	76
E3	25	10.8	12936	9	73.37	27.42	40

It is clear that the model modified E minimizes the depth and the volume of local scour more than the best model C at each discharge.

The water surface profiles for each run were measured as shown in Figures (4.21, 4.22, and 4.23).

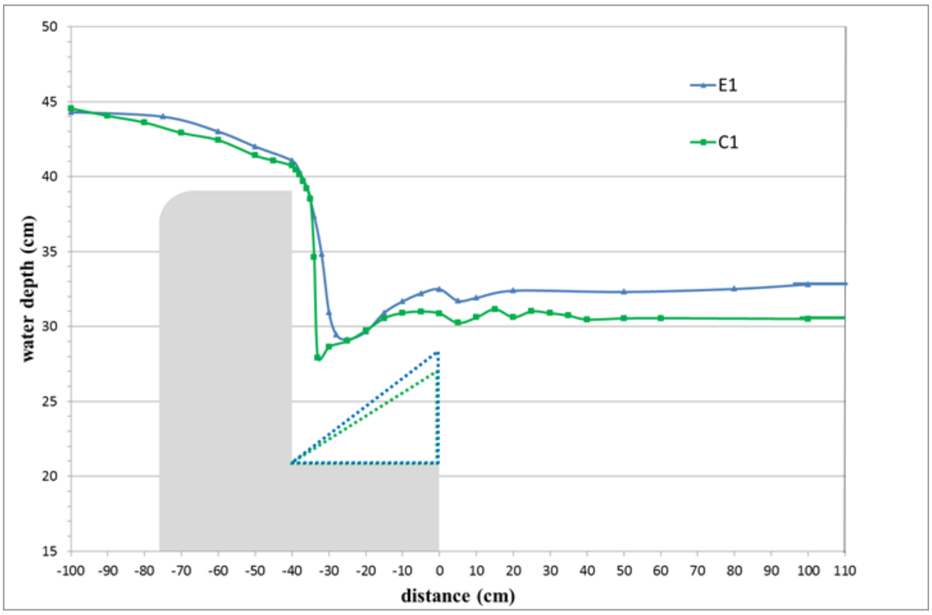

Figure 4.21 Longitudinal water surface profiles at the discharge of 15l/s for modified model E and best model C

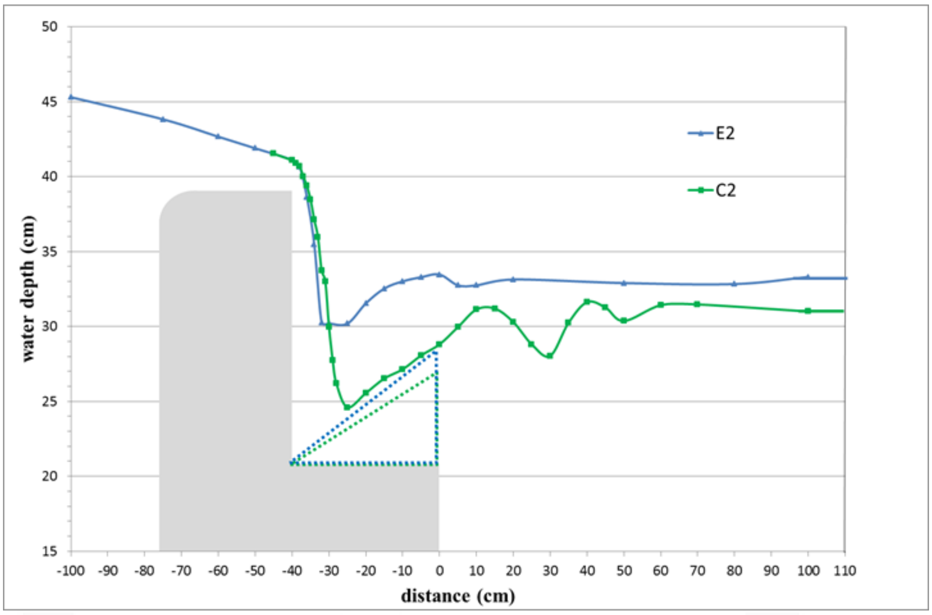

Figure 4.22 Longitudinal water surface profiles at the discharge of 20l/s for modified model E and best model C

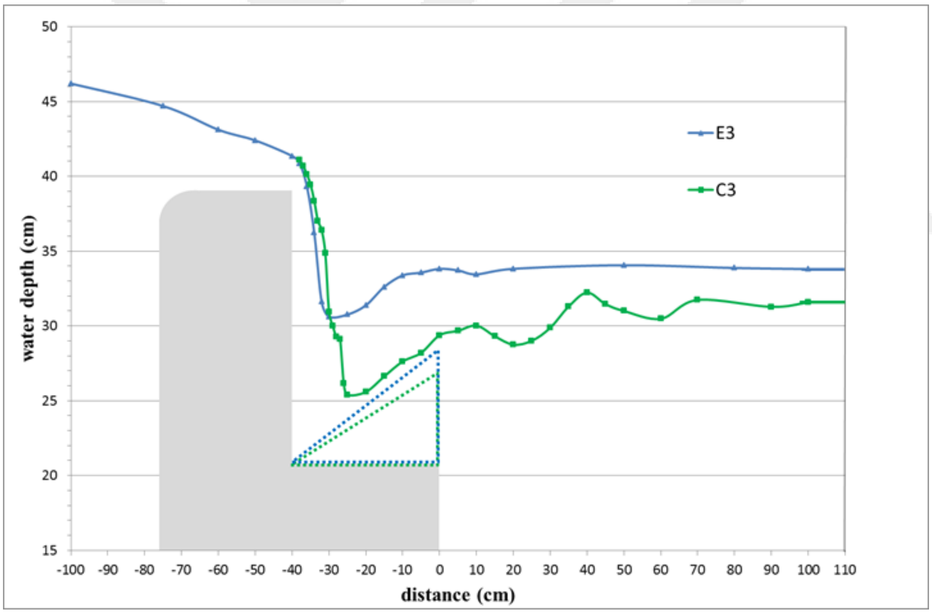

Figure 4.23 Longitudinal water surface profiles at the discharge of 25l/s for modified model E and best model C

It is seen that the water surface at modified model E is smooth, and there is no effect of vortices at downstream (D/S) of the weir, but the water surface at best a model C is more turbulent than model modified E at each discharge.

The rate of scour at each run for modified model E and best model C as shown in Figures (4.24, 4.25, and 4.26).

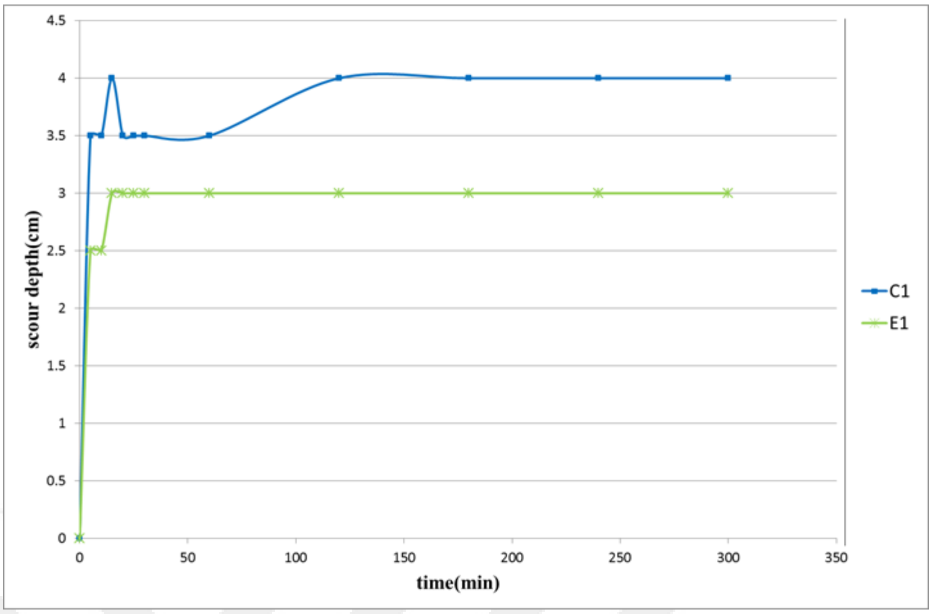

Figure 4.24 Downstream scour development with respect to time at the discharge of 15 l/s for modified model E and best model C

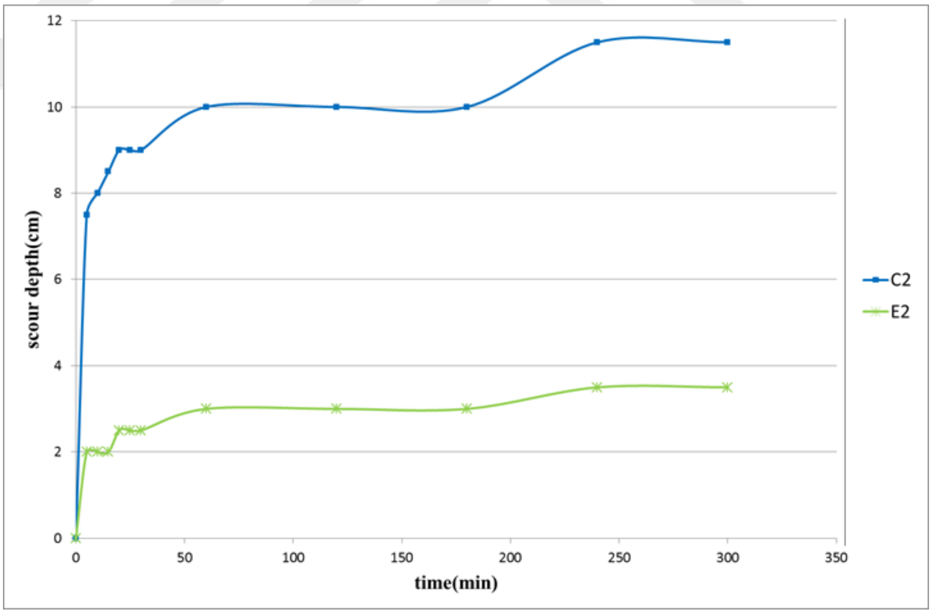

Figure 4.25 Downstream scour development with respect to time at the discharge of 20 l/s for modified model E and best model C

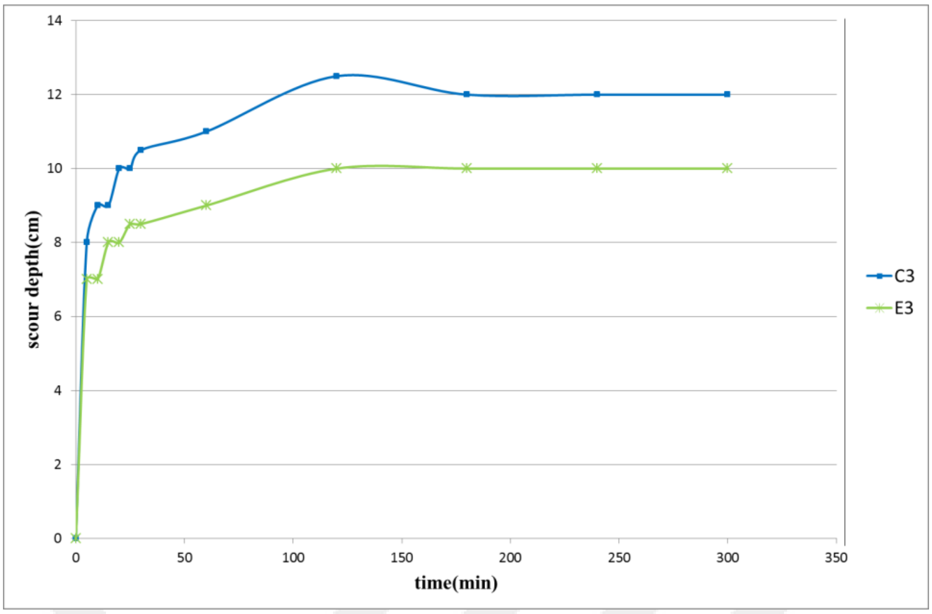

Figure 4.26 Downstream scour development with respect to time at the discharge of 25 l/s for modified model E and best model C

It is clear that the equilibrium got at modified model E a faster than best model C.

The bed profile for each discharge is given in Figures (4.27, 4.28 and 4.29).

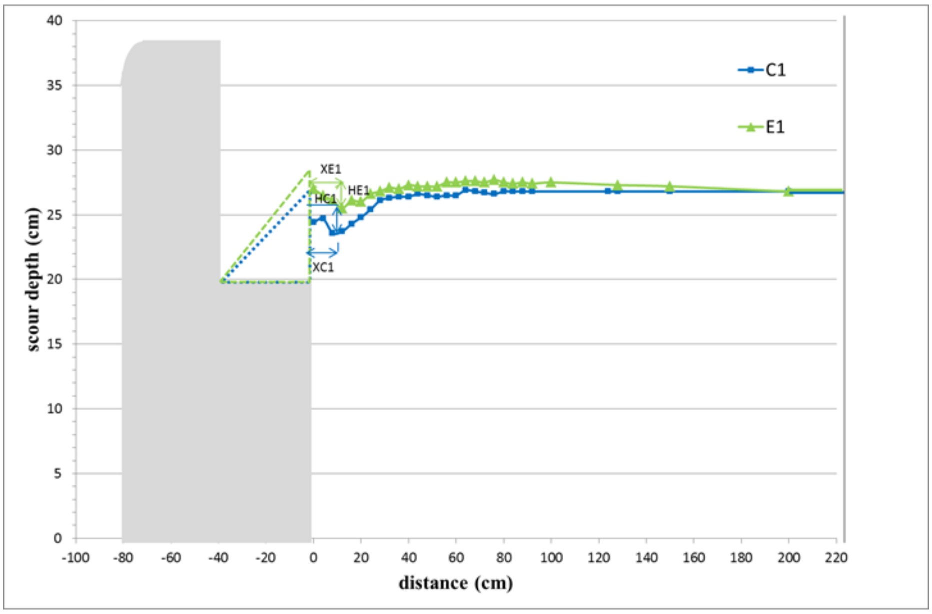

Figure 4.27 Bed profile at the discharge of 15l/s for modified model E and best model C

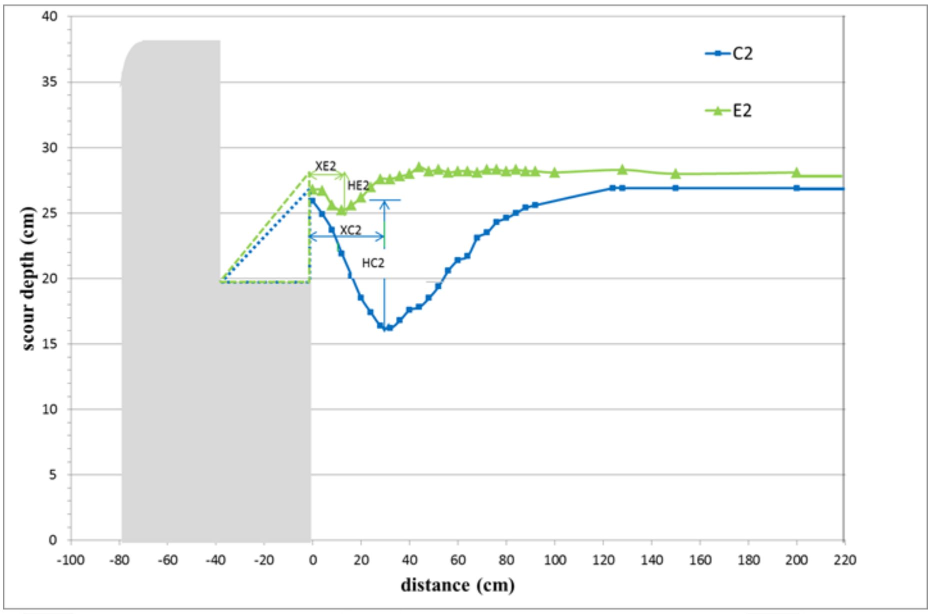

Figure 4.28 Bed profile at the discharge of 20l/s for modified model E and best model C

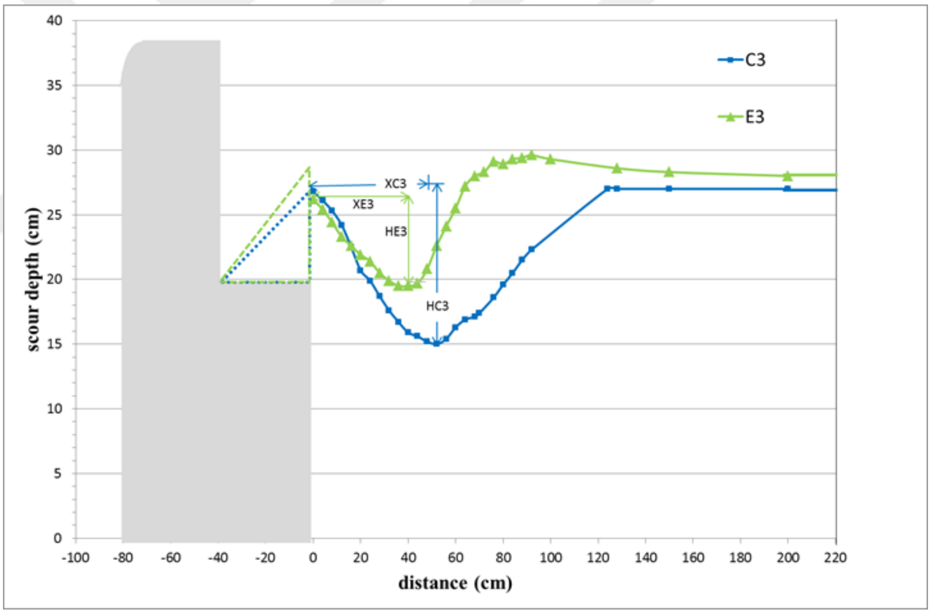

Figure 4.29 Bed profile at the discharge of 25l/s for modified model E and best model C

As shown, that the minimum depth and volume of scour for each discharge has occurred in the modified model E.

Figures (4.30, 4.31 and 4.32) show the scour pattern on the modified model E and best model C.

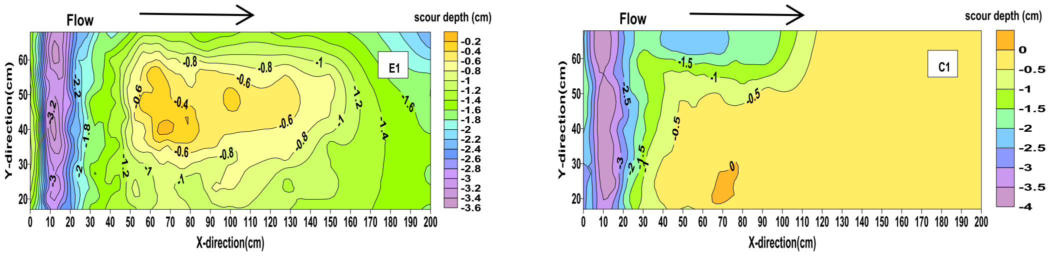

Figure 4.30 The scour pattern in front of models C1 and E1

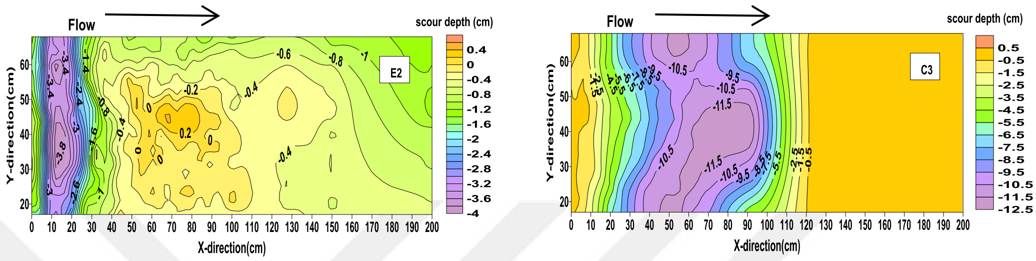

Figure 4.31 The scour pattern in front of models C2 and E2

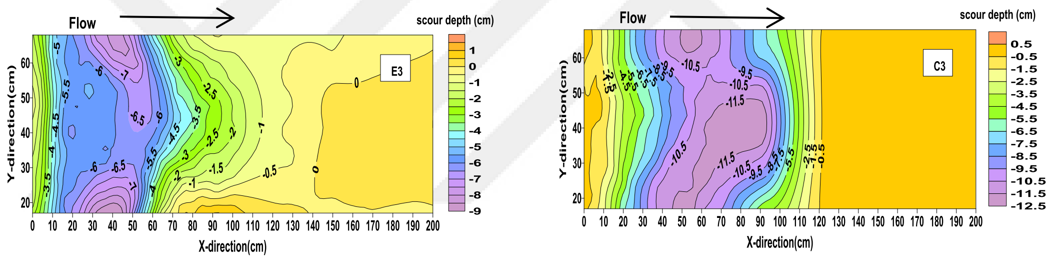

Figure 4.32 The scour pattern in front of models C3 and E3

It is seen from Figure (4.33) that, the effect of the vortex is weak at modified model E, but the best model C is more turbulent than modified model E due to large energy dissipation.

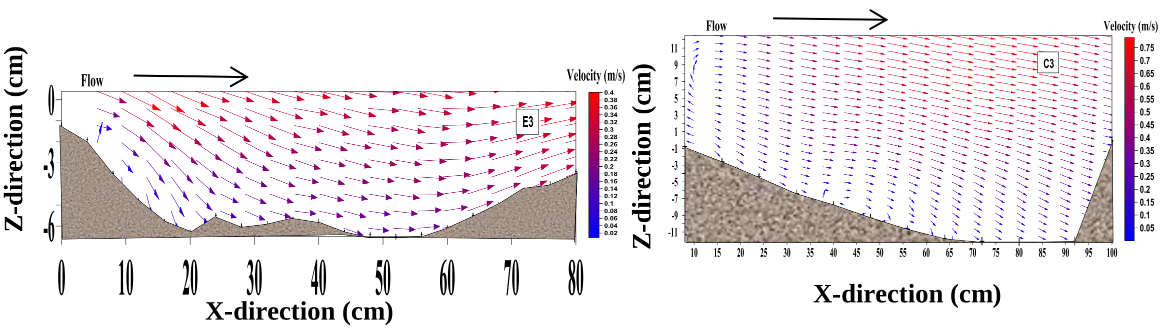

Figure 4.33 Velocity vectors in vertical plane along the center line of the channel for models C3 and E3 and discharge (25 l/s)

Figures (4.34, 4.35, 4.36, 4.37 and 4.36) show the each model during the run.

Figure 4.34 Picture of model A

Figure 4.35 Picture of model B

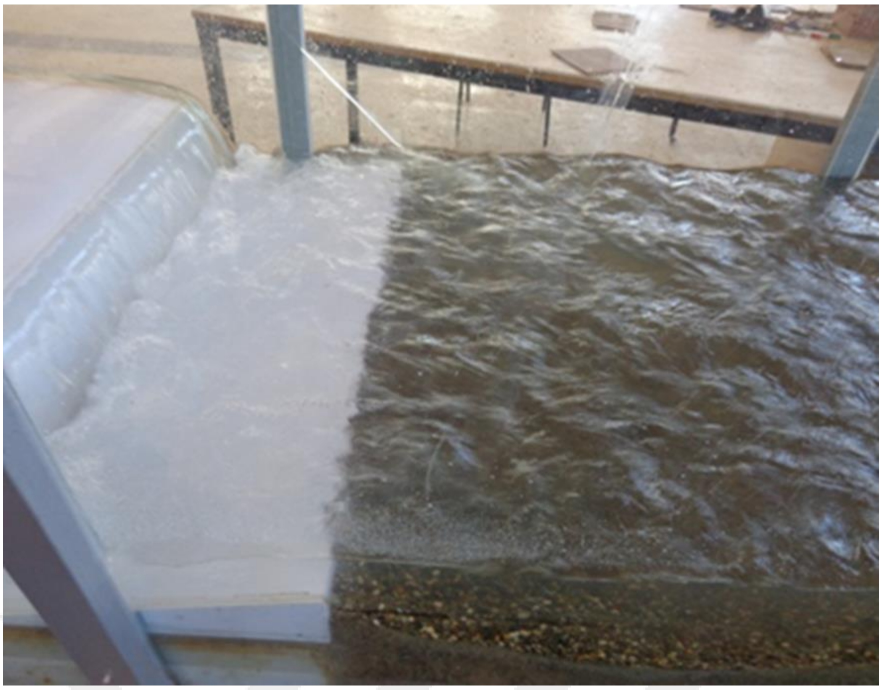

Figure 4.36 Picture of model C

Figure 4.37 Picture of model D

Figure 4.38 Picture of modified model E

It is seen from Figure (4.38) that, the water surface at model modified E is smooth and there is no effect of vortices at downstream (D/S) of the weir, on the contrary, the other models where more turbulent during the run.

4.2 Discussion of experimental results of weir with end sill

Analysis of results included four main aspects; local scour dimension, energy dissipation, water surface profiles, velocity distribution for single step broad crested weir with different height and porosity of the hollow end sill.

4.2.1 Local Scour Dimensions

The depth of local scour for weir with end sill was measured and experimental results of the models will be compared and discussed in this section. The total scour volume, maximum local scour (ds) and local scour distance from the weir (Ls) were compared for each of the seven models as shown in Table (4.7).

Table 4.7 Total volume of scour, maximum depth of scour and local scour distance from the weir for single step broad crested weir with end sill

Model	Q (l/s)	P2 (cm)	dr (cm)	e (%)	Vs (cm^3)	ds (cm)	Ls (cm)
A1	15	21	0	100	27993	11	40
F1	15	24	1	20	12451	7.2	10
G1	15	24	1.5	30	11160	6	16
H1	15	24	1.7	35	12136	6	18
K1	15	27	1	25	13748	10.5	6
M1	15	27	1.1	30	13772	9	12
N1	15	30	1	30	15311	11.5	10
A2	20	21	0	100	42537	12.8	52
F2	20	24	1	20	13663	8.4	15
G2	20	24	1.5	30	11347	6.5	18
H2	20	24	1.7	35	11621	6.5	20
K2	20	27	1	25	16580	11.7	8
M2	20	27	1.1	30	16715	10.5	16
N2	20	30	1	30	22218	13.5	15
A3	25	21	0	100	48583	12.4	68
F3	25	24	1	20	17898	8.9	20
G3	25	24	1.5	30	15686	7.5	26
H3	25	24	1.7	35	15950	7.5	26
K3	25	27	1	25	21031	11.7	15
M3	25	27	1.1	30	22328	11	16
N3	25	30	1	30	47904	17.3	20

It is clear that the model G and H minimizes the scour depth and the volume of local scour more than other models at each discharge because dissipate residual energy and reduce the velocity of the flow to a point where the flow becomes unable to scour the downstream channel bed (Al- Moula, 2014).

The function of the end sill is to ensure the formation of a jump and to control its position under all probable operating conditions lead to reduce the length of the jump and to control the scour (Chow, 1959).

The end sill has the additional function of diffusing the residual portion of high velocity.

The reduction of the local scour and total volume for each run were measured as shown in Table (4.8).

Table 4.8 Reduction total volume and depth of scour for weir with end sill comparing with model A

Model	Q (l/s)	P2 (cm)	dr (cm)	e (%)	Rv (%)	Rd (%)
F1	15	21	1	20	55.52	34.55
G1	15	21	1.5	30	60.13	45.45
H1	15	21	1.7	35	56.65	45.45
K1	15	27	1	25	50.89	4.55
M1	15	27	1.1	30	50.80	18.18
N1	15	30	1	30	45.30	0
F2	20	21	1	20	67.88	34.38
G2	20	21	1.5	30	73.32	49.22
H2	20	21	1.7	35	72.68	49.22
K2	20	27	1	25	61.02	8.59
M2	20	27	1.1	30	60.70	17.97
N2	20	30	1	30	47.77	0
F3	25	21	1	20	63.16	28.23
G3	25	21	1.5	30	67.71	39.52
H3	25	21	1.7	35	67.17	39.52
K3	25	27	1	25	56.71	5.65
M3	25	27	1.1	30	54.00	11.29
N3	25	30	1	30	1.40	0

Scour depth was reduced 45.45 %, 49.22% and 39.52% for models G and H comparison with model A at each discharge. Also, the model G reduces local scour hole volume about 60.13%, 73.32%, and 67.71% compared with models A at each discharge. It is clear that the models G, H minimizes the depth and volume of local scour more than other models due to large energy dissipation.

The values of average and critical velocity for each model are shown in Table (4.9).

Table 4.9 Experimental measurements of average and critical velocities for weir with end sill

Model	Q (l/s)	P2 (cm)	dr (cm)	e (%)	Va (m/s)	Vc (m/s)	Va / Vc
A1	15	21	0	100	1.563	0.319	4.892
F1	15	24	1	20	0.625	0.372	1.680
G1	15	24	1.5	30	0.647	0.370	1.748
H1	15	24	1.7	35	0.721	0.363	1.985
K1	15	27	1	25	0.647	0.370	1.748
M1	15	27	1.1	30	0.647	0.37	1.748
N1	15	30	1	30	0.647	0.370	1.748
A2	20	21	0	100	1.667	0.331	5.028
F2	20	24	1	20	0.676	0.385	1.754
G2	20	24	1.5	30	0.641	0.389	1.649
H2	20	24	1.7	35	0.781	0.376	2.077
K2	20	27	1	25	0.694	0.384	1.811
M2	20	27	1.1	30	0.676	0.385	1.754
N2	20	30	1	30	0.735	0.380	1.935
A3	25	21	0	100	1.736	0.342	5.081
F3	25	24	1	20	0.781	0.390	2.001
G3	25	24	1.5	30	0.744	0.394	1.891
H3	25	24	1.7	35	0.845	0.385	2.192
K3	25	27	1	25	0.977	0.376	2.597
M3	25	27	1.1	30	0.781	0.39	2
N3	25	30	1	30	0.893	0.382	2.339

The water surface for each run of experiments was measured as shown in Figures (4.39, 4.40, and 4.41).

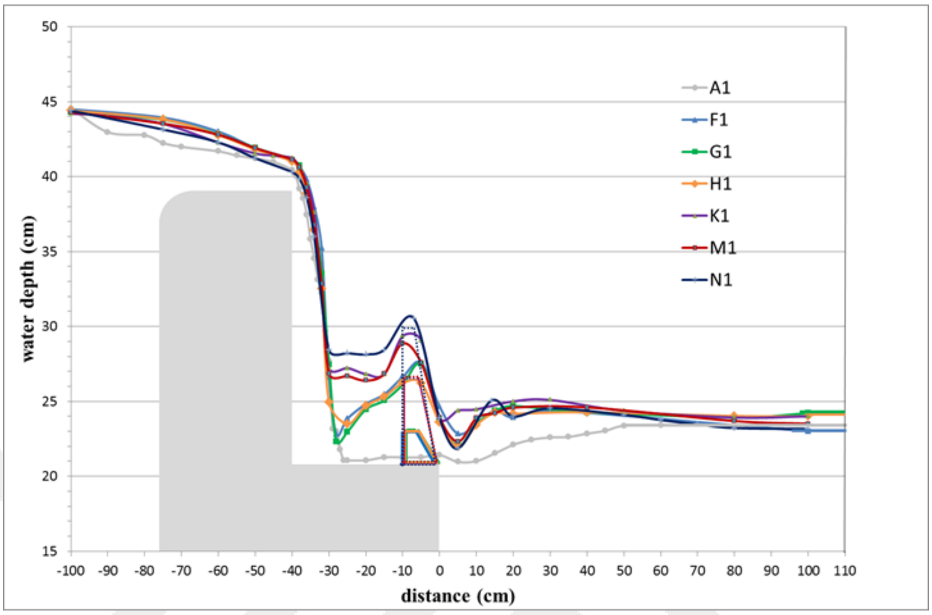

Figure 4.39 Longitudinal water surface profiles at the discharge of 15l/s for weir with end sill

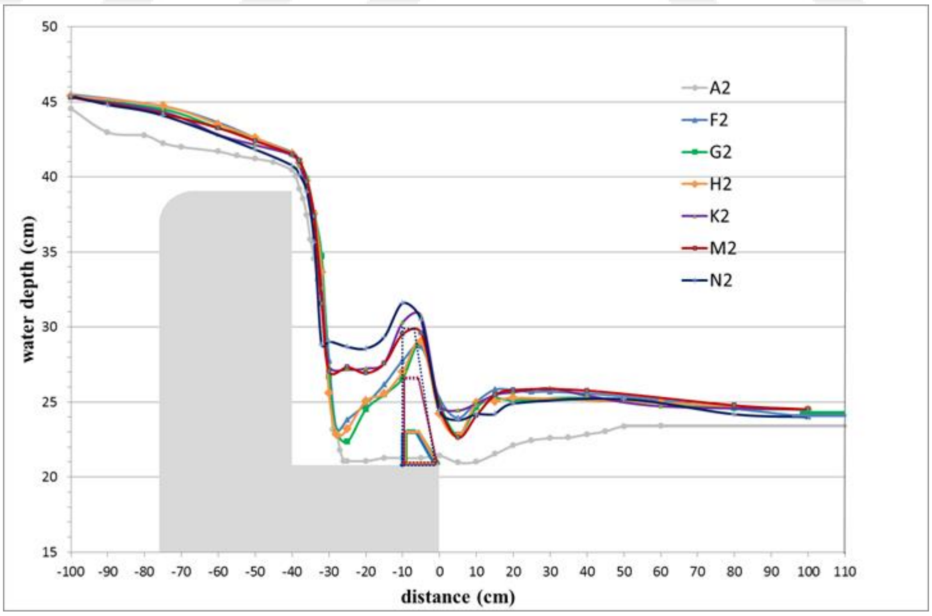

Figure 4.40 Longitudinal water surface profiles at the discharge of 20l/s for weir with end sill

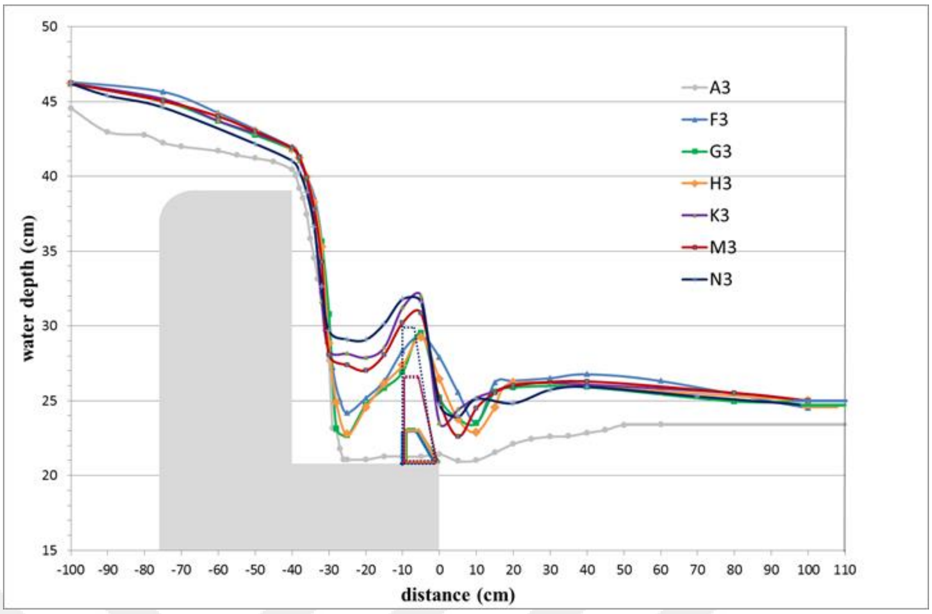

Figure 4.41 Longitudinal water surface profiles at the discharge of 25l/s for weir with end sill

It is seen that the trend of these water surface profiles for all discharges were mostly similar, follow the shape of the model and the water surface at models A, G and H are smooth, but the water surface of other models are more turbulent. The flow regime over the models A, G and H were surface jet flow because the surface is nearly horizontal and smooth, but the flow regime over other models was surface wave flow because of the mainstream following the free and wavy surface and a recirculation zone near the bottom (Tuyen, 2006).

The total energy in the inlet Eu and at the end of weir Et is calculated and shown in Table (4.10).

Table 4.10 Energy dissipation for weir with end sill

Model	Q (l/s)	P2 (cm)	dr (cm)	e (%)	Eu (cm)	Et (cm)	∆E%
A1	15	21	0	100	45.092	30.179	33.072
F1	15	24	1	20	45.092	23.885	47.031
G1	15	24	1.5	30	45.092	23.947	46.894
H1	15	24	1.7	35	45.092	23.685	47.475
K1	15	27	1	25	45.092	24.820	44.958
M1	15	27	1.1	30	45.092	24.12	46.51
N1	15	30	1	30	45.092	24.383	45.927
A2	20	21	0	100	46.103	30.688	33.434
F2	20	24	1	20	46.103	25.274	45.178
G2	20	24	1.5	30	46.103	24.774	46.263
H2	20	24	1.7	35	46.103	24.553	46.743
K2	20	27	1	25	46.103	25.678	44.302
M2	20	27	1.1	30	46.103	25.183	45.377
N2	20	30	1	30	46.103	25.573	44.530
A3	25	21	0	100	47.234	31.254	33.832
F3	25	24	1	20	47.234	26.491	43.916
G3	25	24	1.5	30	47.234	25.780	45.422
H3	25	24	1.7	35	47.234	25.645	45.706
K3	25	27	1	25	47.234	26.645	43.589
M3	25	27	1.1	30	47.234	26.145	44.647
N3	25	30	1	30	47.234	26.691	43.492

It is clear that the high energy dissipation at models G and H have optimum height where hydraulic jump formed between the toe of the weir and the end sill (Ali khani et al., 2010). The relative energy dissipation decreases with increasing the flow rate (Al- Moula, 2014).

The rate of scour at each run is also reduced considerably as shown in Figures (4.42, 4.43, and 4.44).

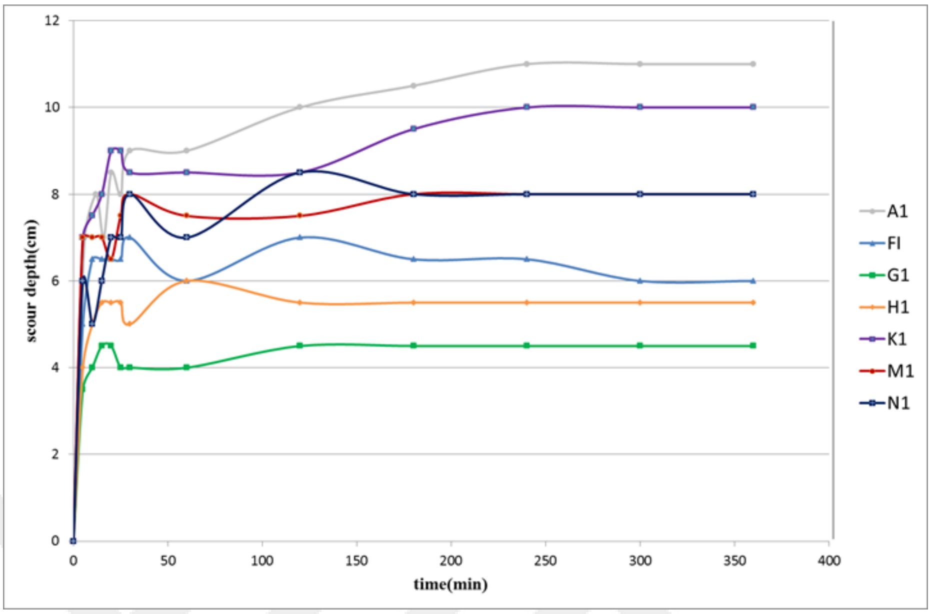

Figure 4.42 Downstream scour development with respect to time at the discharge of 15 l/s for weir with end sill

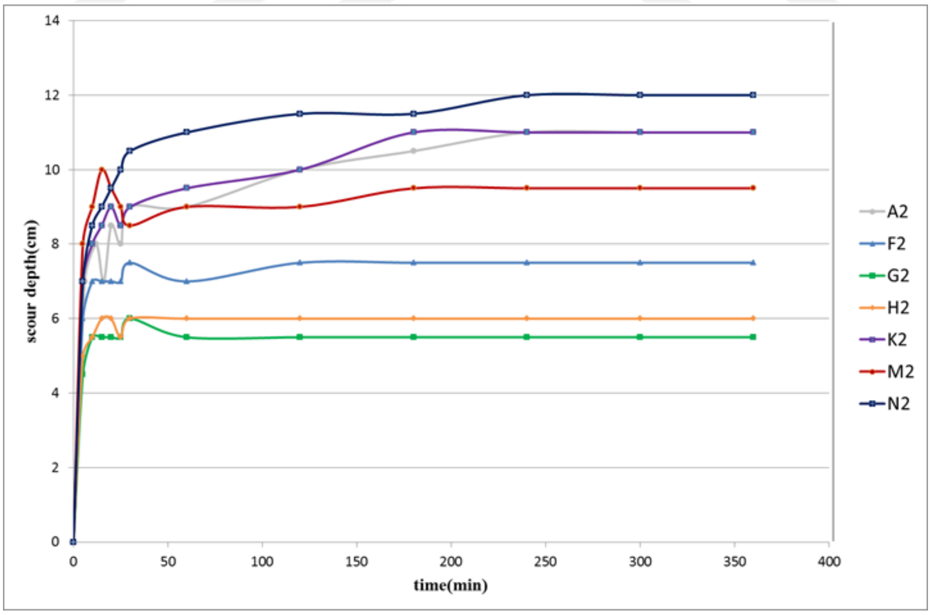

Figure 4.43 Downstream scour development with respect to time at the discharge of 20 l/s for weir with end sill

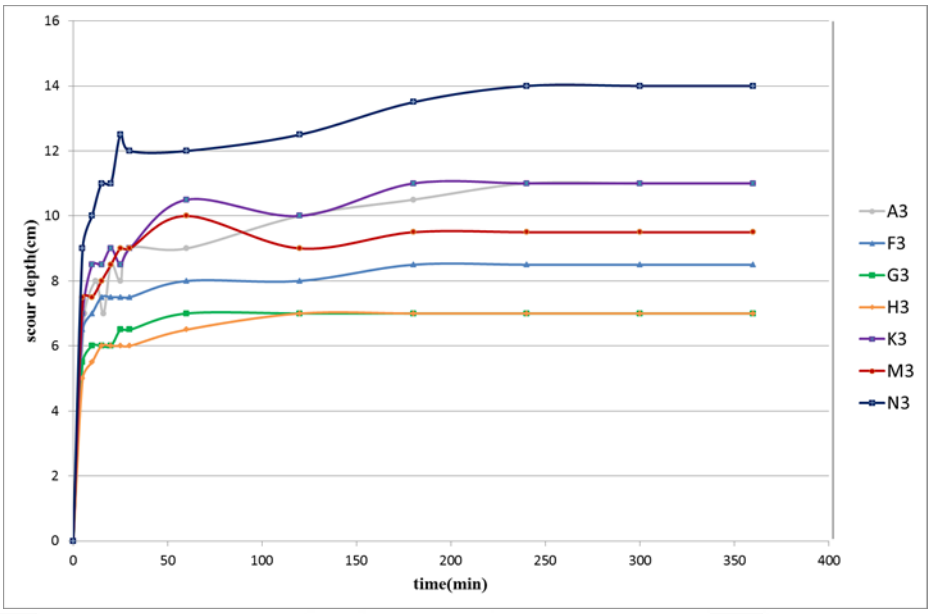

Figure 4.44 Downstream scour development with respect to time at the discharge of 25 l/s for weir with end sill

It is seen that all models reach equilibrium case after 250 minutes. The models G and H are more stable and very slow in scour hole development when compared with other models because the shape of the hole makes stable the surface profile, on the contrary, the other models were more turbulent.

The bed profile for each run is given in Figures (4.45, 4.46 and 4.47).

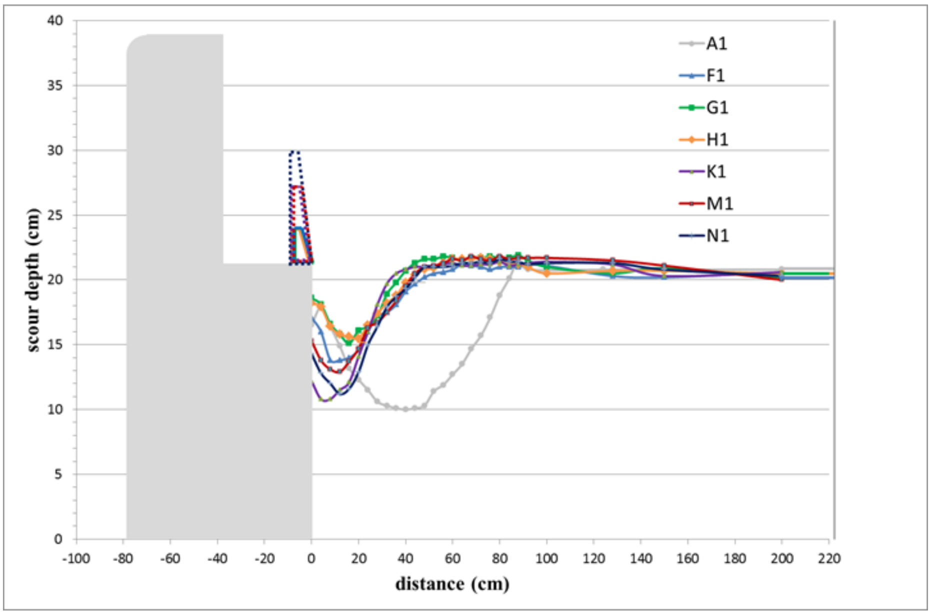

Figure 4.45 Bed profile at the discharge of 15l/s for weir with end sill

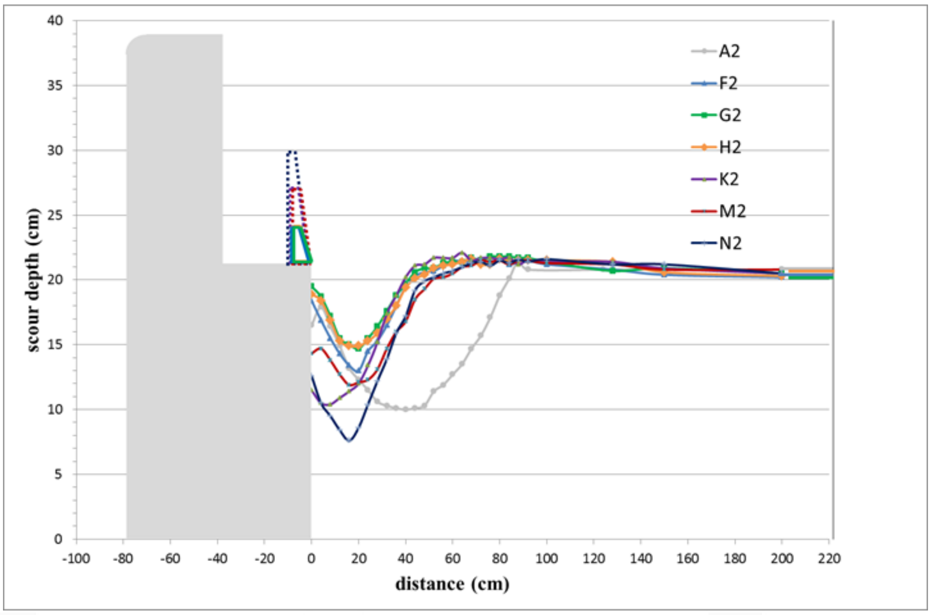

Figure 4.46 Bed profile at the discharge of 20l/s for weir with end sill

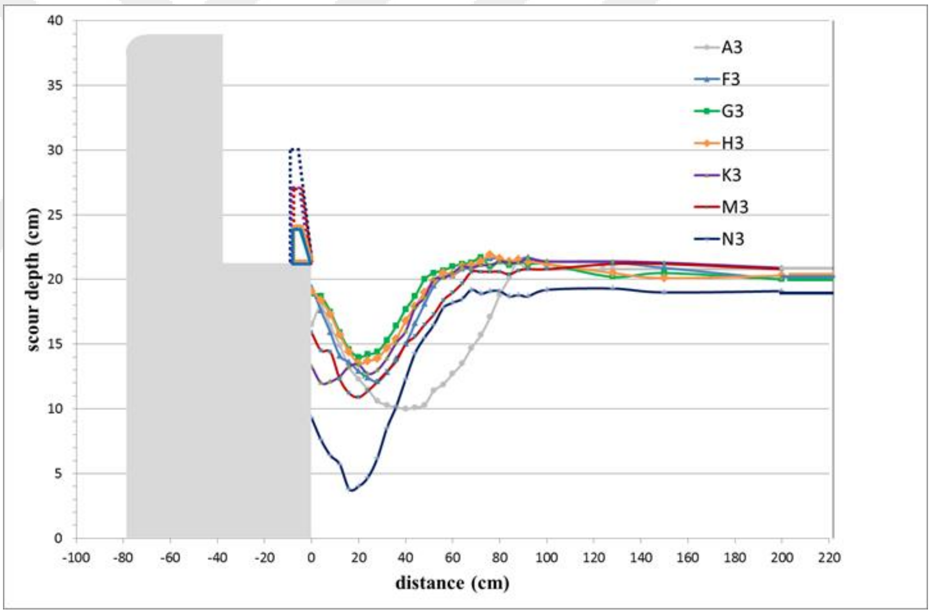

Figure 4.47 Bed profile at the discharge of 25l/s for weir with end sill

As shown in Figures 4.45, 4.46 and 4.47, the maximum scour depth and a minimum distance of scour depth from weir were found after the weir model N because turbulent shear stresses are higher than other models lead to exposure to failure in the future.

Figures (4.48, 4.49, 4.50) show the scour pattern at each model after each run. The models G, H minimizes the scour depth and maximum scour is occurred much away from the end of the weir.

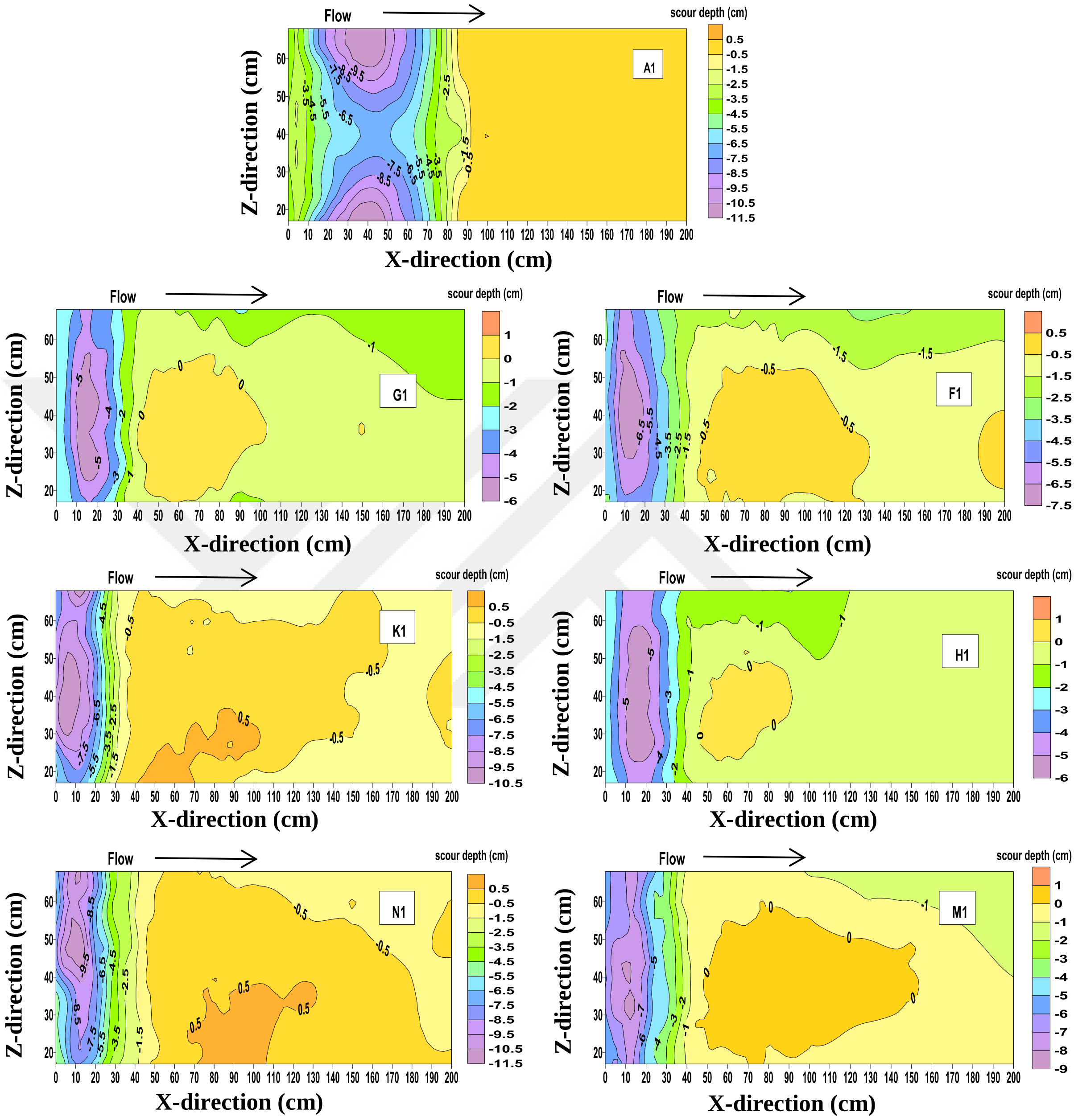

Figure 4.48 The scour pattern in front of models A1, F1, G1, H1, K1, M1 and N1

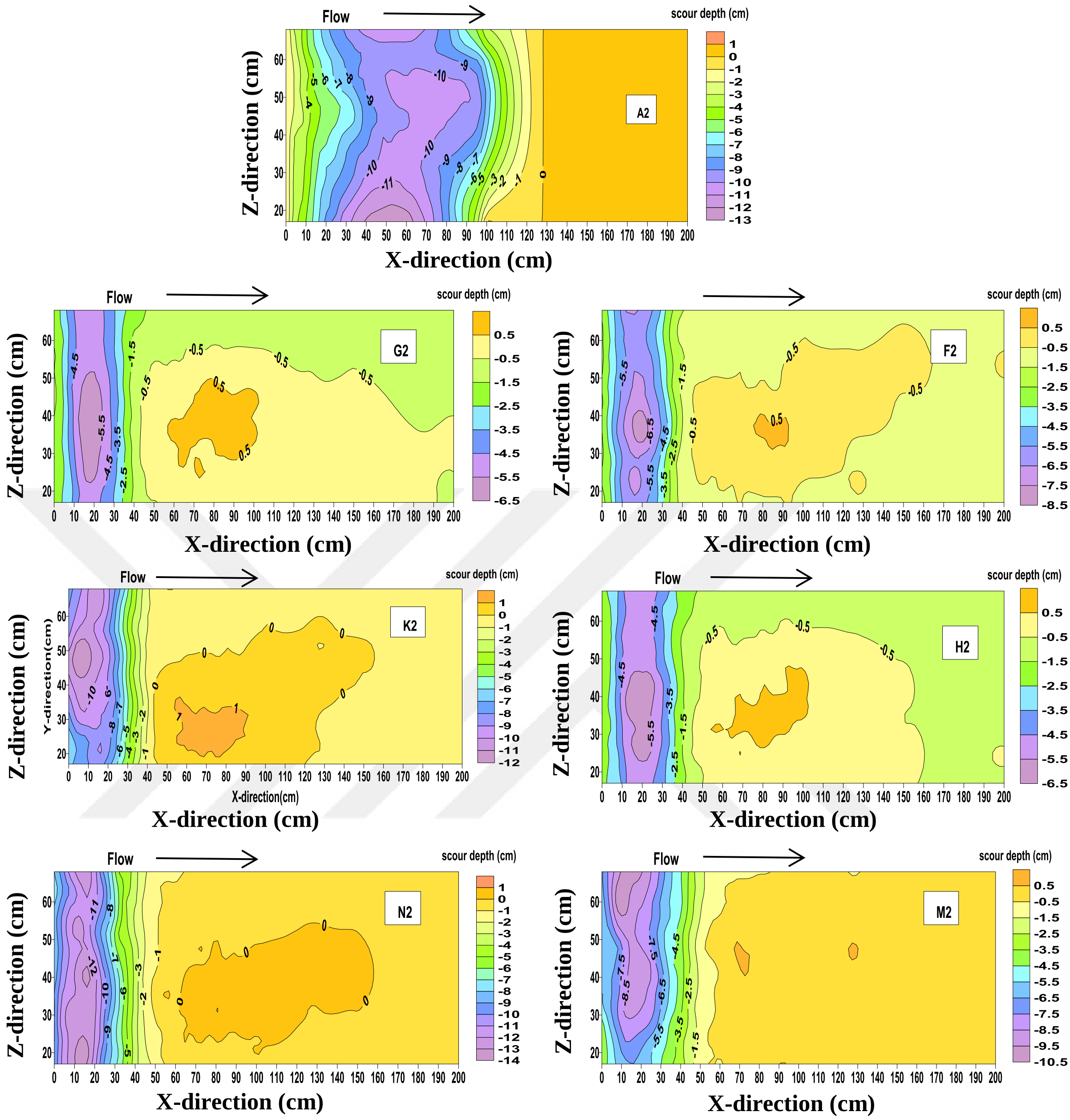

Figure 4.49 The scour pattern in front of models A2, F2, G2, H2, K2, M2 and N2

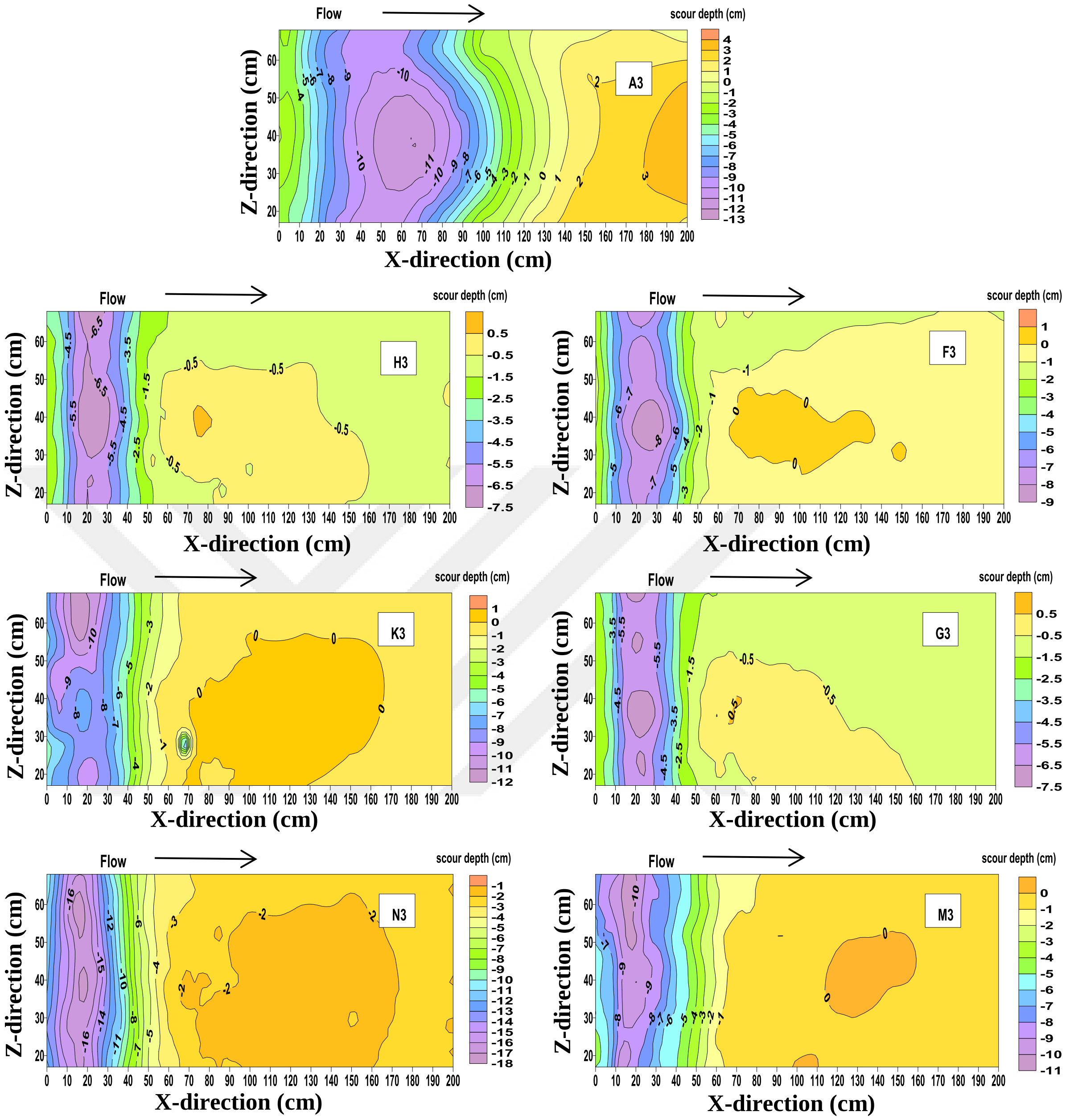

Figure 4.50 The scour pattern in front of models A3, F3, G3, H3, K3, M3 and N3

It is seen from Figures (4.51, 4.52 and 4.53) that, the effect of the vortex is very strong for model N, but the effect of the vortex is reduced for models G, H due to large energy dissipation.

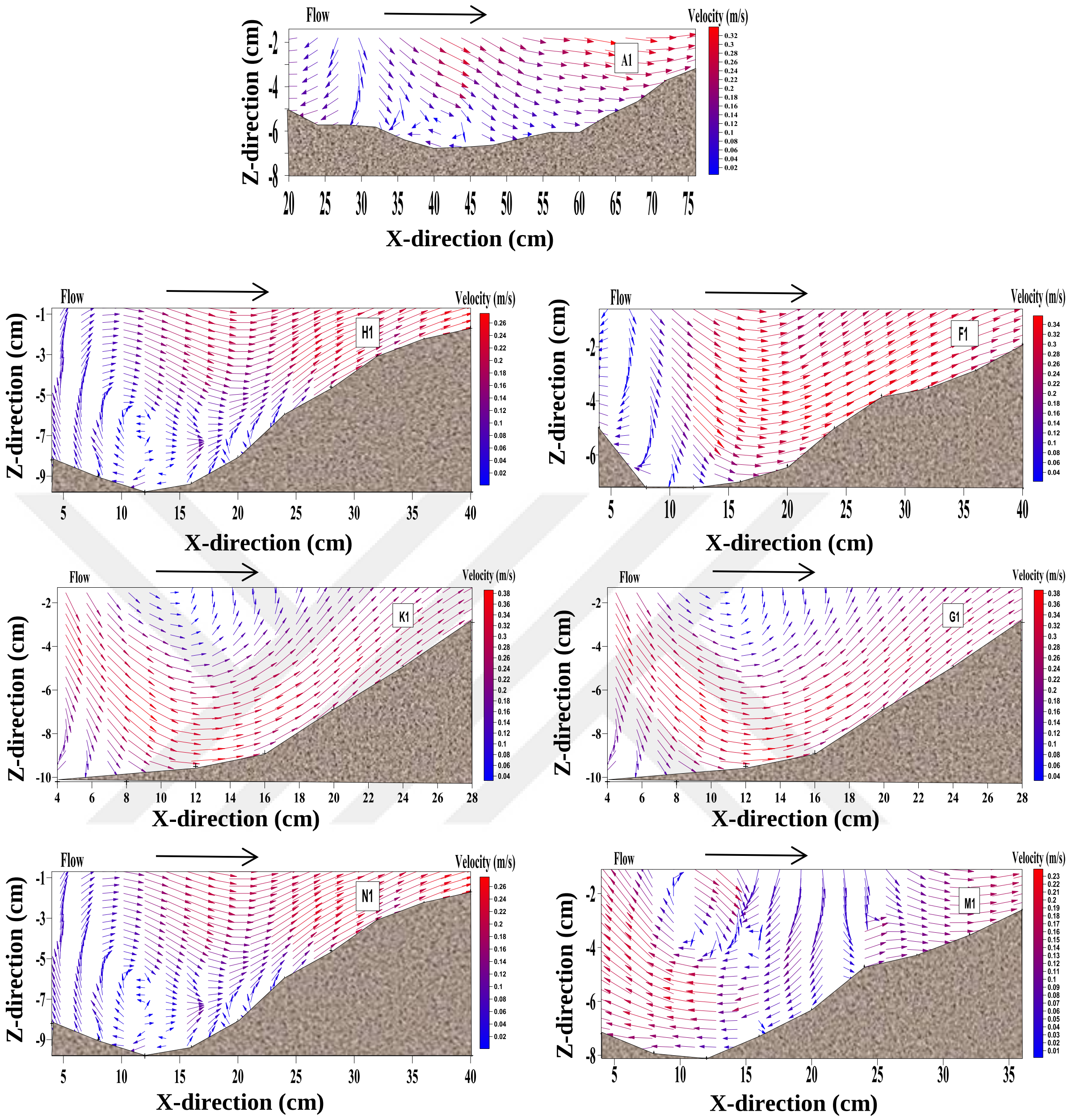

Figure 4.51 Velocity vectors in vertical plane along the center line of the channel for models A1, F1, G1, H1, K1, M1 and N1

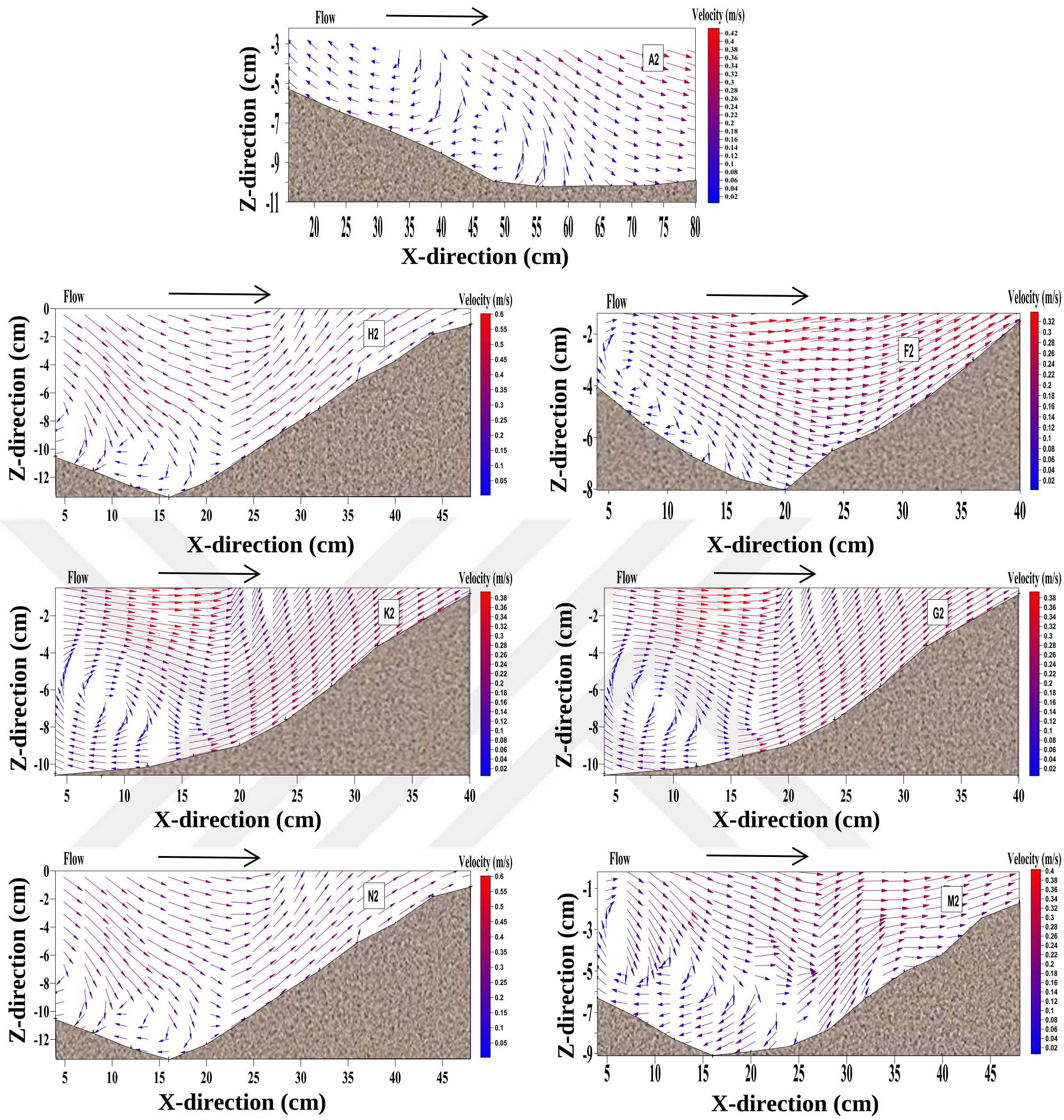

Figure 4.52 Velocity vectors in vertical plane along the center line of the channel for models A2, F2, G2, H2, K2, M2 and N2

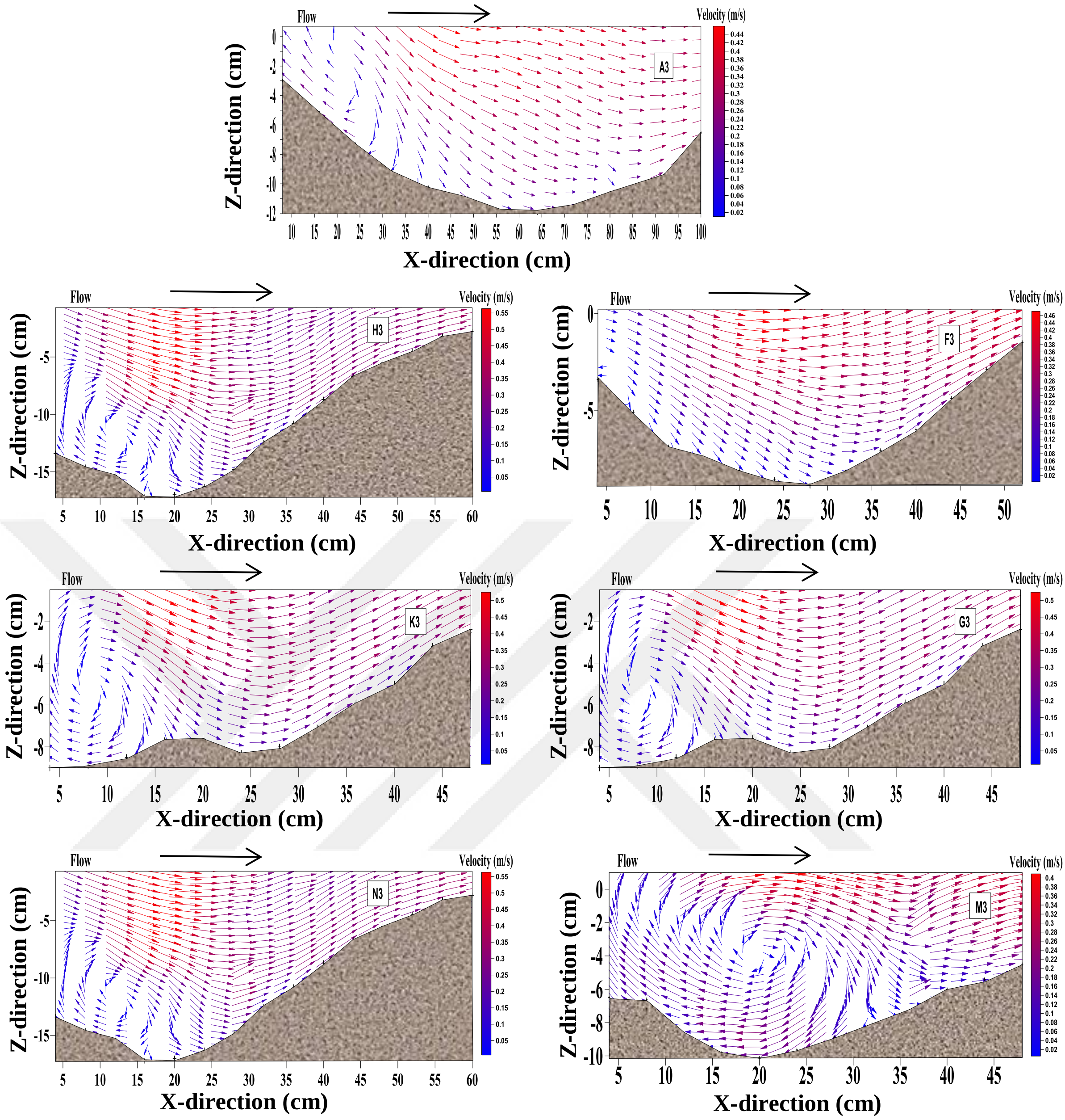

Figure 4.53 Velocity vectors in vertical plane along the center line of the channel for models A3, F3, G3, H3, K3, M3 and N3

The effect of the vortex is reduced for models G and H because the biggest part of the kinetic energy of the flow was dissipated, but other models have the turbulent fluctuations very strong because the biggest part of the kinetic energy of the flow is converted into energy of vortices (Uijttewaal, 2007).

The vortices at the models G and H are surface roller because the flow regime is free flow, but the vortices at other models are bottom roller because the flow regime is transition flow also called recirculation (Tuyen, 2006).

4.2.2 Prediction of scour depth, volume of scour and energy dissipation

By using step-wise regression (full cubic Method) which was developed to predict the maximum scour depth to the upstream water depth, cube root of the volume of scour to the upstream water depth and the energy dissipation ratio between upstream and downstream.

The functional relationship for ΔE%, ds/Yu and $Vs^{1/3}$ /Yu with the main flow parameters may be expressed in dimensionless form as follows:

$$\Delta E\% = f_1\left(\frac{\mathrm{Yt}}{\mathrm{Yu}}, \frac{\mathrm{Yd}}{\mathrm{Yu}}, \mathrm{Fr}, \mathrm{FD}, \mathrm{P2/P1}, \mathrm{dr/P1}, \mathrm{e}\right) \tag{4.14}$$

$$\mathrm{ds/Yu} = f_3\left(\frac{\mathrm{Yt}}{\mathrm{Yu}}, \frac{\mathrm{Yd}}{\mathrm{Yu}}, \mathrm{Fr}, \mathrm{FD}, \mathrm{P2/P1}, \mathrm{dr/P1}, \mathrm{e}\right) \tag{4.15}$$

$$\mathrm{Vs}^{1/3}/\mathrm{Yu} = f_3\left(\frac{\mathrm{Yt}}{\mathrm{Yu}}, \frac{\mathrm{Yd}}{\mathrm{Yu}}, \mathrm{Fr}, \mathrm{FD}, \mathrm{P2/P1}, \mathrm{dr/P1}, \mathrm{e}\right) \tag{4.16}$$

We get equations as below.

ds/Yu= 40.77966 -546.38271*dr/P1*dr/P188.81437*P2/P1*Pt/P1-117.33188*P2/P1 + -0.00584 *Fr*FD (4.17)

The correlation coefficient (R2) for each equation is 75%.

ΔE%=57.855-13.5556*P2/P1*Yd/Yu-0.65099*FD*Yd/Yu-0.74293*Fr*Fr +0.1425*Yd/Yu*e (4.18)

The correlation coefficient (R2) for each equation is 98%.

$Vs^{1/3}$/Yu = 89.46188 +197.5242*P2/P1*P2/P1-257.3654*Pt/P1- 0.001498*e*e- 0.02543*FD*Yt/Yu (4.19)

The correlation coefficient (R2) for each equation is 83%.

A comparison between predicted values by each equation and observed values experimentally is shown in Figures (4.54,4.55 and 4.56).

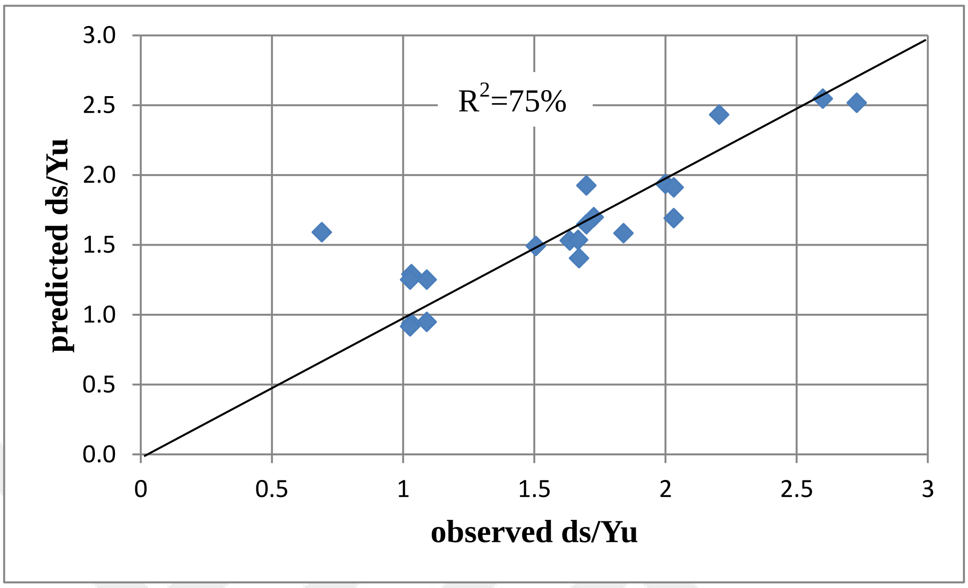

Figure 4.54 Variation of predicted values of ds/Yu with observed ds/Yu for all models

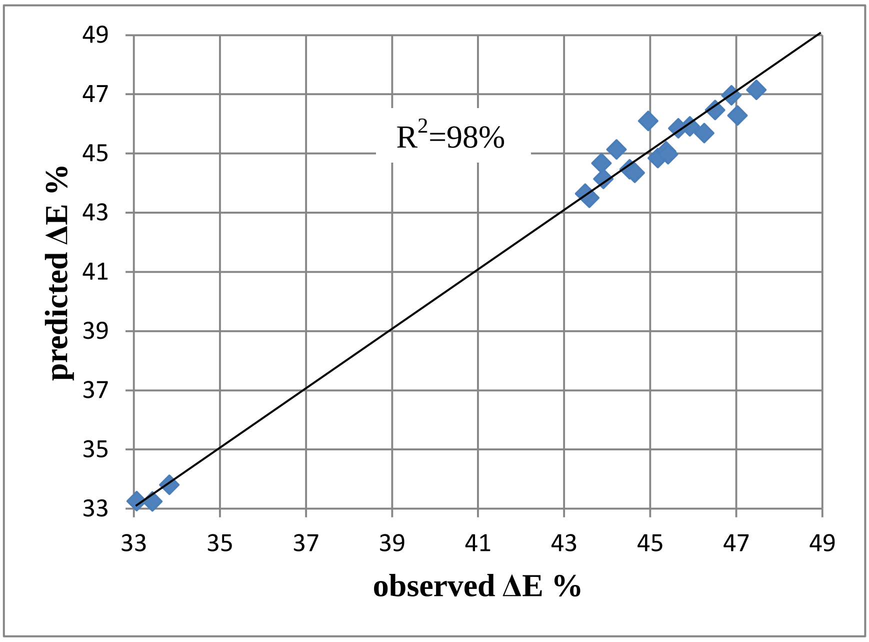

Figure 4.55 Variation of predicted values of ΔE % with observed ΔE % for all models

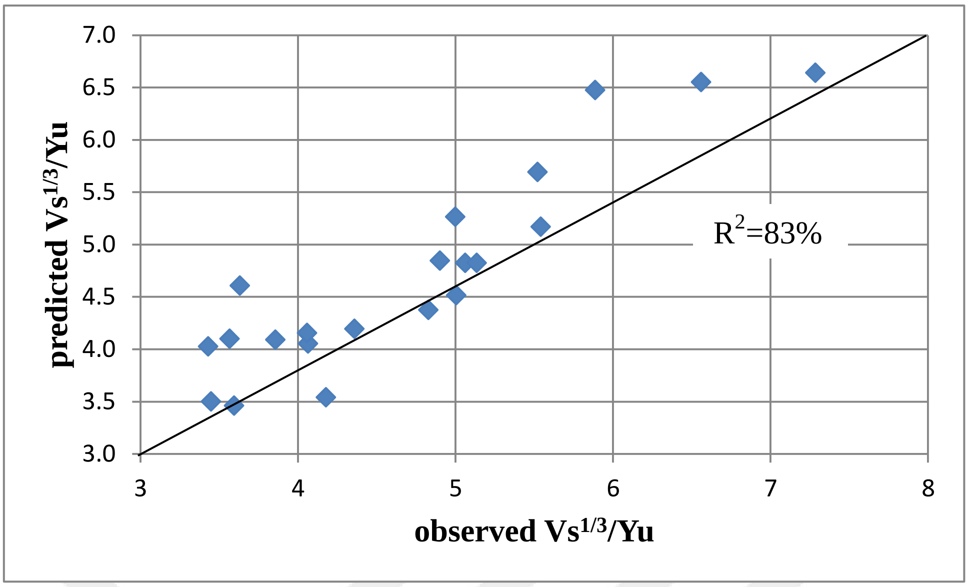

Figure 4.56 Variation of predicted values of $Vs^{1/3}/Yu$ with observed $Vs^{1/3}/Yu$ for all models

Figures (4.57, 4.58, 4.59, 4.60,4.61 and 4.62) show the each model during the run.

Figure 3.57 Picture of model F

Figure 3.58 Picture of model G

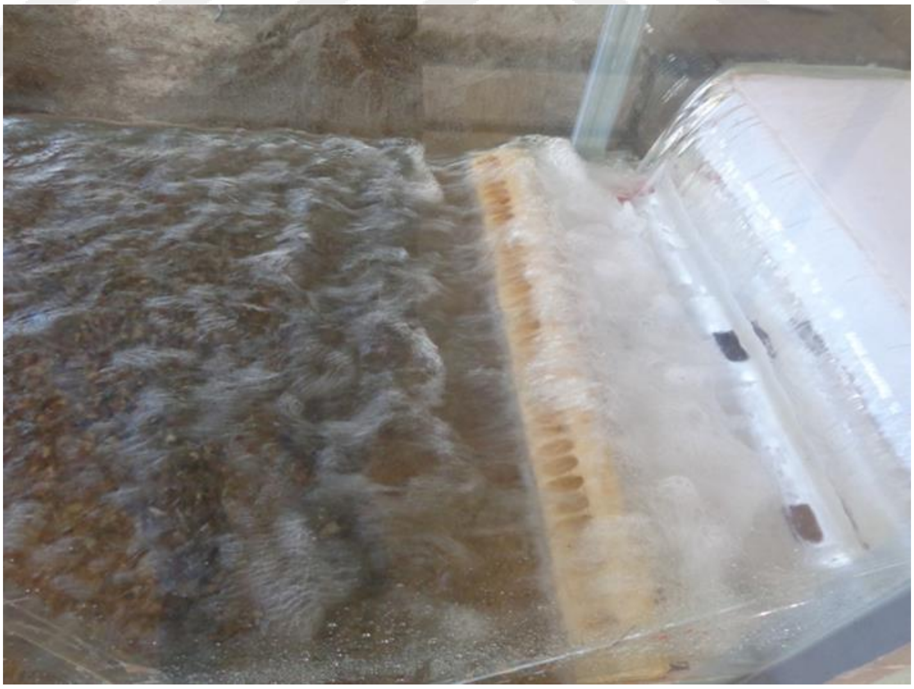

Figure 3.59 Picture of model H

Figure 3.60 Picture of model K

Figure 3.61 Picture of model M

Figure 3.62 Picture of model N

It is seen from Figure (4.58 and 4.59) that, the water surface at model H and model G is smooth and there is no effect of vortices at downstream (D/S) of the weir, on the contrary, the other models where more turbulence during the run.

CHAPTER 5

CONCLUSION AND RECOMMENDATION

5.1 Conclusion:

The present work was an attempt to investigate hydraulic characteristics and parameters that reduce scour due to the change of geometry of the broad crested weir. The current study also provides a new method to reduce the scour depth, the idea of this method is dependent on the change the slope or put an end sill at downstream single step broad crested weir so that it become more effective to reduce scour depth.

The minimum distance of scour from weir was sufficient to prevent failure in the future. In this research, the single broad crested weir was modified to produce minimum local scour and the present improvement also much more economical when it is compared with countermeasures techniques by lining with rubbles and riprap to protect from failure. This research is an experimental study of the application of a new shape of single step broad crested weirs by using end sill with different height and porosity or change the slope at the downstream of single step broad crested weir to reduce local scour on downstream of the weir. Changing the height, porosity or the slope of the step at downstream of the weir was produced minimum local scour more than single step broad crested weir. The results of the comparison between the performances of models under different conditions reveal that single step broad crested weir with an angle (10.8^0) is an effective countermeasure to reduce the depth of scour. The single step broad crested weir with an angle (10.8^0) reduces scour depth, the length of scour hole and volume of scour more than the other models.

We hope that the the designers and engineers will get benefit the results of the present study. From the results, the following conclusions can be drawn from this research:

1. Maximum scour depth was observed to occur at the inclined single step broad crested weir with an angle (13^0) and single step broad crested weir with height End sill 30cm and porosity 30% in all experiments due to the significant effect of down flow which produces a strong vortex.
2. The maximum reduction of scour depth for inclined single step broad crested weir with an angle (10.8^0) was 68.75% and 49.22% for single broad crested weir with height end sill 3 cm and porosity 35% when compared to the single step broad crested weir itself.
3. The inclined single step broad crested weir with an angle (10.8^0) and single broad crested weir with height end sill 3 cm and porosity 35% had a reduction in the scour hole volume of 80.61% and 73.32% respectively when compared to the single step broad crested weir itself.
4. Changing the slope of downstream single step broad crested weir was effective to reduce scour depth more than single step broad crested weir with end sill.
5. For the same discharge, increasing the downstream slope of single step broad crested weir leads to decrease of the maximum depth of scour to a certain level, then further increasing in downstream slope leads to increasing scour depth more than other models because in the meantime increasing downstream slope leads to increase velocity of water instead of reducing it because the geometry helped the water passage more easily.
6. The optimum model was inclined single step broad crested weir with an angle (10.8^0) because it has a minimum of scour depth and volume of scour.
7. Increasing the flow intensity lead to increase in the scour depth, the surface area of scour hole and volume for all models.
8. Changing the geometry of the single step broad crested weir can reduce the scour depth, thereby reducing the potential need for countermeasures.
9. Changing the geometry of the single step broad crested weir much more is economical when it is compared with the traditional Broad crested weir.
10. The effect of the vortex in single broad crested weir with end sill was reduced due to the down flow being deflected away from the weir due to the hollow of end sill.
11. Significantly reduces the intensity of the vortices in downstream of models because the strength of the vortex was inside the weir step.

12. Increasing the height of end sill with increasing the porosity lead to increase the scour depth. Therefore, the single step broad crested weir with 3 cm height of end sill was the best model because it has a minimum porosity (20%).
13. Increasing the height of end sill with increasing diameter of the hole and constant porosity leads to increase the scour depth. Therefore, the single step broad crested weir with 3 cm height of end sill was the best model because it has a maximum diameter (1.5cm).
14. Increasing the diameter of the hole in the end sill with 3 cm height reduce the scour depth.

5.2 Recommendations

1. It would be useful to test the models in the field because It is very important to make additional investigations applying the real-life physical model, this will help in the further understanding of the problem.
2. Study the effects of changing the shape of the hole in the end sill (triangle or square) and checking the efficiency of energy dissipation and reduce the scour depth.
3. Study the effects of using the different shapes of the obstacles on the step of the weir (box or cylinder) and checking the efficiency of energy dissipation and reduce the scour depth.
4. This study could be supplemented with (CFD) analysis to get more results to compare with the obtained scour depths from the experiments.

REFERENCES

Ackers, P., White, W.R., Perkins, J.A., Harrison, A.J.M. (1978), Weirs and Flumes for Flow Measurement, First Edition, John Wiley and Sons, Inc., New York, N.Y., PP. 133-166.

Afshar, H., Hoseini, S. H. (2013). Experimental and 3-D numerical simulation of flow over a rectangular broad-crested weir, *International Journal of Engineering and Advanced Technology*, **2 (6)**, 2249-8958.

Aksoy, A. Ö., Doğan, M.(2016). Experimental investigation of the approach angle effects on the discharge efficiency for broad crested weirs, *Anadolu University Journal of Science and Technology A- Applied Sciences and Engineering*, **17 (2)**, 279-286.

Al- Moula, S. J. S. (2014). Hydraulic Characteristics of Flow over Stepped Spillway with Semicircular Crest, Ph.D. Thesis, Civil Engineering Department, University of Al-Mustansiriyah, Iraq.

Al Naib, S. K. (1997). Fluid Mechanics, Hydraulics and Environmental Engineering: The Essential User-Friendly Books; Including Over 350 Solved Examples; Book One for First and Second Year Undergraduate and Diploma Students and a Reference for Practising Engineers. Research Books.

Albertson, M. L., Dai, Y. B., Jensen, R. A., Rouse, H. (1950). Diffusion of submerged jets, *Transactions of the American Society of Civil Engineers*, **115(1)**, 639-664.

Al-Hashimi, S. A., Madhloom, H. M., Nahi, T. N., & Al-Ansari, N. (2016). Channel Slope Effect on Energy Dissipation of Flow over Broad Crested Weirs, *Engineering*, **8 (12)**, 837.

Al-Hashimi, S., Sulaiman, S.A., Madhloom,H.M. (2015). Determination of Discharge Coefficient of Rectangular Broad-Crested Weir by CFD. *The 2nd*

Ali khani, R., Behrozi-Rad., M. Fathi-Moghadam. (2010). Hydraulic jump in basin with vertical end sill, *International Journal Physical Sciences*, **5 (1)**, 025-029.

Al-Talib, A.N.J. (2007). Laboratory Study of Flow Energy Dissipation Using Stepped Weirs, *MSc. Thesis, Engineering College, Mosul University*.

Aydın, İ., Altan-Sakarya A. B, Şisman, Ç. (2011). Discharge Formula for Rectangular Sharp-Crested Weirs, *Journal of Flow Measurement and Instrumentation*, **22**, 144-151.

Azimi, A. H., Rajaratnam, N. (2009). Discharge characteristics of weir of finite crest length, *Journal of hydraulic engineering*, **135(12)**, 1081-1085.

Azimi,A.H., Rajaratnam,N., David Z. Z. (2013). Discharge Characteristics of Weirs of Finite Crest Length with Upstream and Downstream Ramps, *Journal of Irrigation and Drainage Engineering, ASCE*, **139 (1)**, 75-83.

Badr, K., Mowla, D.(2015). Development of Rectangular Broad-Crested Weirs for Flow Characteristics and Discharge Measurement. *KSCE Journal of Civil Engineering*, **19 (1)**, 136-141.

Bormann, N.E., Julien, P.Y. (1991). Scour downstream of grade-control structures, *Journal of Hydraulic Engineering, ASCE*, **117 (5)**, 579-594.

Bos. M.G. (1976). Discharge measurement structures, Oxford & IBH Publishing Co. New Delhi.

Breusers, H.N.C. (1966). Conformity and time scale in two-dimensional local scour, Proceedings Symposium on model and prototype conformity, Hydraulic Research Laboratory, Poona, pp. 1-8.

Chamani, M.R. , Beirami, M.K. (2002). Flow Characteristics at Drops, *Journal of Hydraulic Engineering, ASCE*, **128 (8)**, 788-791.

Chanson, H. (2001). Hydraulic Design of Stepped Spillways and Downstream Energy Dissipaters, *Dam Energy*, **11 (4)**, 205-242.

Chinnarasri,C., Donjadee, S., Israngkura, U. (2008). Hydraulic characteristics of gabion- stepped weirs. *Journal of Hydraulic Engineering, ASCE,* **134 (8)**, 1147-1152.

Chow, V.T. (1959). Open-Channel Hydraulics, McGraw-Hill, New York.

Clemmons, A.J., Replogle, J.A., Bos, M.G. (1984). Rectangular Measuring Flumes for Lined and Earthen Channels, *Journal of Irrigation and Drainage Engineering, ASCE*, **110 (2)**, 121-137.

Dargahi, B. (2003), Scour development downstream of a spillway, J. Hydraulic Research, 41 (4), 417-426.

De Graauw, A.F.F., Pilarczyk, K.W. (1981). Model-prototype conformity of local scour in non-cohesive sediments beneath overflow-dam, 19th IAHR- Congress, New Delhi (also Delft Hydraulics, PublicationNo.242).

Dehghani, A. A., Bashiri, H., Dehghani, N. (2010). Downstream scour of combined flow over weirs and below gates. *River Flow–Dittrich, Koll, Aberle & Geisenhainer (eds)*, 1201-1205.

Dehghani. A. A, Bashiri. H. (2009). Experimental Investigation of Scouring in Downstream of Combined Flow over Weirs and below Gates, *33rd IAHR Conference*, *Canada,* 978-94.

Dietz, J.W. (1969). Kolkbildung in feinen oder leichten Sohlmaterialien bei strömen dem Abfluß, Mit teilungen Heft 155, Universität Fridericiana Karlsruhe.

Ebrahim N., Heydarnejad, M., (2014). Experimental Investigation of the Effect of Flow Angle of Attack on the Rate of Scour around the Slotted Bridge Pier at Different Levels of River Bend, *IJRASET-International Journal for Research in Applied Science & Engineering Technology,* **2 (12)**, 276-282.

Elyass, S.S. (2012). Effect of Channel Slope on Energy Dissipation of Flow for single step broad-crested weirs, *Journal of Al-Rafidain Engineering, Mosul University*, **16 (3)**, 91-103.

Emiroglu, M. E., Tuna, M. C. (2011). The Effect of Tailwater Depth on the Local Scour Downstream of Stepped-Chutes, *KSCE Journal of Civil Engineering,* **15 (5)**, 907-915.

Fahmy, S.A. (2013). Effect of semi-circular baffle blocks on local scour downstream clear-overfall weirs, *Ain Shams Engineering Journal*, **4**, 675–684.

Farhoudi, J., Alami, S. (2005). Slope effect on discharge efficiency in rectangular broad crested weir with slope upstream face, *International Journal of Civil Engineering,* **3 (1)**, 58- 65.

Fatah, A. K. (2017). Simulation of Local Scouring Downstream of Broad Crested Weirs with Variable Step Angles, MSc. Thesis. Dept. of Civil Engineering, Gaziantep University, Turkey.

Ferziger, J., Peric, M.(1997). Computational Methods for Fluid Dynamics. Springer, Verlag, Berlin.

Fritz, H.M., Hager, W.H. (1998). Hydraulics of Embankment Weirs, *Journal of Hydraulic Engineering, ASCE,* **124 (9)**, 963-971.

Gogus, M., Defne, Z., Ozkandemir, V. (2006). Broad-Crested Weirs with Rectangular Compound Cross Sections, *Journal of Irrigation and Drainage Engineering, ASCE,* **132 (3)**, 272-280.

Gonzalez, C. A., Chanson, H. (2007). Experimental measurements of velocity and pressure distributions on a large broad-crested weir. *Journal Flow Measurement and Instrumentation,* **18 (3)**, 107-113.

Goodarzi, E., Farhoudi, J., Shokri, N. (2012). Flow Characteristics of Rectangular Broad-Crested Weirs with Sloped Upstream Face, *Journal of Hydrology and Hydromechanics,* **60 (2)**, 87-100.

Hager, W.H., Schwalt,M. (1994). Broad-Crested Weir, *Journal of Irrigation and Drainage Engineering, ASCE,* **120 (1)**, 13-26.

Hamill, L. (1999). Bridge Hydraulics, E & FN Spon, London.

Hargreaves, D. M., Morvan, H. P., Wright, N. G. (2007). Validation of the volume of fluid method for free surface calculation: the broad-crested weir, *Engineering Applications of Computational Fluid Mechanics,* **1 (2)**, 136-146.

Hargreaves, D. M., Morvan, H. P., Wrigth, N. G. (2007). Validation of the volume of fluid method for free surface calculation, the broad crested weir, *Engineering applications of computational fluid dynamics*, **1(2)**, 136-147.

Haun, S., Reidar, N., Olsen,B., Feurich, R. (2011). Numerical Modeling of Flow Over Trapezoidal Broad Crested Weir, *Journal of Engineering Applications of Computational Fluid Mechanics,* **5 (3)**, 397- 405.

Hirt, C.W., Nichols, B.D. (1981). Volume of Fluid (VOF) Method for the Dynamics of Free Boundaries, *Journal of Computational Physics,* **39 (1)**, 201-225.

Hoffmans, G. J., & Booij, R. (1993). Two-dimensional mathematical modeling of local scour holes. *Journal of Hydraulic Research*, **31(5)**, 615-634.

Hoffmans, G.J. C.M. (1998). Jet scour in equilibrium phase. *Journal of Hydraulic Engg*., **124(4)**, 430-437.

Hoffmans, G.J., Pilarczyk, K.W.(1995). Local scour downstream of hydraulic structures, *Journal of Hydraulic Engineering, ASCE*. **121(4)**, 326-339.

Hoffmans, G.J.C.M. (1990). Concentration and flow velocity measurements in a local scour hole, Report No.4-90, Faculty of Civil Engineering, Hydraulic and Geotechnical Engineering Division, Delft University of Technology, Delft.

Hoffmans, G.J.C.M. (1992). Two-dimensional mathematical modeling of local scour holes, Doctoral thesis, Faculty of Civil Engineering, Hydraulic and Geotechnical Engineering Division, Delft University of Technology, Delft.

Hoffmans. G.J, Pilarczyk. K.W. (1995). Local scour downstream of hydraulic structures, *Journal of Hydraulic Engineering, ASCE,* **121(4)**, 326-339.

Hoseini, S. H., Afshar, H. (2014). Flow over a broad-crested weir in subcritical flow conditions physical study, *Journal of River Engineering*, **2**, 1-35.

Hoseini, S. H., Jerome, S. H. M., Vahid, M. S. R. (2013). Determination of discharge coefficient of rectangular broad-crested side weir in trapezoidal channel by CFD. *International Journal of Hydraulic Engineering*, **2 (4)**, 64-70.

Hussein, H.H., Elyass, S.S., Shareef, S.J.S. (2009). Local scour evaluation of the downstream single step broad-crested weirs, *11th Scientific Conference of the Technical Education Foundation, Baghdad, Iraq*, pp 198-209.

Hussein, H.H., Juma, I. A.K. Shareef, S.J.S. (2010). Flow characteristics and energy dissipation over single step broad crested weirs, *Journal of Al-Rafidain Engineering, Mosul University*, **18 (5)**, 152-164.

Hussein, H.H., Juma, I.A.K., Shareef, S.J.S. (2011). Improving the hydraulic performance of single step broad-crested weirs, *Journal of Al-Rafidain Engineering, Mosul University*, **7 (1)**, 1-12.

International Conference on Buildings, Construction, and Environmental Engineering, BCEE2-2015, Baghdad, Iraq, pp 123-127.

Jalil, S.A., Ibrahim, S.S., Jafer, R.A. (2014). Surface Roughness Effects on Discharge Coefficient of Broad Crested Weir. *Research Journal of Applied Sciences, Engineering, and Technology*, **7 (24)**, 5227-5233.

Lien, F.S., Leschziner, M.A. (1994). Assessment of Turbulence-Transport Models Including Non-Linear RNG Eddy-Viscosity Formulation and Second-Moment Closure for Flow over a Backward-Facing Step, *Computers, and Fluids*, **23 (8)**, 983-1004.

Liu, C., Hute, A., Wenju, M. (2002). Numerical and Experimental Investigation of Flow over a Semicircular Weir, *Acta Mechanica Sinica*, **18 (6)**, 594-602.

Madadi, M.R., Dalir, A.H., Farsadizadeh, D.(2014). Investigation of Flow Characteristics above Trapezoidal Broad-Crested Weirs. *Flow Measurement and Instrumentation*, **38**, 139-148.

Mason, P. J., Arumugam, K. (1985). Free Jet scour below dams and flip buckets, *Journal of Hydraulic Engineering*, **111 (2)**, 220-235.

Mohammad, E., M. (2005). A conceptual model for flow and sediment routing for a watershed northern Iraq, Ph.D Thesis , Water reesources Dep., College of engineering, Mosul University, Mosul,Iriq.

Mossa, M. (1998). Experimental study on the scour downstream of grade-control structures, Proc., 26th Convegno di Idraulica e Costruzioni Idrauliche, 581-594.

Noori, B. M. , Juma, I. A. (2009). Performance Improvement of Broad Crested Weirs, *Journal of Al-Rafidain Engineering, Mosul University*, **17 (2)**, 95-107.

Noori, B. M., Al- Hafith, A. I. (2007). Performance Improvement of Broad Crested Weirs, *Journal of Al-Rafidain Engineering, Mosul University,* **15 (2)**, 47-62.

Othman, K., Bilal, A., and Suleiman, I. (2012). Morphologic Characteristics of Tigris River with at Mosul City, *Tikrit engineering journal*, **vol**.19 No.3.

Pagliara, S., Palermo, M.(2008). Scour control downstream of block ramps, *Journal of Hydraulic Engineering, ASCE,* **134 (9)**, 1376-138.

Pařílková, J., Říha, J., Zachoval, Z. (2012). The Influence of Roughness on the Discharge Coefficient of a Broad-Crested Weir, *Journal of Hydrology and Hydromechanics,* **60 (2)**, 101-104.

Pilarczyk, K.W. 1984. Interaction water motion and closing elements, The closure of tidal basins, pp. 387-405, Delft University Press, Delft.

Rajaratnam, N. (1981). Erosion by plane turbulent jets, *Journal of Hydraulic Research,* **19 (4)**, 339-358.

Ramamurthy, A.S., Tim, U.S. and Rio, M.V.J. (1988), Characteristics of Square-Edged and Round- Nosed Broad-Crested Weirs, *Journal of Irrigation and Drainage Engineering, ASCE,* **99 (2)**, 61-73.

Raman, G., Mills, A., Othman, S. F., Kibens, V. (2003). Proceedings of the ASME Fluids Engineering Division Summer Meeting. In 2001 ASME Fluids Engineering Division Summer Meeting.

Rao, N. S. L., Rao, M. V. J. (1973). Characteristic of Hydrofoil Weirs, *Journal of Hydraulic Engineering, ASCE,* **99 (2)**, 259-281.

Salmasi, F., Poorescandar, S., Dalir, A.H., Zadeh, D.F. (2012). Discharge Relations for Rectangular Broad-Crested Weirs, *Journal of Agricultural Sciences*, **17**, 324-336.

Sargison, J.E., Percy, A. (2009). Hydraulics of Broad-Crested Weirs with Varying Side Slopes. *Journal of Irrigation and Drainage Engineering, ASCE*, **135 (1)**, 115-118.

Sarker, M. A., Rhodes, D. G. (2000). CFD and physical modeling of free surface over broad-crested weir, Engineering Systems Dept, Cranfield University: UK.

Sarker, M. A., Rhodes, D. G. (2004). Calculation of free surface profile over a rectangular broad crested weir, *Flow measurement and instrumentation*, **15**, 215-219.

Saunders, M.J. (2009). Investigation of the relationship between experimental bridge piers and erosion within a flow, *Courses ENG4111 and ENG4112 Research Project, University of Southern Queensland*.

Shahad, E. (2012). Effect of Channel Slope on Energy Dissipation of Flow for Single Step Broad-Crested Weirs, *Journal of Engineering and Development*, **16(3)**, 91-103.

Şisman, Ç. (2009). Experimental investigation on sharp-crested rectangular weirs, M.S. Thesis, submitted to the Middle East Technical University.

Sobeih M. F., Helal, E. Y., Nassralla, T. H., Abdelaziz, A. A. (2012). Scour depth downstream weir with openings, an *international journal of civil and structural engineering*, **3 (1)**, 259-270.

Subramanya, K. (1986). Flow in open channels, 1st revised edition, Tata McGraw-Hill Published Company Ltd., New Delhi, India, pp 227-238.

Tuyen, N. B. (2006). Flow over oblique weirs, Unpublished M. Sc. Thesis. Delft University of Technology, Netherland.

Uijttewaal, W. (2007). Turbulence in hydraulics CT5312. Delft University of Technology, Delft, The Netherlands, 8(9).

Van Rijn, L.C. (1985). Mathematical models for sediment concentration profiles in a steady flow, Euromech 192, Munich/Neubiberg, Germany, (also Delft Hydraulics, Publication No.365).

Van Rijn, L.C. (1986). Mathematical modeling of suspended sediment in non-uniform flows, *Journal of Hydraulic Engineering, ASCE,* **112(6)**, 433-455.

Vreugdenhil, C.B. 1982. Boundary-layer flow over a sloping bottom, program DUCT, Mathematical investigation, Report S488, Part 2, Delft Hydraulics, Delft.

Whittaker, J.G., Schleiss, A. (1983). Progress Report on the Hydraulic Structure Design Manual, IAHR, chapter 5.4, September.

Yakhot, V., & Orszag, S. A. (1986). Renormalization group analysis of turbulence. I. Basic theory. *Journal of scientific computing,* **1 (1)**, 3-51.

Yazdi, J., Sarkardeh, H., Azamathulla, H.M.,Ghani, A.A. (2010). 3D Simulation of Flow around a Single Spur Dike with Free Surface Flow, *International Journal of River Basin Managemen,* **8 (1)**, 55-62.

Zachoval, Z., Kneblova, M., Rousar, L., Rumann, J., Sulc, J.(2014). Discharge Coefficient of a Rectangular Sharp-Edged Broad-Crested Weir. *Journal of Hydrology and Hydromechanics,* **62 (2)**, 145-149.

Zanke, U. (1978). Zusammenhänge zwischen Strömung und Sedimenttransport Teil 2: Berechnung des Sedimenttransportes hinter befestigten Sohlenstrecken, Sonderfall zweidimensionaler Kolk, Mitteilungen des Franzius-Instituts der TU Hannover, Heft 48.